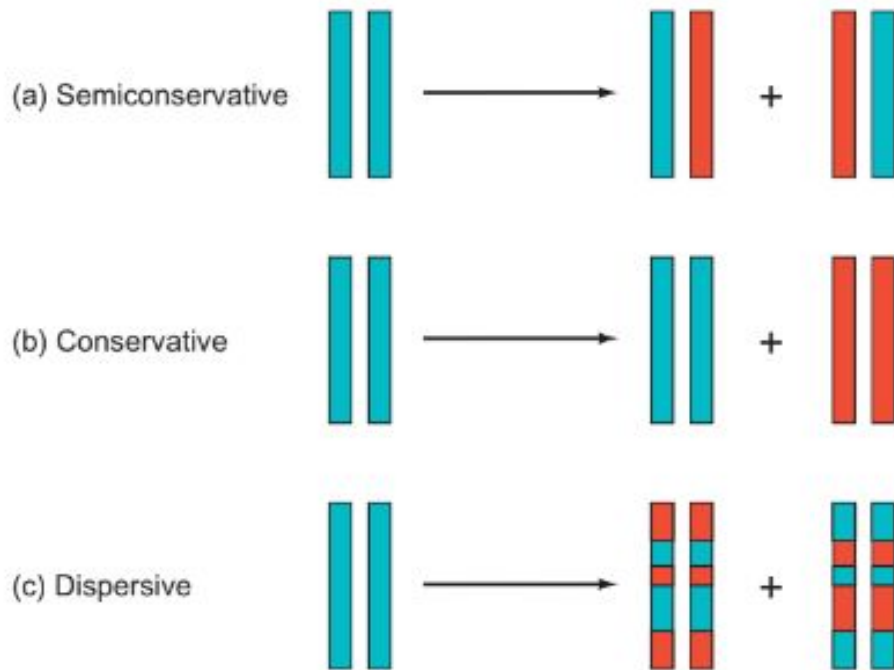


# DNA REPLICATION

M.Sc. semester 1

## SEMI CONSERVATIVE REPLICATION



In 1958, Matthew Meselson and Franklin Stahl performed a classic experiment to distinguish among these three possibilities. They labeled *E. coli* DNA with heavy nitrogen ( $^{15}\text{N}$ ) by growing cells in a medium enriched in this nitrogen isotope. This made the DNA denser than normal. Then they switched the cells to an ordinary medium containing primarily  $^{14}\text{N}$ , for various lengths of time. Finally, they subjected the DNA to CsCl gradient ultracentrifugation to determine the density of the DNA. Figure 20.2 depicts the results of a control experiment that shows that  $^{15}\text{N}$ - and  $^{14}\text{N}$ -DNAs are clearly separated by this method.

**Figure 20.1 Three hypotheses for DNA replication.**

**(a)** Semiconservative replication gives two daughter duplex DNAs, each of which contains one old strand (blue) and one new strand (red).

**(b)** Conservative replication yields two daughter duplexes, one of which has two old strands (blue) and one of which has two new strands (red). **(c)** Dispersive replication gives two daughter duplexes, each of which contains strands that are a mixture of old and new.

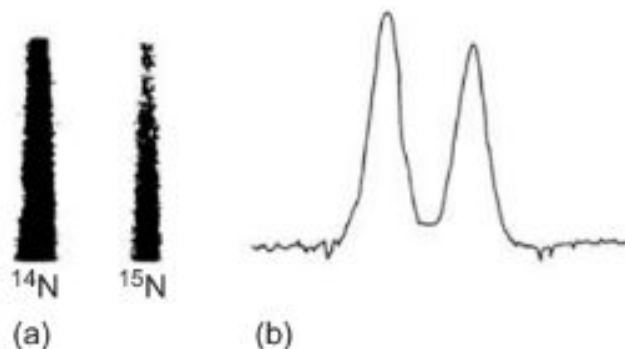
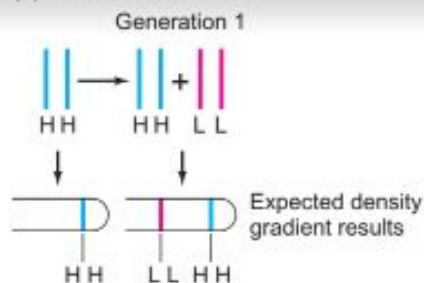


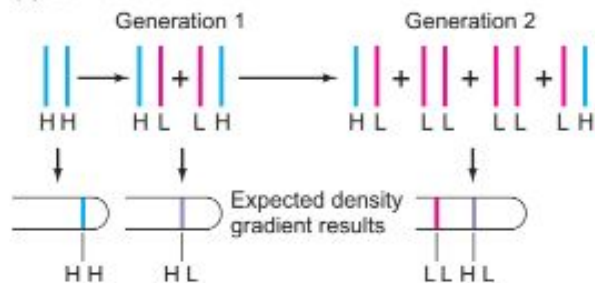
**Figure 20.2 Separation of DNAs by cesium chloride density gradient centrifugation.** DNA containing the normal isotope of nitrogen ( $^{14}\text{N}$ ) was mixed with DNA labeled with a heavy isotope of nitrogen ( $^{15}\text{N}$ ) and subjected to cesium chloride density gradient centrifugation. The two bands had different densities, so they separated cleanly. **(a)** A photograph of the spinning rotor under ultraviolet illumination. Note that this is a photograph through a window in the rotor as it spins. The ultracentrifuge rotor was designed to allow the experimenter to check its contents without stopping the centrifuge. The two dark bands correspond to the two different DNAs that absorb ultraviolet light. **(b)** A graph of the darkness of each band, which gives an idea of the relative amounts of the two kinds of DNA.

(Source: Adapted from Meselson, M. and F. Stahl, The replication of DNA in *Escherichia coli*. *Proceedings of the National Academy of Sciences USA* 44 (1958) p. 673, f. 2.)

(a) Conservative



(b) Semiconservative



(c) Dispersive

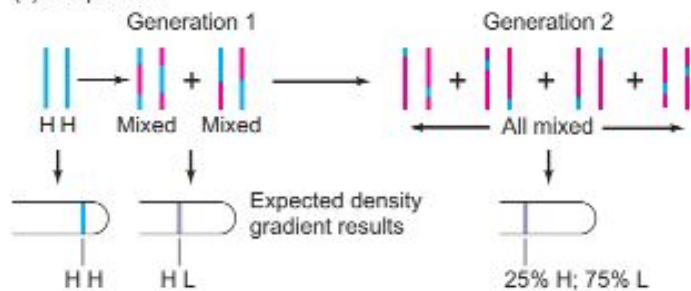


**Figure 20.3 Three replication hypotheses.** The conservative model (a) predicts that after one generation equal amounts of two different DNAs (heavy/heavy [H/H] and light/light [L/L]) will occur. Both the semiconservative (b) and dispersive (c) models predict a single band of DNA with a density halfway between the H/H and L/L densities. Meselson and Stahl's results confirmed the latter prediction, so the conservative mechanism was ruled out. The dispersive model predicts that the DNA after the second generation will have a single density, corresponding to molecules that are 25% H and 75% L. This should give one band of DNA halfway between the L/L and the H/L band. The semiconservative model predicts that equal amounts of two different DNAs (L/L and H/L) will be present after the second generation. Again, the latter prediction matched the experimental results, supporting the semiconservative model.

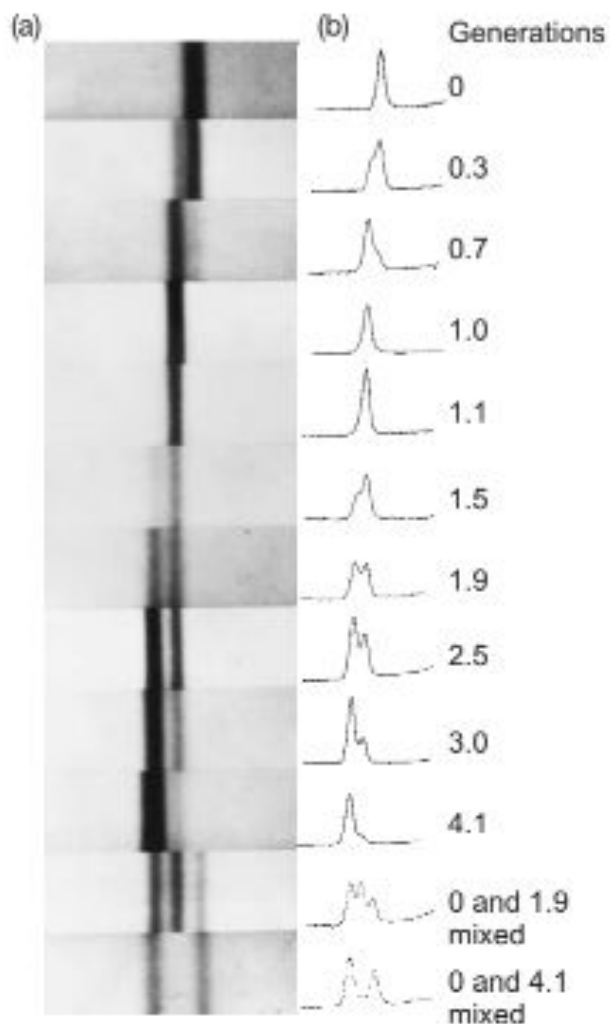


**Figure 20.4 Results of CsCl gradient ultracentrifugation experiment that demonstrates semiconservative DNA replication.** Meselson and Stahl shifted  $^{15}\text{N}$ -labeled *E. coli* cells to a  $^{14}\text{N}$  medium for the number of generations given at right, then subjected the bacterial DNA to CsCl gradient ultracentrifugation. **(a)** Photographs of the spinning centrifuge tubes under ultraviolet illumination. The dark bands correspond to heavy DNA (right) and light DNA (left). A band of intermediate density was also observed between these two and is virtually the only band observed at 1.0 and 1.1 generations. This band corresponds to duplex DNAs in which one strand is labeled with  $^{15}\text{N}$ , and the other with  $^{14}\text{N}$ , as predicted by the semiconservative replication model. After 1.9 generations, Meselson and Stahl observed approximately equal quantities of the intermediate band (H/L) and the L/L band. Again, this is what the semiconservative model predicts. After three and four generations, they saw a progressive depletion of the H/L band, and a corresponding increase in the L/L band, again as we expect if replication is semiconservative. **(b)** Densitometer tracings of the bands in panel (a), which can be used to quantify the amount of DNA in each band. (Source: Meselson, M. and F.W. Stahl, The replication of DNA in *Escherichia coli*, *Proceedings of the National Academy of Sciences USA* 44:675, 1958.)

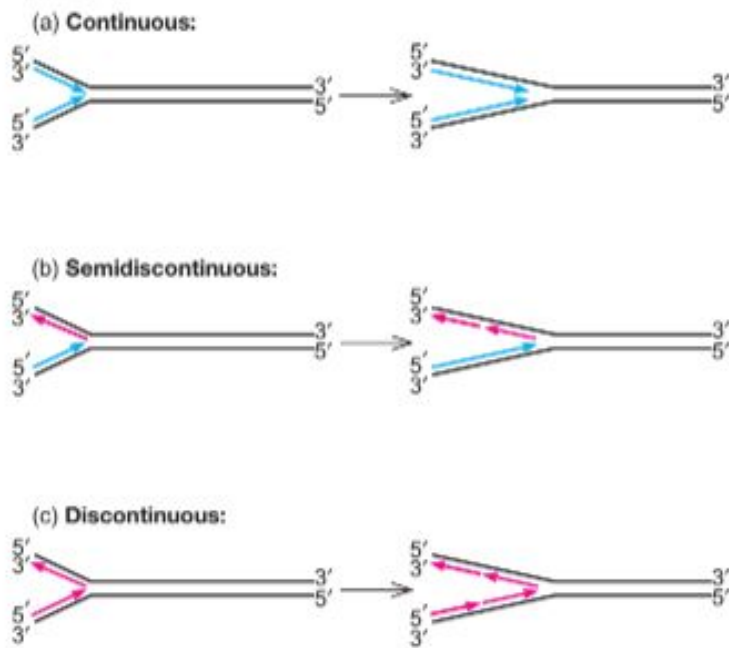


**Figure 20.5 Continuous, semidiscontinuous, and discontinuous models of DNA replication.** (a) Continuous model. As the replicating fork moves to the right, both strands are replicated continuously in the same direction, left to right (blue arrows). The top strand grows in the 3'→5' direction, the bottom strand in the 5'→3' direction. (b) Semidiscontinuous model. Synthesis of one of the new strands (the leading strand, bottom) is continuous (blue arrow), as in the model in panel (a); synthesis of the other (the lagging strand, top) is discontinuous (pink arrows), with the DNA being made in short pieces. Both strands grow in the 5'→3' direction. (c) Discontinuous model. Both leading and lagging strands are made in short pieces (i.e., discontinuously; pink arrows). Both strands grow in the 5'→3' direction.

DNA synthesizing part (DNA polymerase) of all natural replicating machines can make DNA in only one direction: 59→39.

Following this line of reasoning, Reiji Okazaki concluded that both strands could not replicate continuously. DNA polymerase could theoretically make one strand (the leading strand) continuously in the 59→39 direction, but the other strand (the lagging strand) would have to be made discontinuously as shown in Figure 20.5b and c.

The model of semidiscontinuous replication makes two predictions that Okazaki's team tested experimentally: (1) Because at least half of the newly synthesized DNA appears first as short pieces, one ought to be able to label and catch these before they are stitched together by allowing only very short periods (pulses) of labeling with a radioactive DNA precursor. (2) If one eliminates the enzyme (DNA ligase) responsible for stitching together the short pieces of DNA, these short pieces ought to be detectable even with relatively long pulses of DNA precursor.

For his model system, Okazaki chose replication of phage T4 DNA. This had the advantage of simplicity, as well as the availability of T4 ligase mutants. To test the first prediction, Okazaki and colleagues gave shorter and shorter pulses of 3

H-labeled thymidine to *E. coli* cells that were replicating T4 DNA. To be sure of catching short pieces of DNA before they could be joined together, they even administered pulses as short as 2 sec. Finally, they measured the approximate sizes of the newly synthesized DNAs by ultracentrifugation.

Figure 20.6a shows the results. Already at 2 sec, some labeled DNA was visible in the gradient; within the limits of detection, it appeared that all of the label was in very small DNA pieces, 1000–2000 nt long, which remained near the top of the centrifuge tube. With increasing pulse time, another peak of labeled DNA appeared much nearer the bottom of the tube. This was the result of attaching the small, newly formed pieces of labeled DNA to much larger, preformed pieces of DNA that were made before labeling began. These large pieces, because they were unlabeled before the experiment began, did not show up until enough time had elapsed for DNA ligase to join the smaller, labeled pieces to them; this took only a few seconds. The small pieces of DNA that are the initial products of replication have come to be known as Okazaki fragments.

The discovery of Okazaki fragments provided evidence for at least partially discontinuous replication of T4 DNA. This hypothesis was supported by the demonstration that these small DNA fragments accumulated to very high levels when the stitching enzyme, DNA ligase, did not operate. Okazaki's group performed this experiment with the T4 mutant containing a defective DNA ligase gene. Figure 20.6b shows that the peak of Okazaki fragments predominated in this mutant. Even after a full minute of labeling, this was still the major species of labeled DNA, suggesting that Okazaki fragments are not just an artifact of very short labeling times.

The predominant accumulation of small pieces of labeled DNA could be interpreted to mean that replication proceeded discontinuously on both strands, as pictured in Figure 20.5c. Indeed, this was Okazaki and colleagues' interpretation.

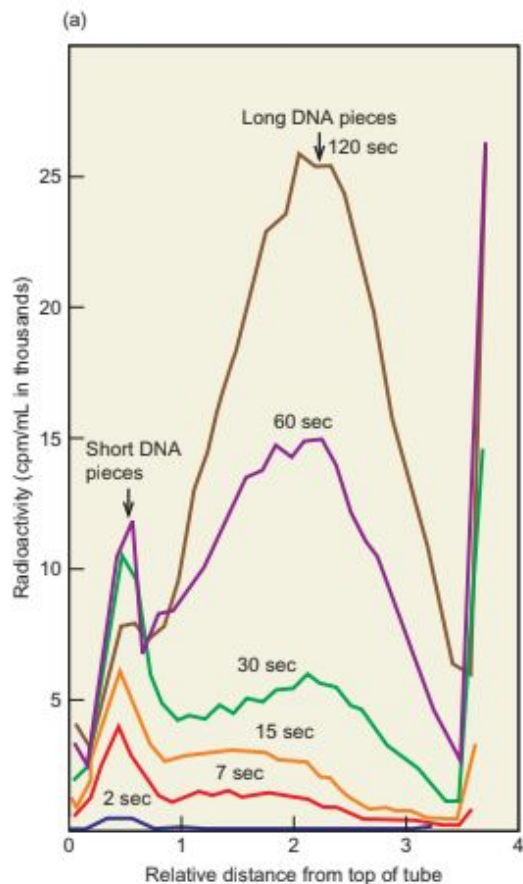
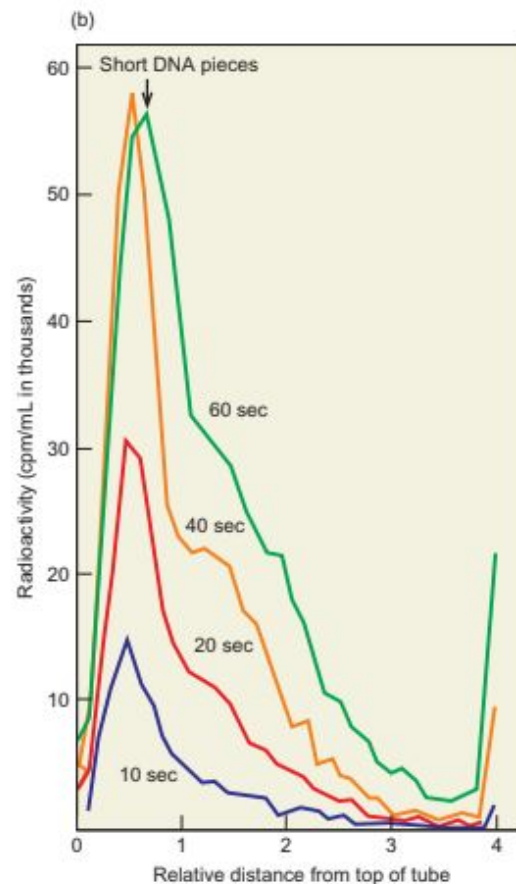


**figure 20.6 Experimental demonstration of at least emidiscontinuous DNA replication. (a)** Okazaki and his colleagues labeled replicating phage T4 DNA with very short pulses of radioactive DNA precursor and separated the product DNAs according to size by ultracentrifugation. At the shortest times, the label went primarily into short DNA pieces (found near the top of the tube), as the

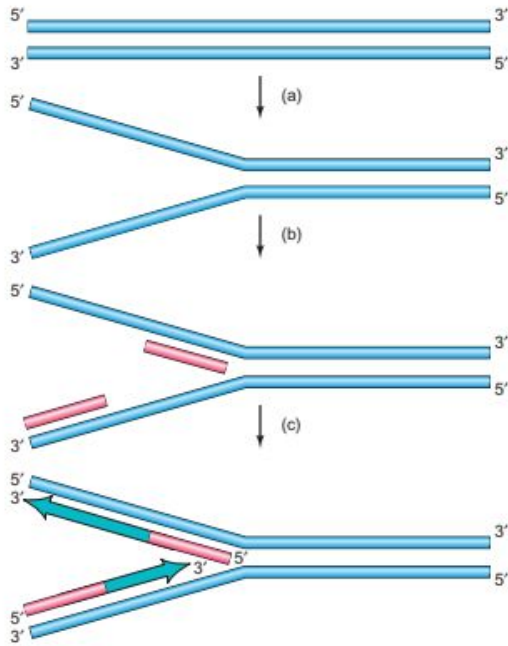


discontinuous model predicted. **(b)** When these workers used a mutant phage with a defective DNA ligase gene, short DNA pieces accumulated even after relatively long labeling times (1 min in the results shown here). (Source: Adapted from R. Okazaki et al., *In vivo mechanism of DNA chain growth, Cold Spring Harbor Symposia on Quantitative Biology*, 33:129-143, 1968.)



synthesis. If we supply a DNA polymerase with all the nucleotides and other small molecules it needs to make DNA, then add either single-stranded or double-stranded DNA with no strand breaks, the polymerase will make no new DNA. What is missing?

We now know that the missing component is a primer, a piece of nucleic acid that the polymerase can “grab onto” and extend by adding nucleotides to its 3'-end. This primer is not DNA, but a short piece of RNA. Figure 20.7 shows a simplified version of this process.



The first line of evidence supporting RNA priming was the finding that replication of M13 phage DNA by an *E. coli* extract is inhibited by the antibiotic rifampicin. This was a surprise because rifampicin inhibits *E. coli* RNA polymerase, not DNA polymerase. The explanation is that M13 uses the *E. coli* RNA polymerase to make RNA primers for its DNA synthesis. However, this is not a general phenomenon. Even *E. coli* does not use its own RNA polymerase for priming; it has a special enzyme system for that purpose.

Perhaps the best evidence for RNA priming was the discovery that DNase cannot completely destroy Okazaki fragments. It leaves little pieces of RNA 10–12 bases long. Most of this work was carried out by Tuneko Okazaki, Reiji Okazaki's wife and scientific colleague. She and her coworkers' first estimate of the primer size was too low—only 1–3 nt. Two problems contributed to this underestimation: (1) Nucleases had already reduced the size of the primers by the time they could be purified, and (2) the investigators had no way of distinguishing degraded from intact primers. In a second set of experiments, completed in 1985, Okazaki's group solved both of these problems and found that intact primers are really about 10–12 nt long.

**Figure 20.7 Priming in DNA synthesis.** (a) The two parental strands (blue) separate. (b) Short RNA primers (pink) are made. (c) DNA polymerase uses the primers as starting points to synthesize progeny DNA strands (green arrows).

To reduce nuclease activity, these workers used mutant bacteria that lacked ribonuclease H or the nuclease activity of DNA polymerase I, or both. This greatly enhanced the yield of the intact primer. To label only intact primer, they used the capping enzyme, guanylyl transferase, and [ $^{32}\text{P}$ ]GTP, to label the 59-ends of these RNAs. Recall from Chapter 15 that guanylyl transferase adds GMP to RNAs with 59-terminal phosphates (ideally, a terminal diphosphate). If the primer were degraded at its 59-end, it would no longer have these phosphates and would therefore not become labeled.

After radiolabeling the primers in this way, these investigators removed the DNA parts of the Okazaki fragments with DNase, then subjected the surviving labeled primers to gel electrophoresis. Figure 20.8 depicts the result. The primers from all the mutant bacteria produced clearly visible bands that corresponded to an RNA with a length of 11 6 1 nt. The wild-type bacteria did not yield a detectable band; nucleases had apparently degraded most or all of their intact primers. Further experiments actually resolved the broad band in Figure 20.8 into three discrete bands with lengths of 10, 11, and 12 nt.

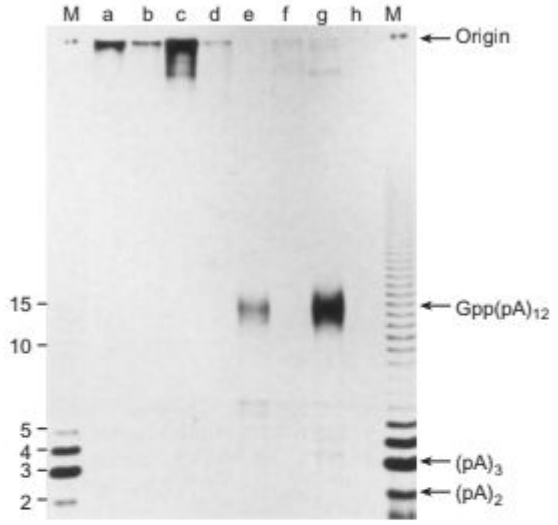


**Figure 20.8 Finding and measuring RNA primers.** Tuneko Okazaki and colleagues isolated Okazaki fragments from wild-type and mutant *E. coli* cells lacking one or both of the nucleases that degrade RNA primers. Next, they labeled the intact primers on the Okazaki fragments with [ $^{32}\text{P}$ ]GTP and a capping enzyme. They destroyed the DNA in the fragments with DNase, leaving only the labeled primers. They subjected these primers to electrophoresis and detected their positions by autoradiography. Lanes M are markers. Lanes a–d, before DNase digestion; lanes e–h, after digestion. Lanes a and e, cells were defective in RNase H; lanes b and f, cells were defective in the nuclease activity of DNA polymerase I; lanes c and g, cells were defective in both RNase H and the nuclease activity of DNA polymerase I; lanes d and h, cells were wild-type. The best yield of primers occurred when both nucleases were defective (lane g), and the primers in all cases were  $11 \pm 1$  nt long. The position of the 13-mer Gpp(pA) $_{12}$  marker is indicated at right.

## Bidirectional Replication

In the early 1960s, John Cairns labeled replicating *E. coli* DNA with a radioactive DNA precursor, then subjected the labeled DNA to autoradiography. Figure 20.9a shows the results, along with Cairns's interpretation. The structure represented in Figure 20.9a is a so-called theta structure because of its resemblance to the Greek letter  $\theta$  (theta). Because it may not be immediately obvious that the DNA in Figure 20.9a looks like a theta, Figure 20.9b provides a schematic diagram of the events in the second round of replication that led to the autoradiograph. This drawing shows that DNA replication begins with the creation of a "bubble"—a small region where the parental strands have separated and progeny DNA has been synthesized. As the bubble expands, the replicating DNA begins to take on the theta shape. We can now recognize the autoradiograph as representing a structure shown in the middle of Figure 20.9b, where the crossbar of the theta has grown long enough to extend above the circular part.

The  $\theta$  structure contains two replicating forks, marked X and Y in Figure 20.9. This raises an important question: Does one of these forks, or do both, represent sites of active DNA replication? In other words, is DNA replication unidirectional, with one fork moving away from the other, which remains fixed at the origin of replication? Or is it bidirectional, with two replicating forks moving in opposite directions away from the origin? Cairns's autoradiographs were not designed to answer this question, but a subsequent study on *Bacillus subtilis* replication performed by Elizabeth Gyurasits and R.B. Wake showed clearly that DNA replication in that bacterium is bidirectional.

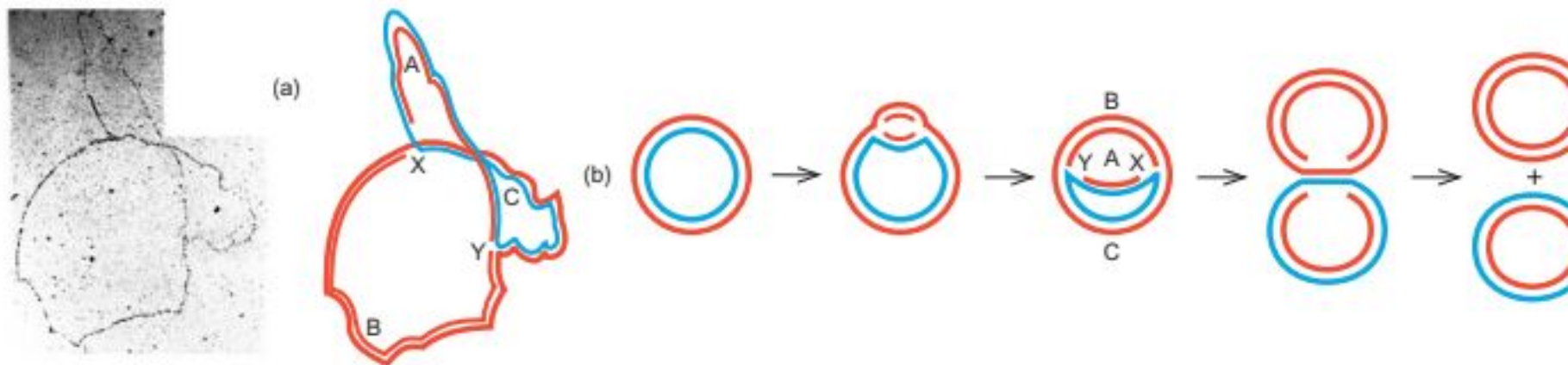


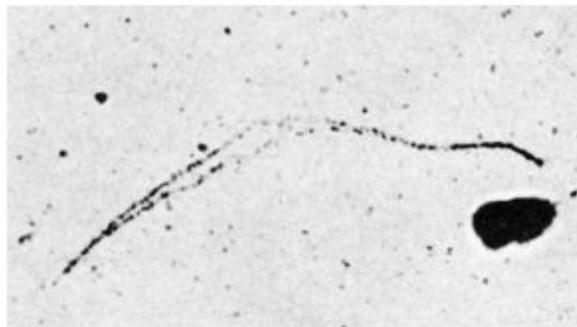
**Figure 20.9 The theta mode of DNA replication in *Escherichia coli*.** (a) An autoradiograph of replicating *E. coli* DNA with an interpretive diagram. The DNA was allowed to replicate for one whole generation and part of a second in the presence of radioactive nucleotides to label the DNA. The interpretive diagram to the right

uses red to represent labeled DNA and blue to represent unlabeled parental DNA. (b) Detailed description of the theta mode of DNA replication. The colors have the same meaning as in panel (a) (Source (a) Cairns, J., *The chromosome of Escherichia coli*. *Cold Spring Harbor Symposium on Quantitative Biology* 28 (1963) p. 44.)

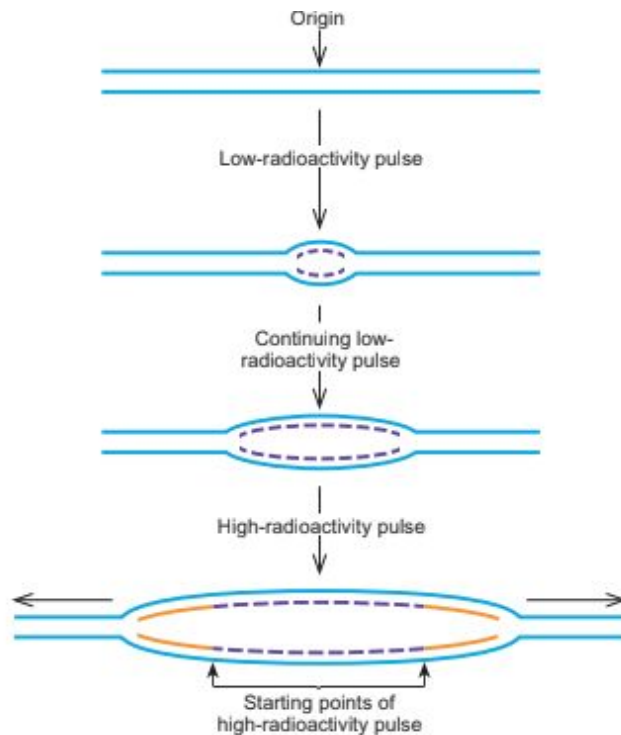
These investigators' strategy was to allow *B. subtilis* cells to grow for a short time in the presence of a weakly radioactive DNA precursor, then for a short time with a more strongly radioactive precursor. The labeled precursor was the same in both cases: [ $^3\text{H}$ ]thymidine. Tritium ( $^3\text{H}$ ) is especially useful for this type of autoradiography because its radioactive emissions are so weak that they do not travel far from their point of origin before they stop in the photographic emulsion and create silver grains. This means that the pattern of silver grains in the autoradiograph will bear a close relationship to the shape of the radioactive DNA. It is important to note that unlabeled DNA does not show up in the autoradiograph. The pulses of label in this experiment were short enough that only the replicating bubbles are visible (Figure 20.10a). You should not mistake these for whole bacterial chromosomes such as in Figure 20.9.

If you look carefully at Figure 20.10a, you will notice that the pattern of silver grains is not uniform. They are concentrated near both forks in the bubble. This extra labeling identifies the regions of DNA that were replicating during the "hot," or high-radioactivity, pulse period. Both forks incorporated extra label, showing that they were both active during the hot pulse. Therefore, DNA replication in *B. subtilis* is bidirectional; two forks arise at a fixed starting point—the origin of replication—and move in opposite directions around the circle until they meet on the other side. Later experiments employing this and other techniques have shown that the *E. coli* chromosome also replicates bidirectionally.

J. Huberman and A. Tsai have performed the same kind of autoradiography experiments in a eukaryote, the fruit fly *Drosophila melanogaster*. Here, the experimenters gave a pulse of strongly radioactive (high specific activity) DNA precursor, followed by a pulse of weakly radioactive (low specific activity) precursor. Alternatively, they reversed the procedure and gave the low specific activity label first, followed by the high. Then they autoradiographed the labeled insect DNA. The spreading of DNA in these experiments did not allow the replicating bubbles to remain open; instead, they collapsed and appear on the autoradiographs as simple streaks of silver grains.



(a)



(b)

**Figure 20.10 Experimental demonstration of bidirectional DNA replication.** (a) Autoradiograph of replicating *Bacillus subtilis* DNA. Dormant bacterial spores were germinated in the presence of low-radioactivity DNA precursor, so the newly formed replicating bubbles immediately became slightly labeled. After the bubbles had grown somewhat, a more radioactive DNA precursor was added to label the DNA for a short period. (b) Interpretation of the autoradiograph. The purple color represents the slightly labeled DNA strands produced

during the low-radioactivity pulse. The orange color represents the more highly labeled DNA strands produced during the later, high-radioactivity pulse. Because both forks picked up the high-radioactivity label, both must have been functioning during the high-radioactivity pulse. DNA replication in *B. subtilis* is therefore bidirectional. (Source: (a) Gyurasits, E.B. and R.J. Wake, Bidirectional chromosome replication in *Bacillus subtilis*. *Journal of Molecular Biology* 73 (1973) p. 58, by permission of Elsevier.)

One end of a streak marks where labeling began; the other shows where it ended. But the point of this experiment is that the streaks always appear in pairs (Figure 20.11a). The pairs of streaks represent the two replicating forks that have moved apart from a common starting point. Why doesn't the labeling start in the middle, at the origin of replication, the way it did in the experiment with *B. subtilis* DNA? In the *B. subtilis* experiment, the investigators were able to synchronize their cells by allowing them to germinate from spores, all starting at the same time. That way they could get label into the cells before any of them had started making DNA (i.e., before germination). Such synchronization was not tried in the *Drosophila* experiments, where it would have been much more difficult. As a result, replication usually began before the label was added, so a blank area arises in the middle where replication was occurring but no label could be incorporated.

Notice the shape of the pairs of streaks in Figure 20.11a. They taper to a point, moving outward, rather like an old-fashioned waxed mustache. That means the DNA incorporated highly radioactive label first, then more weakly radioactive label, leading to a tapering off of radioactivity moving outward in both directions from the origin of replication. The opposite experiment—"cooler" label first, followed by "hotter" label—would give a reverse mustache, with points on the inside. It is possible, of course, that closely spaced, independent origins of replication gave rise to these pairs of streaks. But we would not expect that such origins would always give replication in opposite directions. Surely some would lead to replication in the same direction, producing asymmetric autoradiographs such as the hypothetical one in Figure 20.11b. But these were not seen. Thus, these autoradiography experiments confirm that each pair of streaks we see really represents one origin of replication, rather than two that are close together. It therefore appears that replication of *Drosophila* DNA is bidirectional.

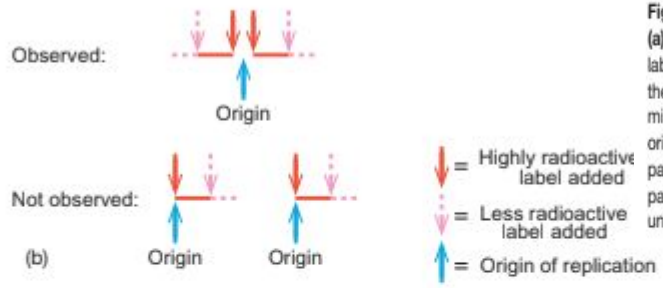
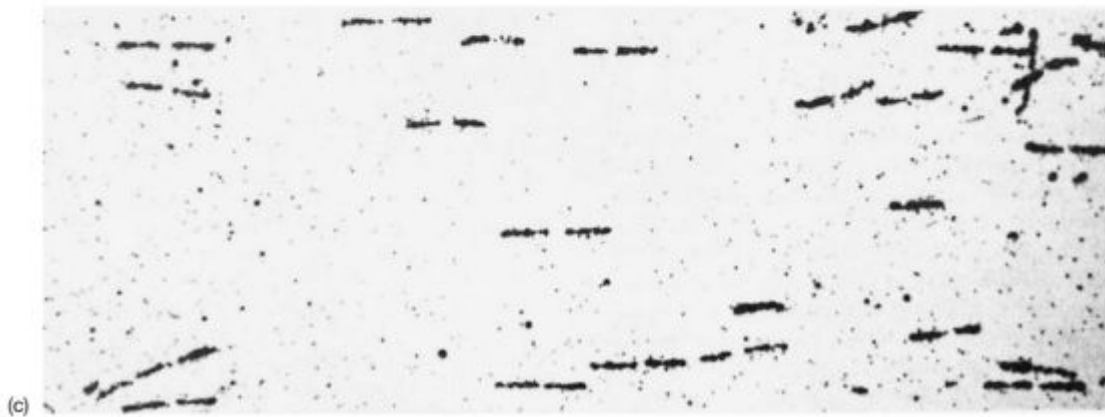


**Figure 20.11 Bidirectional DNA replication in eukaryotes.**  
**(a)** Autoradiograph of replicating *Drosophila melanogaster* DNA, pulse-labeled first with high-radioactivity DNA precursor, then with low. Note the pairs of streaks (denoted by brackets) tapering away from the middle. This reflects the pattern of labeling of a replicon with a central origin and two replicating forks. **(b)** Idealized diagram showing the patterns observed with high-, then low-radioactivity labeling, and the pattern expected if the pairs of streaks represent two independent unidirectional replicons whose replicating forks move in the same

direction. The latter pattern was not observed. **(c)** Autoradiograph of replicating embryonic *Triturus vulgaris* DNA. Note the constant size and shape of the pairs of streaks, suggesting that all the corresponding replicons began replicating at the same time. (Sources: (a) Huberman, J.A. and A. Tsai, Direction of DNA replication in mammalian cells. *Journal of Molecular Biology* 75 (1973) p. 8, by permission of Elsevier. (c) Callan, H.G., DNA replication in the chromosomes of eukaryotes. *Cold Spring Harbor Symposia on Quantitative Biology* 38 (1973) f. 4c, p. 195.)



(c)



These experiments were done with *Drosophila* cells originally derived from mature fruit flies and then cultured *in vitro*. H.G. Callan and his colleagues performed the same type of experiment using highly radioactive label and embryonic amphibian cells. These experiments (with embryonic cells of the newt) gave the striking results shown in Figure 20.11c. In contrast to the pattern in adult insect cells, the pairs of streaks here are all the same. They are all approximately the same length and they all have the same size space in the middle. This tells us that replication at all these origins began simultaneously. This must be so, because the addition of label caught all the forks at the same point—the same distance away from their respective origins of replication. This phenomenon probably helps explain how embryonic newt cells complete their DNA replication so rapidly (in as little as an hour, compared to 40 h in adult cells): Replication at all origins begins simultaneously, rather than in a staggered fashion.

This discussion of origins of replication helps us define an important term: replicon. The DNA under the control of one origin of replication is called a replicon. The *E. coli* chromosome is a single replicon because it replicates from a single origin. Obviously, eukaryotic chromosomes have many replicons; otherwise, it would take far too long to replicate a whole chromosome. Not all DNAs replicate bidirectionally. Michael Lovett used electron microscopic evidence to show that the replication of the plasmid ColE1 in *E. coli* occurs unidirectionally, with only one replicating fork.

## Rolling Circle Replication

Certain circular DNAs replicate, not by the  $\theta$  mode we have already discussed, but by a mechanism called rolling circle replication. The E. coli phages with single-stranded circular DNA genomes, such as  $\phi$ X174, use a relatively simple form of rolling circle replication in which a double-stranded replicative form (RFI) gives rise to many copies of a single-stranded progeny DNA, as illustrated in simplified form in Figure 20.12. The intermediates (steps b and c in Figure 20.12) give this mechanism the rolling circle name because the double-stranded part of the replicating DNA can be considered to be rolling counterclockwise and trailing out the progeny single-stranded DNA, rather like a roll of toilet paper unrolling as it speeds across the floor. This intermediate also somewhat resembles an upside-down Greek letter  $\sigma$  (sigma), so this mechanism is sometimes called the  $\sigma$  mode, to distinguish it from the  $\theta$  mode.

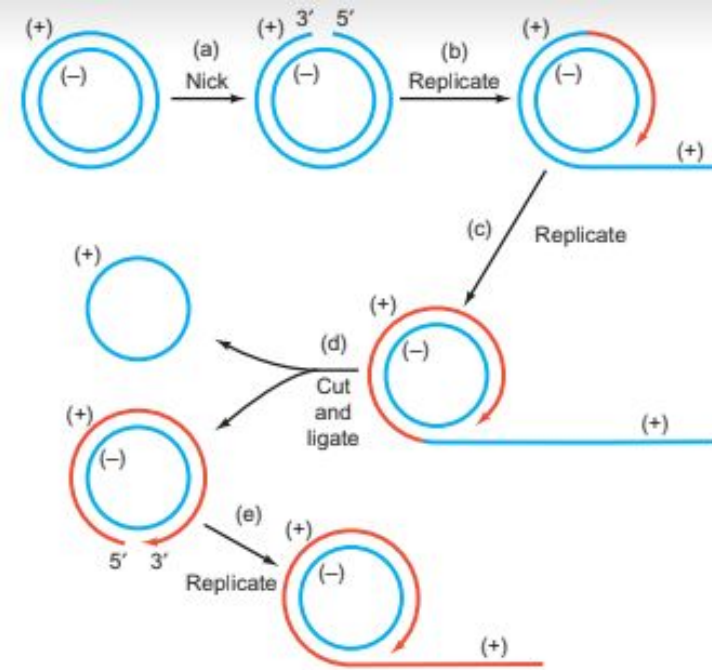


**Figure 20.12 Schematic representation of rolling circle replication that produces single-stranded circular progeny DNAs.** (a) An endonuclease creates a nick in the positive strand of the double-stranded replicative form. (b) The free 3'-end created by the nick serves as the primer for positive strand elongation, as the other end of the positive strand is displaced. The negative strand is the template. Red denotes newly-synthesized DNA. (c) Further replication occurs, as the positive strand approaches double length. The circle can be considered to be rolling counterclockwise. (d) The unit length of positive strand DNA that has been displaced is cleaved off by an endonuclease and circularized. (e) Replication continues, producing another new positive strand, using the negative strand as template. This process repeats over and over to yield many copies of the circular positive strand.

The rolling circle mechanism is not confined to production of single-stranded DNA. Some phages (e.g.,  $\lambda$ ) use this mechanism to replicate double-stranded DNA. During the early phase of  $\lambda$  DNA replication, the phage follows the  $\theta$  mode of replication to produce several copies of circular DNA. These circular DNAs are not packaged into phage particles; they serve as templates for rolling circle synthesis of linear  $\lambda$  DNA molecules that are packaged. Figure 20.13 shows how this rolling circle operates. Here, the replicating fork looks much more like that in *E. coli* DNA replication, with (perhaps) continuous synthesis on the leading strand (the one going around the circle) and discontinuous synthesis on the lagging strand. In  $\lambda$ , the progeny DNA reaches lengths that are several genomes long before it is packaged.

The multiple-length DNAs are called concatemers. The packaging mechanism is designed to provide each phage head with one genome's worth of linear DNA, so the concatemer is cut enzymatically at the *cos* sites flanking each complete  $\lambda$  genome on the concatemer.

## Enzymology of DNA Replication

Over 30 different polypeptides cooperate in replicating the *E. coli* DNA. Let us begin by examining the activities of some of these proteins and their homologs in other organisms, starting with the DNA polymerases—the enzymes that make DNA. Three DNA Polymerases in *E. coli* Arthur Kornberg discovered the first *E. coli* DNA polymerase in 1958. Because we now know that it is only one of three DNA polymerases, we call it DNA polymerase I (pol I). In the absence of evidence for other cellular DNA polymerases, many molecular biologists assumed that pol I was the polymerase responsible for replicating the bacterial genome. As we will see, this assumption was incorrect. Nevertheless, we begin our discussion of DNA polymerases with pol I because it is relatively simple and well understood, yet it exhibits the essential characteristics of a DNA synthesizing enzyme.

**Pol I** Although pol I is a single 102-kD polypeptide chain, it is remarkably versatile. It catalyzes three quite distinct reactions. It has a DNA polymerase activity, of course, but it also has two different exonuclease activities: a 3' → 5', and a 5' → 3' exonuclease activity. Why does a DNA polymerase also need two exonuclease activities? The 3' → 5' activity is important in proofreading newly synthesized DNA (Figure 20.14). If pol I has just added the wrong nucleotide to a growing DNA chain, this nucleotide will not base-pair properly with its partner in the parental strand and should be removed. Accordingly, pol I pauses and the 3' → 5' exonuclease removes the mispaired nucleotide, allowing replication to continue. This greatly increases the fidelity, or accuracy, of DNA synthesis.

The 5'→3' exonuclease activity allows pol I to degrade a strand ahead of the advancing polymerase, so it can remove and replace a strand all in one pass of the polymerase, at least in vitro. This DNA degradation function is useful because pol I seems to be involved primarily in DNA repair (including removal and replacement of RNA primers), for which destruction of damaged or mismatched DNA (or RNA primers) and its replacement by good DNA is required. Figure 20.15 illustrates this process for primer removal and replacement.

Another important feature of pol I is that it can be cleaved by mild proteolytic treatment into two polypeptides: a large fragment (the Klenow fragment), which has the polymerase and proofreading (3'→5' exonuclease) activities; and a small fragment with the 5'→3' exonuclease activity. The Klenow fragment is frequently used in molecular biology when DNA synthesis is required and destruction of one of the parental DNA strands, or the primer, is undesirable. For example, the Klenow fragment is often used to perform DNA end-filling and can also be used to sequence a DNA. On the other hand, the whole pol I is used to perform nick translation to label a probe in vitro, because nick translation depends on 5'→3' degradation of DNA ahead of the moving fork.

Thomas Steitz and colleagues determined the crystal structure of the Klenow fragment in 1987, giving us our first look at the fine structure of a DNA-synthesizing machine. The most obvious feature of the structure is a great cleft between two  $\alpha$ -helices. This is the presumed binding site for the DNA that is being replicated. In fact, all of the known polymerase structures, including that of T7 RNA polymerase, are very similar, and have been likened to a hand. In the Klenow fragment, one  $\alpha$ -helix is part of the “fingers” domain, the other is part of the “thumb” domain, and the  $\beta$ -pleated sheet between them is part of the “palm” domain. The palm domain contains three conserved aspartate residues that are essential for catalysis. They are thought to coordinate magnesium ions that catalyze the polymerase reaction.



**Figure 20.14 Proofreading in DNA synthesis.** (a) An adenine nucleotide (pink) has been mistakenly incorporated across from a guanine. This destroys the perfect base pairing required at the 3'-end of the primer, so the replicating machinery stalls. (b) This pause then

allows Pol I to use its 3'→5' exonuclease function to remove the mismatched nucleotide. (c) With the appropriate base-pairing restored, Pol I is free to continue DNA synthesis.

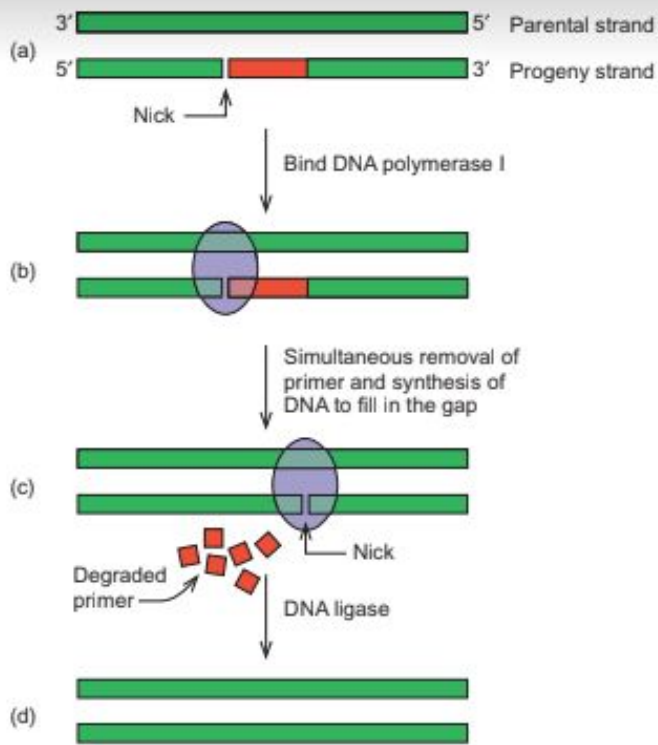


**Figure 20.15 Removing primers and joining nascent DNA fragments.** (a) There are two adjacent progeny DNA fragments, the right-hand one containing an RNA primer (red) at its 5'-end. The two fragments are separated by a single-stranded break called a nick. (b) DNA polymerase I binds to the double-stranded DNA at the nick. (c) The 5'→3' exonuclease and polymerase activities of DNA polymerase I simultaneously remove the primer and fill in the resulting gap by extending the left-hand DNA fragment rightward. The polymerase leaves degraded primer in its wake. (d) DNA ligase seals the remaining nick by forming a phosphodiester bond between the left-hand and right-hand progeny DNA fragments.

Is the cleft in the polymerase structure really the DNA binding site? To find out, Steitz and colleagues turned to another DNA polymerase, the Taq polymerase. They made a cocrystal of Taq polymerase and a model double-stranded DNA template containing 8 bp and a blunt end at the 3'-end of the nontemplate (primer) strand. Taq polymerase is the polymerase from the thermophilic bacterium *Thermus aquaticus* that is widely used in PCR. Its polymerase domain is very similar to that of the Klenow fragment—so much so that it is called the “KF portion,” for “Klenow fragment” portion, of the enzyme. Figure 20.16 shows the results of x-ray crystallography studies on the Taq polymerase–DNA complex. The primer strand (red) has its 3'-end close to the three essential aspartate residues in the palm domain, but not quite close enough for magnesium ions to bridge between the carboxyl groups of the aspartates and the 3'-hydroxyl group of the primer strand. Thus, this structure is not exactly like a catalytically productive one, perhaps in part because the magnesium ions are missing.

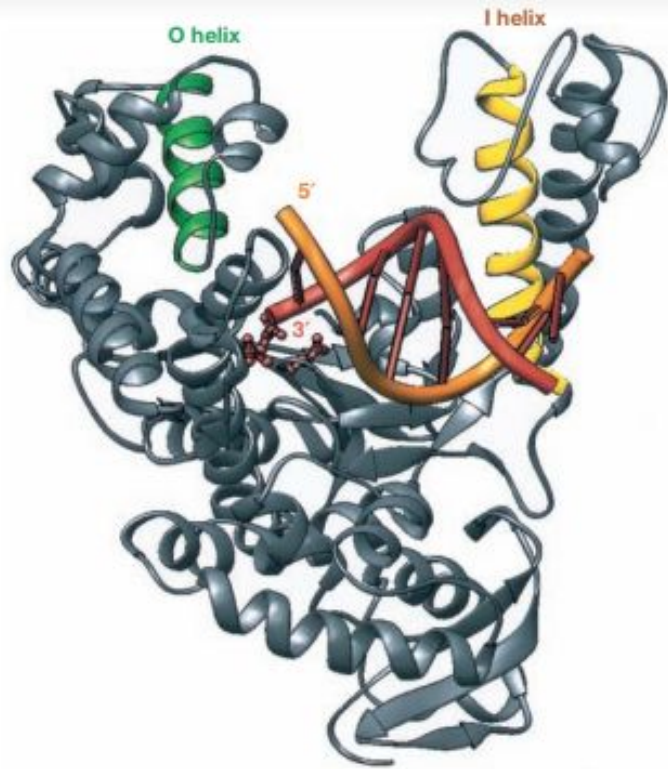


**Figure 20.16** Cocrystal structure of *Taq* DNA polymerase with a double-stranded model DNA template. The O helix and I helix of the “fingers” and “thumb” of the polymerase “hand” are in green and yellow, respectively. The template and primer strands of the model DNA are in orange and red, respectively. The three essential aspartate side chains in the “palm” are represented by small red balls near the 3′-end of the primer strand. (Source: Eom, S.H., J. Wang and T.A. Steitz, Structure of *Taq* polymerase with DNA at the polymerase active site. *Nature* 382 (18 July 1996) f. 2a, p. 280. Copyright © Macmillan Magazines, Ltd.)

In 1969, Paula DeLucia and John Cairns isolated a mutant with a defect in the *polA* gene, which encodes pol I. This mutant (*polA1*) lacked pol I activity, yet it was viable, strongly suggesting that pol I was not really the DNA-replicating enzyme. Instead, pol I seems to play a dominant role in repair of DNA damage. It fills in the gaps left when damaged DNA is removed. The finding that pol I is not essential spurred a renewed search for the real DNA replicase, and in 1971, Thomas Kornberg and Malcolm Gefter discovered two new polymerase activities: DNA polymerases II and III (pol II and pol III). We will see that pol III is the actual replicating enzyme.



Pol II and Pol III Pol II could be readily separated from pol I by phosphocellulose chromatography, but pol III had been masked in wild-type cells by the preponderance of pol I. Next, Kornberg, Gefter, and colleagues used genetic means to search for the polymerase that is required for DNA replication. They tested the pol II and III activities in 15 different *E. coli* strains that were temperature-sensitive for DNA replication. Most of these strains were polA12, which made it easier to measure pol III activity after phosphocellulose chromatography because there was no competing pol I activity. In those few cases where pol I was active, Gefter and colleagues used N-ethylmaleimide to knock out pol III so its activity could be measured as the difference between the activities in the presence and absence of the inhibitor.

The most striking finding was that there were five strains with mutations in the *dnaE* gene. In four of these, the pol III activity was very temperature-sensitive, and in the fifth it was slightly temperature-sensitive. On the other hand, none of the mutants affected pol II at all. These results led to three conclusions: First, the *dnaE* gene encodes pol III. Second, the *dnaE* gene does not encode pol II, and pol II and pol III are therefore separate activities. Third, because defects in the gene encoding pol III interfere with DNA replication, pol III is indispensable for DNA replication. It would have been nice to conclude that pol II is not required for DNA replication, but that was not possible because no mutants in the gene encoding pol II were tested. However, in separate work, these investigators isolated mutants with inactive pol II, and these mutants were still viable, showing that pol II is not necessary for DNA replication. Thus, pol III is the enzyme that replicates the *E. coli* DNA.

**The Pol III Holoenzyme** The enzyme that carries out the elongation of primers to make both the leading and lagging strands of DNA is called DNA polymerase III holoenzyme (pol III holoenzyme). The “holoenzyme” designation indicates that this is a multisubunit enzyme, and indeed it is: As Table 20.1 illustrates, the holoenzyme contains 10 different polypeptides. On dilution, this holoenzyme dissociates into several different subassemblies, also as indicated in Table 20.1.

**Table 20.1 Subunit Composition of *E. coli* DNA Polymerase III Holoenzyme**

Subunit	Molecular mass (kD)	Function	Subassemblies		
$\alpha$	129.9	DNA polymerase	Core	Pol III'	Pol III holoenzyme
$\epsilon$	27.5	3'→5' exonuclease			
$\theta$	8.6	Stimulates $\epsilon$ exonuclease			
$\tau$	71.1	Dimerizes core Binds $\gamma$ complex	Pol III*		
$\gamma$	47.5	Binds ATP			
$\delta$	38.7	Binds to $\beta$	$\gamma$ complex (DNA-dependent ATPase)		
$\delta'$	36.9	Binds to $\gamma$ and $\delta$			
$\chi$	16.6	Binds to SSB			
$\psi$	15.2	Binds to $\chi$ and $\gamma$			
$\beta$	40.6	Sliding clamp			

\*Pol III holoenzyme minus the  $\beta$ -subunit.

Source: Reprinted from Herendeel, D.R. and T.T. Kelly, DNA Polymerase III: Running rings around the fork *Cell* 84:6, 1996. Copyright © 1996, with permission from Elsevier.

Each pol III subassembly is capable of DNA polymerization, but only very slowly. This suggested that something important is missing from the subassemblies because DNA replication in vivo is extremely rapid. The replicating fork in *E. coli* moves at the amazing rate of 1000 nt/sec. (Imagine the sheer mechanics involved in unwinding parental DNA, correctly pairing 1000 nt with partners in the parental DNA strands, and forming 1000 phosphodiester bonds every second!) In vitro, the holoenzyme goes almost that fast: about 700 nt/sec, suggesting that this is the entity that replicates DNA in vivo. The other two DNA polymerases in the cell, pol I and pol II, are not ordinarily found in holoenzyme forms, and they replicate DNA much more slowly than the pol III holoenzyme does. Charles McHenry and Weldon Crow purified DNA polymerase III to near-homogeneity and found that three polypeptides compose the core of pol III: the  $\alpha$ -,  $\epsilon$ -, and  $\theta$ -subunits. These have molecular masses of 130, 27.5, and 10 kD, respectively. The rest of the subunits of the holoenzyme dissociated during purification, but the core subunits were bound tightly together. In this section, we will examine the pol III core more thoroughly, but we will save our discussion of the other polypeptides in the pol III holoenzyme for Chapter 21 because they play important roles in initiation and elongation of DNA synthesis.

The  $\alpha$ -subunit of the pol III core has the DNA polymerase activity, but this was not easy to determine because the  $\alpha$ -subunit is so difficult to separate from the other core subunits. When Hisaji Maki and Arthur Kornberg cloned and overexpressed the gene for the  $\alpha$ -subunit, they finally paved the way for purifying the polymerase activity because the overproduced  $\alpha$ -subunit was in great excess over the other two subunits. When they tested this purified  $\alpha$ -subunit for DNA polymerase activity, they found that it had activity similar to the same amount of core. Thus, the  $\alpha$ -subunit contributes the DNA polymerase activity to the core.

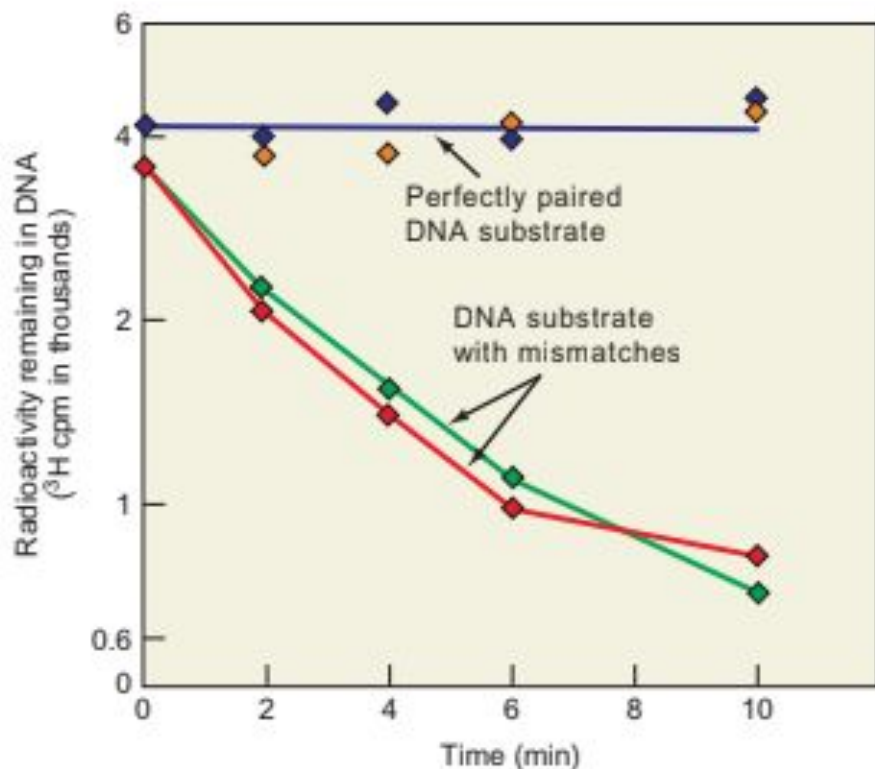


**Figure 20.17 Exonuclease activity of  $\epsilon$ -subunit and pol III core with substrates that are perfectly base-paired or that have mismatches.** Scheuermann and Echols incubated the purified  $\epsilon$ -subunit with  $^3\text{H}$ -labeled synthetic DNAs and measured the amount of radioactivity remaining in the DNAs after increasing lengths of time. Symbols: blue and green, pol III core; orange and red,  $\epsilon$ -subunit.

The pol III core has a 3'→5' exonuclease activity that removes mispaired bases as soon as they are incorporated, allowing the polymerase to proofread its work. This is similar to the 3'→5' exonuclease activity of the pol I Klenow fragment. Scheuermann and Echols used the overexpression strategy to demonstrate that the core  $\epsilon$ -subunit has this exonuclease activity. They overexpressed the  $\epsilon$ -subunit (the product of the *dnaQ* gene) and purified it through various steps. After the last step, DEAE-Sephacel chromatography, the  $\epsilon$ -subunit was essentially pure. Next, Richard Scheuermann and Harrison Echols tested this purified  $\epsilon$ -subunit, as well as core pol III, for exonuclease activity. Figure 20.17 shows that the core and the  $\epsilon$ -subunit both have exonuclease activity, and they are both specific for mispaired DNA substrates, having no measurable activity on perfectly paired DNAs. This is what we expect for the proofreading activity. This activity also explains why *dnaQ* mutants are subject to excess mutations ( $10^3$ – $10^5$  more than in wild-type cells). Without adequate proofreading, many more mismatched bases fail to be removed and persist as mutations. Thus, we call *dnaQ* mutants mutator mutants, and the gene has even been referred to as the *mutD* gene because of this mutator phenotype.

Relatively little work has been performed on the  $\alpha$ -subunit of the core. Its function, other than a stimulation of  $\epsilon$  exonuclease activity, is unknown. However, it is clear that the  $\alpha$ - and  $\epsilon$ -subunits cooperate to boost each other's activity in the core polymerase. The DNA polymerase activity of the  $\alpha$ -subunit increases by about two-fold in the core, compared with the free subunit, and the activity of the  $\epsilon$ -subunit increases by about 10–80-fold when it joins the core.

## Fidelity of Replication

The proofreading mechanism of pol III (and pol I) greatly increases the fidelity of DNA replication. The pol III core makes about one pairing mistake in one hundred thousand *in vitro*—not a very good record, considering that even the *E. coli* genome contains over four million base pairs. At this rate, replication would introduce errors into a significant percentage of genes every generation. Fortunately, proofreading allows the polymerase another mechanism by which to get the base pairing right. The error rate of this second pass is presumably the same as that of the first pass, or about  $10^{-5}$ . This predicts that the actual error rate with proofreading would be  $10^{-5} \times 10^{-5} = 10^{-10}$ , and that is close to the actual error rate of the pol III holoenzyme *in vivo*, which is  $10^{-10}$ – $10^{-11}$ . (The added fidelity comes at least in part from mismatch repair, which we will discuss later in this chapter.) This is a tolerable level of fidelity. In fact, it is better than perfect fidelity because it allows for mutations, some of which help the organism to adapt to a changing environment through evolution.

Consider the implications of the proofreading mechanism, which removes a mispaired nucleotide at the 3'-end of a DNA progeny strand (recall Figure 20.14). DNA polymerase cannot operate without a base-paired nucleotide to add to, which means that it cannot start a new DNA chain unless a primer is already there. That explains the need for primers, but why primers made of RNA? The reason seems to be the following: Primers are made with more errors, because their synthesis is not subject to proofreading. Making primers out of RNA guarantees that they will be recognized, removed, and replaced with DNA by extending the neighboring Okazaki fragment. The latter process is, of course, relatively error-free, because it is catalyzed by pol I, which has a proofreading function.

## Multiple Eukaryotic DNA Polymerases

**Table 20.2 Probable Roles of Some Eukaryotic DNA Polymerases**

Enzyme	Probable role
DNA polymerase $\alpha$	Priming of replication of both strands
DNA polymerase $\delta$	Elongation of lagging strand
DNA polymerase $\epsilon$	Elongation of leading strand
DNA polymerase $\beta$	DNA repair
DNA polymerase $\gamma$	Replication of mitochondrial DNA

Much less is known about the proteins involved in eukaryotic DNA replication, but we do know that multiple DNA polymerases take part in the process, and we also have a good idea of the roles these enzymes play. Table 20.2 lists the major mammalian DNA polymerases and their probable roles.

It had been thought that polymerase  $\alpha$  synthesized the lagging strand because of the low processivity of this enzyme. Processivity is the tendency of a polymerase to stick with the replicating job once it starts. The *E. coli* polymerase III holoenzyme is

highly processive. Once it starts on a DNA chain, it remains bound to the template, making DNA for a long time. Because it does not fall off the template very often, which would require a pause as a new polymerase bound and took over, the overall speed of *E. coli* DNA replication is very rapid. Polymerase  $\delta$  is much more processive than polymerase  $\alpha$ . Thus, it was proposed that the less processive DNA polymerase  $\alpha$  synthesized the lagging strand, which is made in short pieces. However, it now appears that polymerase  $\alpha$ , the only eukaryotic DNA polymerase with primase activity, makes the primers for both strands. Then DNA polymerase epsilon  $\epsilon$  elongates the leading strand and DNA polymerase  $\delta$  elongates the lagging strand.

Actually, much of the processivity of polymerases  $\delta$  and  $\epsilon$  comes, not from the polymerase itself, but from an associated protein called proliferating cell nuclear antigen, or PCNA. This protein, which is enriched in proliferating cells that are actively replicating their DNA, enhances the processivity of polymerase  $\delta$  by a factor of 40. That is, PCNA causes the polymerase to travel 40 times farther elongating a DNA chain before falling off the template. PCNA works by physically clamping the polymerase onto the template.

In marked contrast, polymerase  $\beta$  is not processive at all. It usually adds only one nucleotide to a growing DNA chain and then falls off, requiring a new polymerase to bind and add the next nucleotide. This fits with its postulated role as a repair enzyme that needs to make only short stretches of DNA to fill in gaps created when primers or mismatched bases are excised. In addition, the level of polymerase  $\beta$  in a cell is not affected by the rate of division of the cell, which suggests that this enzyme is not involved in DNA replication. If it were, we would expect it to be more prevalent in rapidly dividing cells, as polymerases  $\delta$  and  $\epsilon$  are.

Polymerase  $\gamma$  is found in mitochondria, not in the nucleus. Therefore, we conclude that this enzyme is responsible for replicating mitochondrial DNA.



# Strand Separation

In our discussion of the general features of DNA replication, we have been assuming that the two DNA strands at the fork somehow unwind. This does not happen automatically as DNA polymerase does its job; the two parental strands hold tightly to each other, and it takes energy and enzyme action to separate them.

**Helicase** The enzyme that harnesses the chemical energy of ATP to separate the two parental DNA strands at the replicating fork is called a helicase. We have already seen an example of helicase action in our discussion of the DNA helicase activity of TFIIH, which unwinds a short region of DNA to help create the transcription bubble in eukaryotes. That DNA melting is transient, in contrast to the permanent strand separation needed to advance a replicating fork.

Many DNA helicases have been identified in *E. coli* cells. The problem is finding which of these is involved in DNA replication. The first three to be investigated—the *rep* helicase, and DNA helicases II and III—could be mutated without inhibiting cellular multiplication. This made it unlikely that any of these three enzymes could participate in something as vital to cell survival as DNA replication; we would anticipate that defects in the helicase that participates in DNA replication would be lethal.

One way to generate mutants with defects in essential genes is to make the mutations conditional, usually temperature-sensitive. That way, one can grow the mutant cells at a low temperature at which the mutation is not expressed, then shift the temperature up to observe the mutant phenotype. As early as 1968, François Jacob and his colleagues discovered two classes of temperature-sensitive mutants in *E. coli* DNA replication. Type 1 mutants showed an immediate shut-off of DNA synthesis on raising the temperature from 30°C to 40°C, whereas type 2 mutants showed only a gradual decrease in the rate of DNA synthesis at elevated temperature.

One of the type 1 mutants was the *dnaB* mutant; DNA synthesis in *E. coli* cells carrying temperature-sensitive mutations in the *dnaB* gene stopped short as soon as the temperature rose to the nonpermissive level. This is what we would expect if *dnaB* encodes the DNA helicase required for replication. Without a functional helicase, the fork cannot move, and DNA synthesis must halt immediately. Furthermore, the *dnaB* product (DnaB) was known to be an ATPase, which we also expect of a DNA helicase, and the DnaB protein was found associated with the primase, which makes primers for DNA replication.

All of these findings suggested that DnaB is the DNA helicase that unwinds the DNA double helix during *E. coli* DNA replication. All that remained was to show that DnaB has DNA helicase activity. Jonathan LeBowitz and Roger McMacken did this in 1986. They used the helicase substrate shown in Figure 20.18a, which is a circular M13 phage DNA, annealed to a shorter piece of linear DNA, which was labeled at its 5'-end. Figure 20.18a also shows how the helicase assay worked. LeBowitz and McMacken incubated the labeled substrate with DnaB, or other proteins, and then electrophoresed the products. If the protein had helicase activity, it would unwind the double-helical DNA and separate the two strands. Then the short, labeled DNA would migrate independently of the larger, unlabeled DNA, and would have a much higher electrophoretic mobility.

Figure 20.18b shows the results of the assay. DnaB alone had helicase activity, and this was stimulated by DnaG, and by SSB, a single-stranded DNA-binding protein that we will introduce next. Neither DnaG nor SSB, by themselves or together, had any DNA helicase activity. Thus, DnaB is the helicase that unwinds the DNA at the replicating fork.

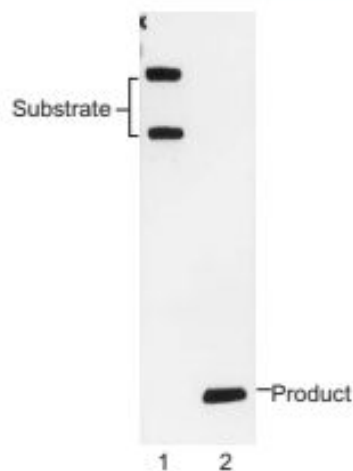
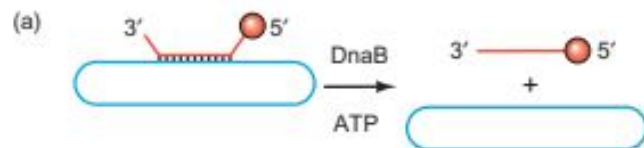
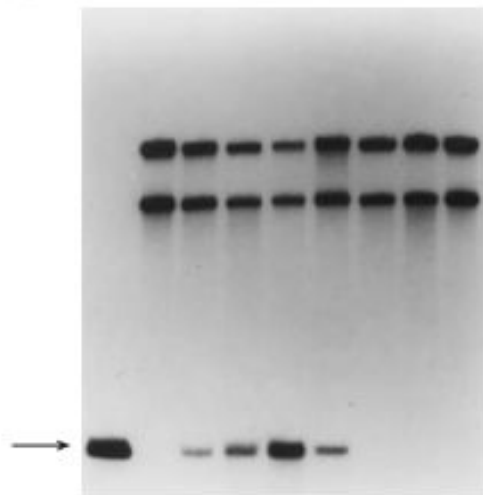


**Figure 20.18 DNA helicase assay.** (a) Principle of assay. LeBowitz and McMacken made a helicase substrate (top) by  $^{32}\text{P}$ -labeling a single-stranded 1.06-kb DNA fragment (red) at its 5'-end and annealing the fragment to an unlabeled single-stranded recombinant M13 DNA bearing a complementary 1.06-kb region. The dnaB protein, or any DNA helicase, can unwind the double-stranded region of the substrate and liberate the labeled short piece of DNA (red) from its longer, circular partner. Bottom: Electrophoresis of the substrate (lane 1) yields two bands, which probably correspond to linear and circular versions of the long DNA annealed to the labeled, short DNA. Electrophoresis of the short DNA by itself (lane 2) shows that it has a much higher mobility than the substrate (see band labeled "Product").

(b) 

Addition	1	2	3	4	5	6	7	8	9
dnaB	-	+	+	+	+	-	-	-	-
dnaG	-	-	-	+	+	+	+	-	+
SSB	-	-	+	+	-	+	+	-	-



(b) Helicase assay results. LeBowitz and McMacken performed the assay outlined in (a) with the additions (DnaB, DnaG, and SSB) indicated at top. The electrophoresis results are given at bottom. Lane 1 is a control with the unannealed, labeled short DNA to show its electrophoretic behavior (arrow). Lane 3 shows that DnaB has helicase activity on its own, but lanes 4 and 5 demonstrate that the other proteins stimulate this activity. On the other hand, lanes 7-9 show that the other two proteins have no helicase activity without DnaB. (Source: LeBowitz, J.H. and R. McMacken, *The Escherichia coli dnaB replication protein is a DNA helicase. Journal of Biological Chemistry* 261 (5 April 1986) figs. 2, 3, pp. 4740-41. American Society for Biochemistry and Molecular Biology.)

## Single-Strand DNA-Binding Proteins

Another class of proteins, called single-strand DNA-binding proteins (SSBs), also participate in DNA strand separation during replication. These proteins do not catalyze strand separation, as helicases do. Instead, they bind selectively to single-stranded DNA as soon as it forms and coat it so it cannot anneal to re-form a double helix. The single-stranded DNA can form by natural “breathing” (transient local separation of strands, especially in A–T-rich regions) or as a result of helicase action, then SSB catches it and keeps it in single-stranded form. The best-studied SSBs are bacterial. The *E. coli* protein is called SSB and is the product of the *ssb* gene. The T4 phage protein is gp32, which stands for “gene product 32” (the product of gene 32 of phage T4). The M13 phage protein is gp5 (the product of the phage gene 5). All of these proteins act cooperatively: The binding of one protein facilitates the binding of the next. For example, the binding of the first molecule of gp32 to single-stranded DNA raises the affinity for the next molecule a thousandfold. Thus, once the first molecule of gp32 binds, the second binds easily, and so does the third, and so forth. This results in a chain of gp32 molecules coating a single-stranded DNA region. The chain will even extend into a double-stranded hairpin, melting it, as long as the free energy released in cooperative gp32 binding through the hairpin exceeds the free energy released by forming the hairpin. In practice, this means that relatively small, or poorly base-paired hairpins will be melted, but long, or well base-paired ones will remain intact. The gp32 protein binds to DNA as a chain of monomers, whereas gp5 binds as a string of dimers, and *E. coli* SSB binds as a chain of tetramers, with about 65 nt of single-stranded DNA wound around each SSB tetramer.

By now we have had some hints that the name “single-strand DNA-binding protein” is a little misleading. These proteins do indeed bind to single-stranded DNA, but so do many other proteins we have studied in previous chapters, including RNA polymerase. But the SSBs do much more. We have already seen that they trap DNA in single-stranded form, but they also specifically stimulate their homologous DNA polymerases. For example, gp32 stimulates the T4 DNA polymerase, but it does not stimulate phage T7 polymerase or *E. coli* DNA polymerase I.

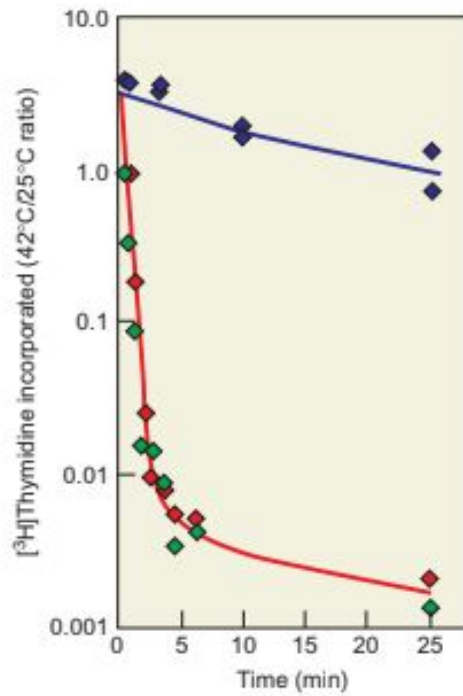


**Figure 20.19 Temperature-sensitivity of DNA synthesis in cells infected by T4 phage with a temperature-sensitive mutation in the SSB (gp32) gene.** Curtis and Alberts measured the relative incorporation of [<sup>3</sup>H]thymidine after 1 min pulses at 42° and 25°C in cells infected with T4 phage mutants having mutations in the following genes: gene 23, blue; gene 32 plus gene 23, red; and gene 32 plus gene 49, green. The amber mutations in genes 23 and 49 have no effect on DNA synthesis. Thus, the observed drop in DNA synthesis is due to the *ts* mutation in gene 32. (Source: Adapted from Curtis, M.J. and B. Alberts, Studies on the structure of intracellular bacteriophage T4 DNA, *Journal of Molecular Biology*, 102: 793–816, 1976.)

Are the activities of the SSBs important? In fact, they are essential. Temperature-sensitive mutations in the *ssb* gene of *E. coli* render the cell inviable at the nonpermissive temperature. In cells infected by the *tsP7* mutant of phage T4, with a temperature-sensitive gp32, phage DNA replication stops within 2 min after shifting to the nonpermissive temperature (Figure 20.19). Furthermore, the phage DNA begins to be degraded. This behavior suggests that one function of gp32 is to protect from degradation the single-stranded DNA created during phage DNA replication.

Based on the importance of the SSBs in prokaryotes, it is surprising that SSBs with similar importance have not yet been found in eukaryotes. However, a host SSB has been found to be essential for replication of SV40 DNA in human cells. This protein, called RF-A, or human SSB, binds selectively to single-stranded DNA and stimulates the DNA helicase activity of the viral large T antigen. Because this is a host protein, we assume that it plays a role in the uninfected human cell as well, but we do not know yet what that role is. We also know that virus-encoded SSBs play a major role in replication of certain eukaryotic viral DNAs, including adenovirus and herpesvirus DNAs.

# Topoisomerases

Sometimes we refer to the separation of DNA strands as “unzipping.” We should not forget, when using this term, that DNA is not like a zipper with straight, parallel sides. It is a double helix. Therefore, when the two strands of DNA separate, they must rotate around each other. Helicase could handle this task alone if the DNA were linear and unnaturally short, but closed circular DNAs, such as the *E. coli* chromosome, present a special problem. As the DNA unwinds at the replicating fork, a compensating winding up of DNA will occur elsewhere in the circle. This tightening of the helix will create intolerable strain unless it is relieved. Cairns recognized this problem in 1963 when he first observed circular DNA molecules in *E. coli*, and he proposed a “swivel” in the DNA duplex that would allow the DNA strands on either side to rotate to relieve the strain (Figure 20.20). We now know that an enzyme known as DNA gyrase serves the swivel function. DNA gyrase belongs to a class of enzymes called topoisomerases that introduce transient single- or double-stranded breaks into DNA and thereby allow it to change its shape, or topology.

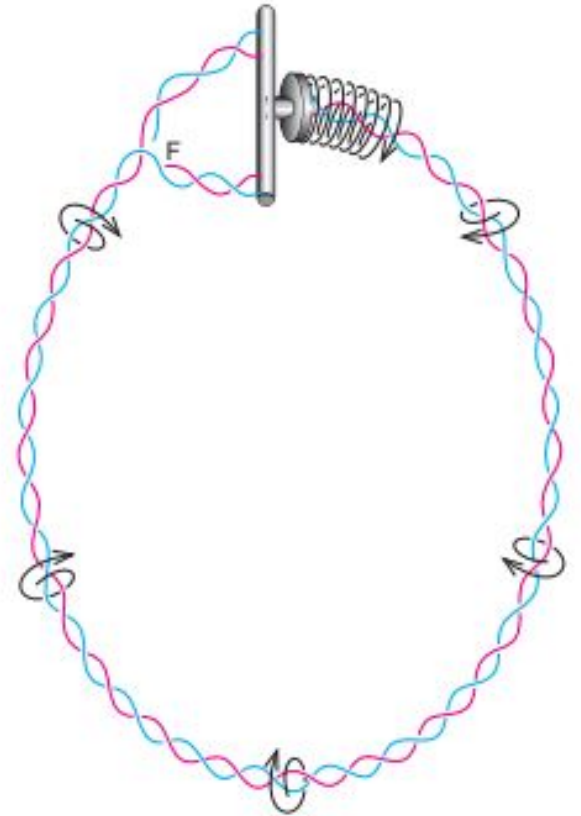


**Figure 20.20 Cairns's swivel concept.** As the closed circular DNA replicates, the two strands must separate at the fork (F). The strain of this unwinding would be released by a swivel mechanism. Cairns actually envisioned the swivel as a machine that rotated actively and thus drove the unwinding of DNA at the fork.

To understand how the topoisomerases work, we need to look more closely at the phenomenon of supercoiled, or superhelical, DNA. All naturally occurring, closed circular, double-stranded DNAs studied so far exist as supercoils. Closed circular DNAs are those with no single-strand breaks, or nicks. When a cell makes such a DNA, it causes some unwinding of the double helix; the DNA is then said to be “underwound.” As long as both strands are intact, no free rotation can occur around the bonds in either strand’s backbone, so the DNA cannot relieve the strain of underwinding except by supercoiling. The supercoils introduced by underwinding are called “negative,” by convention. This is the kind of supercoiling found in most organisms; however, positive supercoils do exist in extreme thermophiles, which have a reverse DNA gyrase that introduces positive supercoils, thus stabilizing the DNA against the boiling temperatures in which these organisms live.

You can visualize the supercoiling process as follows: Take a medium to large rubber band, and hold it at the top with one hand. With your other hand, twist the side of the rubber band through one full turn. You should notice that the rubber band resists the turning as strain is introduced, then relieves the strain by forming a supercoil (a figure 8). The more you twist, the more supercoiling you will observe: one superhelical turn for every full twist you introduce. Reverse the twist and you will see supercoiling of the opposite handedness or sign. If you release your grip on the side of the rubber band, of course the superhelix will relax. In DNA, it is only necessary to cut one strand to relax a supercoil because the other strand can rotate freely.

Unwinding DNA at the replicating fork would form positive rather than negative supercoils if no other way for relaxing the strain existed. That is because replication permanently unwinds one region of the DNA without nicking it, forcing the rest of the DNA to become overwound, and therefore positively supercoiled, to compensate. To visualize this, look at the circular arrow ahead of the replicating fork (F) in Figure 20.20. Notice how twisting the DNA in the direction of the arrow causes unwinding behind the arrow but overwinding ahead of it. Imagine inserting your finger into the DNA just behind the fork and moving it in the direction of the moving fork to force the DNA strands apart. You can imagine how this would force the DNA to rotate in the direction of the circular arrow, which overwinds the DNA helix. This overwinding strain would resist your finger more and more as it moved around the circle. Therefore, unwinding the DNA at the replicating fork introduces positive superhelical strain that must be constantly relaxed so replication will not be retarded. You can appreciate this when you think of how the rubber band increasingly resisted your twisting as it became more tightly wound. In principle, any enzyme that is able to relax this strain could serve as a swivel. In fact, of all the topoisomerases in an *E. coli* cell, only one, DNA gyrase, appears to perform this function.

Topoisomerases are classified according to whether they operate by causing single- or double-stranded breaks in DNA. Those in the first class (type I topoisomerases, e.g., topoisomerase I of *E. coli*) introduce temporary single-stranded breaks. Enzymes in the second class (type II topoisomerases, e.g., DNA gyrase of *E. coli*) break and reseal both DNA strands. Why is *E. coli* topoisomerase I incapable of providing the swivel function needed in DNA replication? Because it can relax only negative supercoils, not the positive ones that form in replicating DNA ahead of the fork. Obviously, the nicks created by these enzymes do not allow free rotation in either direction. But DNA gyrase pumps negative supercoils into closed circular DNA and therefore counteracts the tendency to form positive ones. Hence, it can operate as a swivel.



## Initiation

As we have seen, initiation of DNA replication means primer synthesis. Different organisms use different mechanisms to make primers; even different phages that infect *E. coli* (coliphages) use quite different primer synthesis strategies. The coliphages were convenient tools to probe *E. coli* DNA replication because they are so simple that they have to rely primarily on host proteins to replicate their DNAs.

### Priming in *E. coli*

As mentioned in Chapter 20, the first example of coliphage primer synthesis was found by accident in M13 phage, when this phage was discovered to use the host RNA polymerase as its primase (primer-synthesizing enzyme). But *E. coli* and its other phages do not use the host RNA polymerase as a primase. Instead, they employ a **primase** called **DnaG**, which is the product of the *E. coli* *dnaG* gene. Arthur Kornberg noted that *E. coli* and most of its phages need at least one more protein (**DnaB**, a DNA helicase introduced in Chapter 20) to form primers, at least on the lagging strand.

Arthur Kornberg and colleagues discovered the importance of DnaB with an assay in which single-stranded φX174 phage DNA (without SSB) is converted to double-stranded form. Synthesis of the second strand of phage DNA required primer synthesis, then DNA replication. The DNA replication part used pol III holoenzyme, so the other required proteins should be the ones needed for primer synthesis. Kornberg and colleagues found that three proteins: DnaG (the primase), DnaB, and pol III holoenzyme were required in this assay. Thus, DnaG and DnaB were apparently needed for primer synthesis. Kornberg coined the term primosome to refer to the collection of proteins needed to make primers for a given replicating DNA. Usually this is just two proteins, DnaG and DnaB, although other proteins may be needed to assemble the primosome.

The *E. coli* primosome is mobile and can repeatedly synthesize primers as it moves around the uncoated circular fX174 phage DNA. As such, it is also well suited for the repetitious task of priming Okazaki fragments on at least the lagging strand of *E. coli* DNA. This contrasts with the activity of RNA polymerase or primase alone, which prime DNA synthesis at only one spot—the origin of replication. Two different general approaches were used to identify the important components of the *E. coli* DNA replication system, with DNA from phages fX174 and G4 as model substrates. The first approach was a combination genetic–biochemical one, the strategy of which was to isolate mutants with defects in their ability to replicate phage DNA, then to complement extracts from these mutants with proteins from wild-type cells. The mutant extracts were incapable of replicating the phage DNA *in vitro* unless the right wild-type protein was added. Using this system as an assay, the protein can be highly purified and then characterized. The second approach was the classical biochemical one: Purify all of the components needed and then add them all back together to reconstitute the replication system *in vitro*.

**The Origin of Replication in *E. coli*** Before we discuss priming further, let us consider the unique site at which DNA replication begins in *E. coli*: *oriC*. An origin of replication is a DNA site at which DNA replication begins and which is essential for proper replication to occur. We can locate the place where replication begins by several means, but how do we know how much of the DNA around the initiation site is essential for replication to begin? One way is to clone a DNA fragment, including the initiation site, into a plasmid that lacks its own origin of replication but has an antibiotic resistance gene. Then we can use the antibiotic to select for autonomously replicating plasmids. Any cell that replicates in the presence of the antibiotic must have a plasmid with a functional origin. Once we have such an *oriC* plasmid, we can begin trimming and mutating the DNA fragment containing *oriC* to find the minimal effective DNA sequence. The minimal origin in *E. coli* is 245 bp long. Some features of the origins are conserved in bacteria, and the spacing between them is also conserved.

Figure 21.1 illustrates the steps in initiation at *oriC*. The origin includes four 9-mers with the consensus sequence TTATCCACA. Two of these are in one orientation, and two are in the opposite orientation. DNase foot-printing shows that these 9-mers are binding sites for the *dnaA* product (DnaA). These 9-mers are therefore sometimes called *dnaA* boxes. DnaA appears to facilitate the binding of DnaB to the origin.

DnaA helps DnaB bind at the origin by stimulating the melting of three 13-mer repeats at the left end of *oriC* to form an open complex. This is analogous to the open promoter complex. DnaB can then bind to the melted DNA region. Another protein, DnaC, binds to DnaB and helps deliver it to the origin.

The evidence also strongly suggests that DnaA directly assists the binding of DnaB. Here is one line of evidence that points in this direction. A *dnaA* box resides in the stem of a hairpin stem loop in a plasmid called R6K. When DnaA binds to this DNA, DnaB (with the help of DnaC) can also bind. Here, no DNA melting appears to occur, so we infer that DnaA directly affects binding between DNA and DnaB.

At least two other factors participate in open complex formation at *oriC*. The first of these is RNA polymerase. This enzyme does not serve as a primase, as it does in M13 phage replication, but it still serves an essential function. We know RNA polymerase action is required, because rifampicin blocks primosome assembly. The role of RNA polymerase seems to be to synthesize a short piece of RNA that creates an R loop (Chapter 14). The R loop can be adjacent to *oriC*, rather than within it.

The second factor is **HU protein**. This is a small basic DNA-binding protein that can induce bending in double-stranded DNA. This bending, together with the R loop, presumably destabilizes the DNA double helix and facilitates melting of the DNA to form the open complex.

Finally, DnaB stimulates the binding of the primase (DnaG), completing the primosome. Priming can now occur, so DNA replication can get started. The primosome remains with the replication machinery, or replisome, as it carries out elongation, and serves at least two functions. First, it must operate repeatedly in priming Okazaki fragment synthesis to build the lagging strand. Second, DnaB serves as the helicase that unwinds DNA to provide templates for both the leading and lagging strands. To accomplish this task, DnaB moves in the 5'→3' direction on the lagging strand template—the same direction in which the replicating fork is moving. This anchors the primosome to the lagging strand template, where it is needed for priming Okazaki fragment synthesis.

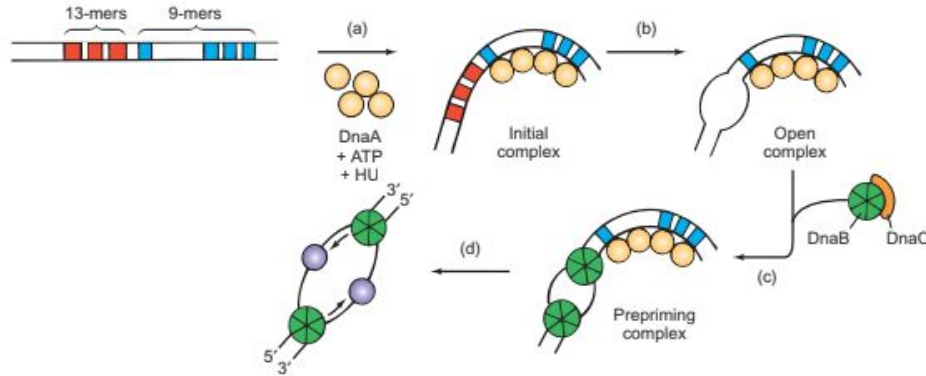


**Figure 21.1 Priming at *oriC*.** (a) Formation of the initial complex. First, DnaA (yellow) binds ATP and forms a multimer. Along with the HU protein, the DnaA/ATP complex binds to the DNA, encompassing the four 9-mers. In all, this complex covers about 200 bp. HU protein probably induces the bend in the DNA pictured here. (b) Formation of the open complex. The binding of DnaA, along with the bending induced by HU protein, apparently destabilizes the adjacent 13-mer repeats and causes local DNA melting there. This allows the binding of

DnaB protein to the melted region. (c) Formation of the prepriming complex. DnaC binds to the DnaB protein and helps deliver it to the DNA. (d) Priming. Finally, primase (purple) binds to the prepriming complex and converts it to the primosome, which can make primers to initiate DNA replication. Primers are represented by arrows. (Source: Adapted from *DNA Replication*, 2/e, (plate 15) by Arthur Kornberg and Tania Baker.)

## Priming in Eukaryotes

Eukaryotic replication is considerably more complex than the bacterial replication we have just studied. One complicating factor is the much bigger size of eukaryotic genomes. This, coupled with the slower movement of eukaryotic replicating forks, means that each chromosome must have multiple origins. Otherwise, replication would not finish within the time allotted—the S phase of the cell cycle—which can be as short as a few minutes. Because of this multiplicity and other factors, identification of eukaryotic origins of replication has lagged considerably behind similar work in prokaryotes. However, when molecular biologists face a complex problem, they frequently resort to simpler systems such as viruses to give them clues about the viruses' more complex hosts. Scientists followed this strategy to identify the origin of replication in the simple monkey virus SV40 as early as 1972. Let us begin our study of eukaryotic origins of replication there, then move on to origins in yeast.

**The Origin of Replication in SV40** Two research groups, one headed by Norman Salzman, the other by Daniel Nathans, identified the SV40 origin of replication in 1972 and showed that DNA replication proceeded bidirectionally from this origin. Salzman's strategy was to use EcoRI to cleave replicating SV40 DNA molecules at a unique site. (Although this enzyme had only a short time before been discovered and characterized, Salzman knew that SV40 DNA contained only a single EcoRI site.) After cutting the replicating SV40 DNA with EcoRI, Salzman and colleagues visualized the molecules by electron microscopy. They observed only a single replicating bubble, which indicated a single origin of replication. Furthermore, as they followed the growth of this bubble, they found that it grew at both ends, showing that both replicating forks were moving away from the single origin. This analysis revealed that the origin lies 33% of the genome length from the EcoRI site. But which direction from the EcoRI site? Because the SV40 DNA is circular, and these pictures contain no other markers besides the single EcoRI site, we cannot tell. But Nathans used another restriction enzyme (HindII), and his results, combined with these, placed the origin at a site overlapping the SV40 control region, adjacent to the GC boxes and the 72-bp repeat enhancer.

The minimal ori sequence (the ori core) is 64 bp long and includes several essential elements (1) four pentamers (59-GAGGC-39), which are the binding site for large T antigen, the major product of the viral early region; (2) a 15-bp palindrome, which is the earliest region melted during DNA replication; and (3) a 17-bp region consisting only of A–T pairs, which probably facilitates melting of the nearby palindrome region.

Other elements surrounding the ori core also participate in initiation. These include two additional large T antigen-binding sites, and the GC boxes to the left of the ori core. The GC boxes provide about a 10-fold stimulation of initiation of replication. If the number of GC boxes is reduced, or if they are moved only 180 bp away from ori, this stimulation is reduced or eliminated. This effect is somewhat akin to the participation of RNA polymerase in initiation at oriC in *E. coli*. One difference: At the SV40 ori, no transcription need occur; binding of the transcription factor Sp1 to the GC boxes is sufficient to stimulate initiation of replication.

Once large T antigen binds at the SV40 ori, its DNA helicase activity unwinds the DNA and prepares the way for primer synthesis. Just as in bacteria, eukaryotic primers are made of RNA. The primase in eukaryotic cells associates with DNA polymerase  $\alpha$ , and this also serves as the primase for SV40 replication.



**Figure 21.2** Location of the SV40 *ori* in the transcription control region. The core *ori* sequence (green) encompasses part of the early region TATA box and the cluster of early transcription initiation sites. Pink arrows denote bidirectional replication away from the replication initiation site. Black arrows denote transcription initiation sites.

The Origin of Replication in Yeast So far, yeast has provided most of our information about eukaryotic origins of replication. This is not surprising, because yeasts are among the simplest eukaryotes, and they lend themselves well to genetic analysis. As a result, yeast genetics are well understood. As early as 1979, C.L. Hsiao and J. Carbon discovered a yeast DNA sequence that could replicate independently of the yeast chromosomes, suggesting that it contains an origin of replication. This DNA fragment contained the yeast ARG41 gene. Cloned into a plasmid, it transformed *arg42* yeast cells to ARG41, as demonstrated by their growth on medium lacking arginine. Any yeast cells that grew must have incorporated the ARG41 gene of the plasmid and, furthermore, must be propagating that gene somehow. One way to propagate the gene would be by incorporating it into the host chromosomes by recombination, but that was known to occur with a low frequency—about  $10^{-26}$ – $10^{-27}$ . Hsiao and Carbon obtained ARG41 cells at a much higher frequency—about  $10^{-4}$ . Furthermore, shuttling the plasmid back and forth between yeast and *E. coli* caused no change in the plasmid structure, whereas recombination with the yeast genome would have changed it noticeably. Thus, these investigators concluded that the yeast DNA fragment they had cloned in the plasmid probably contained an origin of replication. Also in 1979, R.W. Davis and colleagues performed a similar study with a plasmid containing a yeast DNA fragment that converted *trp2* yeast cells to TRP1. They named the 850-bp yeast fragment autonomously replicating sequence 1, or ARS1. Although these early studies were suggestive, they failed to establish that DNA replication actually begins in the ARS sequences. To demonstrate that ARS1 really does have this key characteristic of an origin of replication, Bonita Brewer and Walton Fangman used two-dimensional electrophoresis to detect the site of replication initiation in a plasmid bearing ARS1. This technique depends on the fact that circular and branched DNAs migrate more slowly than linear DNAs of the same size during gel electrophoresis, especially at high voltage or high agarose concentration.

Brewer and Fangman prepared a yeast plasmid bearing ARS1 as the only origin of replication. They allowed this plasmid to replicate in synchronized yeast cells and then isolated replication intermediates (RIs). They linearized these RIs with a restriction endonuclease, then electrophoresed them in the first dimension under conditions (low voltage and low agarose concentration) that separate DNA molecules roughly according to their sizes. Then they electrophoresed the DNAs in the second dimension using higher voltage and agarose concentrations that cause retardation of branched and circular molecules. Finally, they Southern blotted the DNAs in the gel and probed the blot with a labeled plasmid-specific DNA.

Figure 21.3 shows an idealized version of the behavior of various branched and circular RIs of a hypothetical 1-kb fragment. Simple Y's (panel a) begin as essentially linear 1-kb fragments with a tiny Y at their right ends; these would behave almost like linear 1-kb fragments. As the fork moves from right to left, the Y grows larger and the mobility of the fragment in the second (vertical) dimension slows. Then, as the Y grows even larger, the fragment begins to look more and more like a linear 2-kb fragment, with just a short stem on the Y. This is represented by the horizontal linear form with a short

vertical stem in panel (a). Because these forms resemble linear shapes more and more as the fork moves, their mobility increases correspondingly, until the fork has nearly reached the end of the fragment. At this point, they have a shape and mobility that is almost like a true linear 2-kb fragment. This behavior gives rise to an arc-shaped pattern, where the apex of the

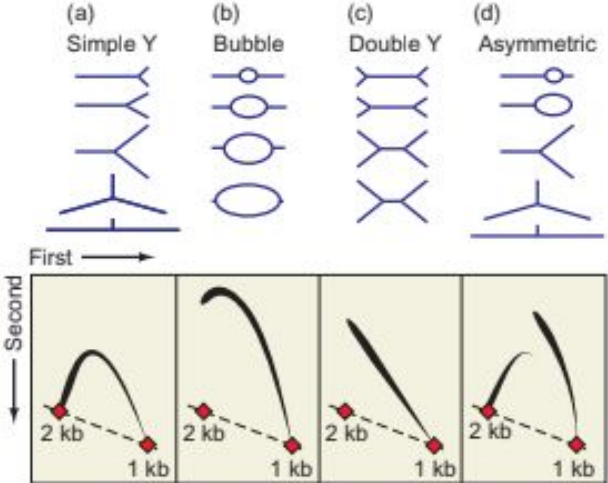


**Figure 21.3** Theoretical behaviors of various types of replication intermediates on two-dimensional gel electrophoresis. The top parts of panels a–d are cartoons showing the shapes of growing simple Y's, bubbles, double Y's, and asymmetric bubbles that convert to simple Y's as replication progresses. The bottom parts of each panel are cartoons that depict the expected deviation of the changing mobilities of each type of growing RI from the mobilities of linear forms growing progressively from 1 to 2 kb (dashed lines). (Source: Adapted



arc corresponds to a Y that is half-replicated, at which point it is least like a linear molecule.

Figure 21.3b shows what to expect for a bubble-shaped fragment. Again, we begin with a 1-kb linear fragment, but this time with a tiny bubble right in the middle. As the bubble grows larger, the mobility of the fragment slows more and more, yielding the arc shown at the bottom of the panel. Panel (c) shows the behavior of a double Y, where the RI becomes progressively more branched as the two forks approach the center of the fragment. Accordingly, the mobility of the RI decreases almost linearly. Finally, panel (d) shows what happens to a bubble that is asymmetrically placed in the fragment. It begins as a bubble, but then, when one fork passes the restriction site at the right end of the fragment, it converts to a Y. The mobilities of the RIs reflect this discontinuity: The curve begins like that of a bubble, then abruptly changes to that of a Y, with an obvious discontinuity showing exactly when the fork passed the restriction site and converted the bubble to a Y.

This kind of behavior is especially valuable in mapping the origin of replication. In panel (d), for example, we can see that the discontinuity occurs in the middle of the curve, when the mobility in the first dimension was that of a 1.5-kb fragment. This tells us that the arms of the Y are each 500 bp long. Assuming that the two forks are moving at an equal rate, we can conclude that the origin of replication was 250 bp from the right end of the fragment. Now let us see how this works in practice. Brewer and Fangman chose restriction enzymes that would cleave the plasmid with its ARS1 just once, but in locations that would be especially informative if the origin of replication really lies within ARS1. Figure 21.4 shows the locations of the two restriction sites, at top, and the experimental results, at bottom. The first thing to notice about the autoradiographs is that they are simple and correspond to the patterns we have seen in Figure 21.3. This means that there is a single origin of replication; otherwise, there would have been a mixture of different kinds of RIs, and the results would have been more complex.

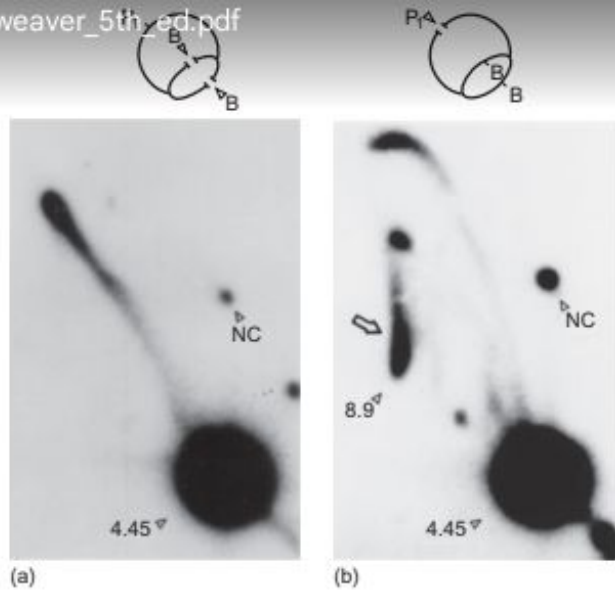
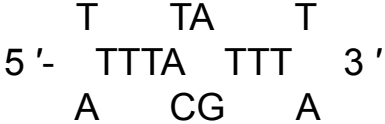


**Figure 21.4 Locating the origin of replication in ARS1.** (a) Results of cleaving 2- $\mu$ m plasmid with *Bgl*III. Top: cartoon showing the shape expected when an RI is cut with *Bgl*III, assuming the origin lies adjacent to the *Bgl*III site within ARS1. The bubble contains DNA that has already replicated, so there are two copies of the *Bgl*III site (arrowheads labeled B), both of which are cut to yield the double-Y intermediate depicted. Bottom: experimental results showing the straight curve expected of double-Y intermediates. (b) Results of cleaving the plasmid with *Pvu*II. Top: cartoon showing the shape expected when an RI is cut with *Pvu*II, assuming the origin lies almost across the circle from the *Pvu*II site within ARS1. Bottom: experimental results showing the rising arc, with a discontinuity near the end. This is what we expect for a bubble-shaped RI that converts to a nearly linear Y as one of the replication forks passes a *Pvu*II site. Both of these results confirm the expectations for an origin of replication within ARS1. NC denotes nicked circles. The large open arrow points to large Y's or very asymmetric double Y's that result when a replicating fork passes a *Pvu*II site. Numbers refer to sizes in kb. (Source: Brewer, B.J. and W.L. Fangman,

The predicted origin within ARS1 lies adjacent to a *Bgl*III site (B, in panel a). Thus, if the RI is cleaved with this enzyme, it should yield double-Y RIs. Indeed, as we see in the lower part of panel (a), the autoradiograph is nearly linear—just as we expect for a double-Y RI. Panel (b) shows that a *Pvu*II site (P) lies almost halfway around the plasmid from the predicted origin. Therefore, cleaving with *Pvu*II should yield the bubble-shaped RI shown at the top of panel (b). The autoradiograph at the bottom of panel (b) shows that Brewer and Fangman observed the discontinuity expected for a bubble-shaped RI that converts at the very end to a very large single Y, as one fork reaches the *Pvu*II site, then perhaps to a very asymmetric double Y as the fork passes that site. Both of these results place the origin of replication adjacent to the *Bgl*III site, just where we expect it if ARS1 contains the origin.

York Marahrens and Bruce Stillman performed linker scanning experiments to define the important regions within ARS1. They constructed a plasmid very similar to the one used by Brewer and Fangman, containing (1) ARS1 in a 185-bp DNA sequence; (2) a yeast centromere; and (3) a selectable marker—URA3—which confers on *ura3-52* yeast cells the ability to grow in uracil-free medium. Then they performed linker scanning (Chapter 10) by systematically substituting an 8-bp *Xho*I linker for the normal DNA at sites spanning the ARS1 region. They transformed yeast cells with each of the linker scanning mutants and selected for transformed cells with uracil-free medium. Some of the transformants containing mutant ARS1 sequences grew more slowly than those containing wild-type ARS1 sequences. Because the centromere in each plasmid ensured proper segregation of the plasmid, the most likely explanation for poor growth was poor replication due to mutation of ARS1.

To check this hypothesis, Marahrens and Stillman grew all the transformants in a nonselective medium containing uracil for 14 generations, then challenged them again with a uracil-free medium to see which ones had not maintained the plasmid well. The mutations in these unstable plasmids presumably interfered with ARS1 function. Figure 21.5 shows the results. Four regions of ARS1 appear to be important. These were named A, B1, B2, and B3 in order of decreasing effect on plasmid stability. Element A is 15 bp long, and contains an 11-bp ARS consensus sequence:



When it was mutated, all ARS1 activity was lost. The other regions had a less drastic effect, especially in selective medium. However, mutations in B3 had an apparent effect on the bending of the plasmid, as assayed by gel electrophoresis. The stained gel below the bar graph shows increased electrophoretic mobility of the mutants in the B3 region. Marahrens and Stillman interpreted this as altered bending of the ARS1 in the presence of the replicating machinery.

The existence of four important regions within ARS1 raises the question whether these are also sufficient for ARS function. To find out, Marahrens and Stillman constructed a synthetic ARS1 with wild-type versions of all four regions, spaced just as in the wild-type ARS1, but with random sequences in between. A plasmid bearing this synthetic ARS1 was almost as stable under nonselective conditions as one bearing a wild-type ARS1. Thus, the four DNA elements defined by linker scanning are sufficient for ARS1 activity. Finally, these workers replaced the wild-type 15-bp region A with the 11-bp ARS consensus sequence. This reduced plasmid stability dramatically, suggesting that the other 4 bp in region A are also important for ARS activity.

## **Elongation**

Once a primer is in place, real DNA synthesis (elongation) can begin. We have already identified the pol III holoenzyme as the enzyme that carries out elongation in *E. coli*, and DNA polymerases  $\delta$  and  $\epsilon$  as the enzymes that elongate the lagging and leading strands, respectively, in eukaryotes. The *E. coli* system is especially well characterized, and the data point to an elegant method of coordinating the synthesis of lagging and leading strands in a way that keeps the pol III holoenzyme engaged with the template so replication can be highly processive, and therefore very rapid. Let us focus on this *E. coli* elongation mechanism, beginning with a discussion of the speed of elongation.

### **Speed of Replication**

Minsen Mok and Kenneth Mariani performed one of the studies that measured the rate of fork movement in vitro with the pol III holoenzyme. They created a synthetic circular template for rolling circle replication, illustrated in Figure 21.6. This template contained a  $^{32}\text{P}$ -labeled, tailed, full-length strand with a free 3'-hydroxyl group for priming. Mok and Mariani incubated this template with either holoenzyme plus preprimosomal proteins and SSB, or plus DnaB helicase alone. At 10-sec intervals, they removed the labeled product DNAs and measured their lengths by electrophoresis. Panels (a) and (b) in Figure 21.7 depict the results with the two reactions, and Figure 21.7c shows plots of the rates of fork movement with the two reactions. Both plots yielded rates of 730 nt/sec, close to the in vivo rate of almost 1000 nt/sec.

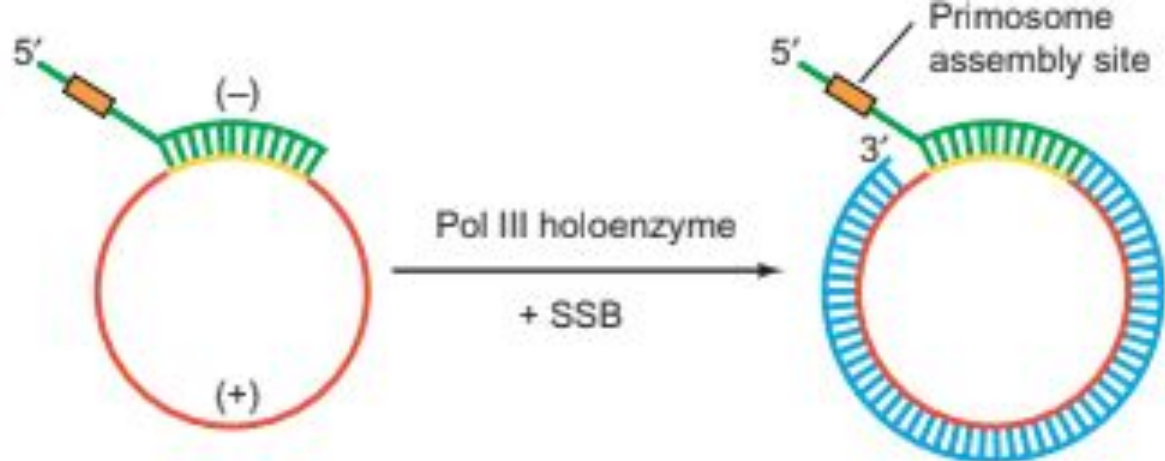


**Figure 21.6 Synthesis of template used to measure fork velocity *in vitro*.** Mok and Marians started with the 6702-nt positive strand (red) from the f1 phage and annealed it to a primer (green) that hybridized over a 282-nt region (yellow). This primer contained a primosome assembly site (orange). Mok and Marians elongated the primer with pol III holoenzyme and single-strand binding protein (SSB) to create the negative strand (blue). The product was a double-stranded template for multiple rounds of rolling circle replication, in which the free 3'-end could serve as the primer. (Source: Adapted from Mok, M. and K.J. Marians, *The Escherichia coli preprimosome and DNA B helicase can form replication forks that move at the same rate. Journal of Biological Chemistry* 262:16645, 1987.)

Furthermore, the elongation in these reactions with holoenzyme was highly processive. As we have mentioned, processivity is the ability of the enzyme to stick to its job a long time without falling off and having to reinitiate. This is essential because reinitiation is a time-consuming process, and little time can be wasted in DNA replication. To measure processivity, Mok and Marians performed the same elongation assay as described in Figure 21.7, but included either of two substances that would prevent reinitiation if the holoenzyme dissociated from the template. These substances were a competing DNA, poly(dA), and an antibody directed against the  $\beta$ -subunit of the holoenzyme. In the presence of either of these competitors, the elongation rate was just as fast as in their absence, indicating that the holoenzyme did not dissociate from the template throughout the process of elongation of the primer by at least 30 kb. Thus, the holoenzyme is highly processive in vitro, just as it is in vivo.

### **The Pol III Holoenzyme and Processivity of Replication**

The pol III core by itself is a very poor polymerase. It puts together about 10 nt and then falls off the template. Then it has to spend about a minute reassociating with the template and the nascent DNA strand. This contrasts sharply with the situation in the cell, where the replicating fork moves at the rate of almost 1000 nt/sec. Obviously, something important is missing from the core.

That “something” is an agent that confers processivity on the holoenzyme, allowing it to remain engaged with the template while polymerizing at least 50,000 nt before stopping—quite a contrast to the 10 nt polymerized by the core before it stops. Why such a drastic difference? The holoenzyme owes its processivity to a “sliding clamp” that holds the enzyme on the template for a long time. The  $\beta$ -subunit of the holoenzyme performs this sliding clamp function, but it cannot associate by itself with the preinitiation complex (core plus DNA template). It needs a clamp loader to help it join the complex, and a group of subunits called the  $\gamma$  complex provides this help. The  $\gamma$  complex includes the  $\gamma$ -,  $\delta$ -,  $\delta'$ -,  $\chi$ -, and  $\epsilon$ -subunits. In this section, we will examine the activities of the  $\beta$  clamp and the clamp loader.

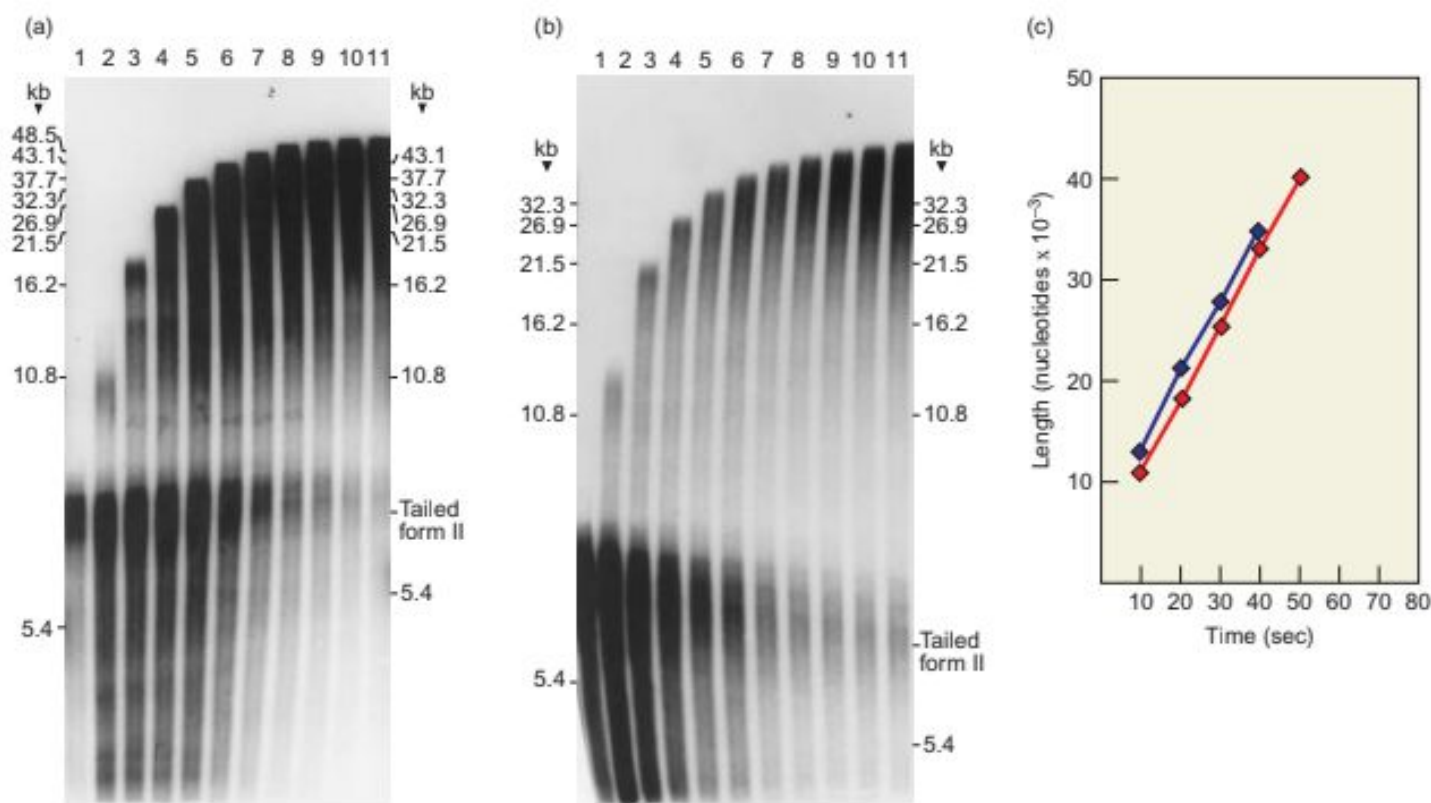


**Figure 21.7 Measuring the rate of fork movement in vitro.** Mok and Marians labeled the negative strand of the tailed template in Figure 21.6 and used it in *in vitro* reactions with pol III holoenzyme plus: **(a)** the preprimosomal proteins (the primosomal proteins minus DnaG); or **(b)** DnaB alone. They took samples from the reactions at 10-sec intervals, beginning with lanes 1 at zero time and lanes 2 at 10 sec, electrophoresed them, and then autoradiographed the gel. Recall that electrophoretic mobilities are a log function, not a linear

function, of mass. The numbers on the left in each panel are marker sizes, not the sizes of DNA products. Panel **(c)** shows a plot of the results from the first five and four time points from panels **(a)** (red) and **(b)** (blue), respectively. (Source: Mok M. and K.J. Marians, *The Escherichia coli* preprimosome and DNA B helicase can form replication forks that move at the same rate. *Journal of Biological Chemistry* 262 no. 34 (5 Dec 1987) f. 6a-b, p. 16650. Copyright © American Society for Biochemistry and Molecular Biology.)



## The b clamp

One way we can imagine the b-subunit conferring processivity on the pol III core is by binding both the core complex and DNA. That way, it would tie the core to the DNA and keep it there—hence the term b clamp. In the course of probing this possibility, Mike O'Donnell and colleagues demonstrated direct interaction between the b- and  $\epsilon$ -subunits. They mixed various combinations of subunits, then separated subunit complexes from individual subunits by gel filtration. They detected subunits by gel electrophoresis, and activity by adding the missing subunits and measuring DNA synthesis. Figure 21.8 depicts the electrophoresis results. It is clear that a and  $\epsilon$  bind to each other, as we would expect, because they are both part of the core. Furthermore, a,  $\epsilon$ , and b form a complex, but which subunit does b bind to, a or  $\epsilon$ ? Panels (d) and (e) show the answer: b binds to a alone (both subunits peak in fractions 60–64), but not to  $\epsilon$  alone (b peaks in fractions 68–70, whereas  $\epsilon$  peaks in fractions 76–78). Thus, a is the core subunit to which b binds.

This scheme demands that b be able to slide along the DNA as a and  $\epsilon$  together replicate it. This in turn suggests that the b clamp would remain bound to a circular DNA, but could slide right off the ends of a linear DNA. To test this possibility, O'Donnell and colleagues performed the experiment reported in Figure 21.9. The general strategy of this experiment was to load 3 H-labeled b dimers onto circular, double-stranded phage DNA with the help of the g complex, then to treat the DNA in various ways to see if the b dimers could dissociate from the DNA. The assay for b-binding to DNA was gel filtration. Independent b dimers emerge from a gel filtration column much later than they do when they are bound to DNA.

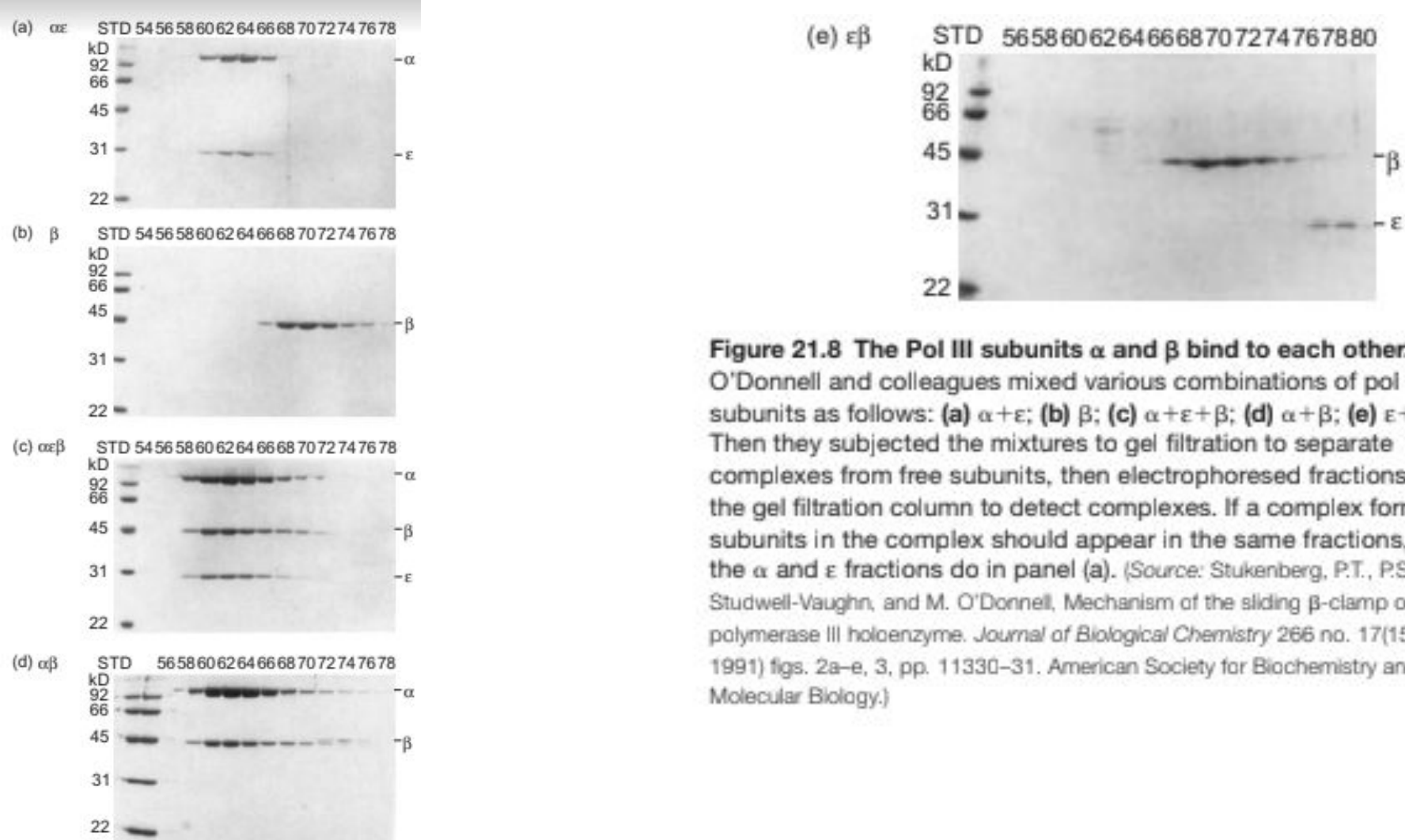


**Figure 21.8 The Pol III subunits  $\alpha$  and  $\beta$  bind to each other.** O'Donnell and colleagues mixed various combinations of pol III subunits as follows: **(a)**  $\alpha + \epsilon$ ; **(b)**  $\beta$ ; **(c)**  $\alpha + \epsilon + \beta$ ; **(d)**  $\alpha + \beta$ ; **(e)**  $\epsilon + \beta$ . Then they subjected the mixtures to gel filtration to separate complexes from free subunits, then electrophoresed fractions from the gel filtration column to detect complexes. If a complex formed, the subunits in the complex should appear in the same fractions, as the  $\alpha$  and  $\epsilon$  fractions do in panel (a). (Source: Stukenberg, P.T., P.S. Studwell-Vaughn, and M. O'Donnell, Mechanism of the sliding  $\beta$ -clamp of DNA polymerase III holoenzyme. *Journal of Biological Chemistry* 266 no. 17(15 June 1991) figs. 2a-e, 3, pp. 11330-31. American Society for Biochemistry and Molecular Biology.)

In panel (a), the DNA was treated with SmaI to linearize the DNA, then examined to see whether the b clamp had slid off. It remained bound to circular DNA, but had dissociated from linearized DNA, apparently by sliding off the ends. Panel (b) demonstrates that the nick in the circular DNA is not what caused retention of the b dimer, because the nick can be removed with DNA ligase, and the b dimer remains bound to the DNA. The inset shows electrophoretic evidence that the ligase really did remove the nick because the nicked form disappeared and the closed circular form was enhanced. Panel (c) shows that adding more b-subunit to the loading reaction increased the number of b dimers bound to the circular DNA. In fact, more than 20 molecules of b-subunit could be bound per molecule of circular DNA. This is what we would expect if many holoenzymes can replicate the DNA in tandem.

If the b dimers are lost from linear DNA by sliding off the ends, one ought to be able to prevent their loss by binding other proteins to the ends of the DNA. O'Donnell's group did this in experiments, not shown here, by binding two different proteins to the ends of the DNA and demonstrating that the b dimers no longer fell off. Indeed, single-stranded tails at the ends of the DNA, even without protein attached, proved to be an impediment to the b dimers sliding off.

Mike O'Donnell and John Kuriyan used x-ray crystallography to study the structure of the b clamp. The pictures they produced provided a perfect rationale for the ability of the b clamp to remain bound to a circular DNA but not to a linear one: The b dimer forms a ring that can fit around the DNA. Thus, like a ring on a string, it can readily fall off if the string is linear, but not if the string is circular. Figure 21.10 is one of the models O'Donnell and Kuriyan constructed; it shows the ring structure of the b dimer, with a scale model of B-form DNA placed in the middle.

In 2008, O'Donnell and colleagues obtained the structure of a co-crystal of a b dimer bound to a primed DNA template. Figure 21.11 shows this crystal structure, which demonstrates that the b clamp really does encircle the DNA, as the model in Figure 21.10 predicted. However, this newer structure shows the actual geometry of DNA within the b clamp, and it contains a bit of a surprise: Instead of extending straight through the b clamp, like a finger through a ring, the DNA is tilted about 22 degrees with respect to a horizontal line through the clamp. Furthermore, the DNA contacts the side chains of two amino acids, arginine 24 and glutamine 149, both of which lie on the C-terminal face of the b clamp. This protein–DNA contact probably contributes to the tilt of the DNA with respect to the b dimer.

As mentioned in Chapter 20, eukaryotes also have a processivity factor called PCNA, which performs the same function as the bacterial b clamp. The primary structure of PCNA bears no apparent similarity to that of the b clamp, and the eukaryotic protein is only two-thirds the size of its prokaryotic counterpart. Nevertheless, x-ray crystallography performed by Kuriyan and his colleagues demonstrated that yeast PCNA forms a trimer with a structure arrestingly similar to that of the b clamp dimer: a ring that can encircle a DNA molecule, as shown in Figure 21.12.

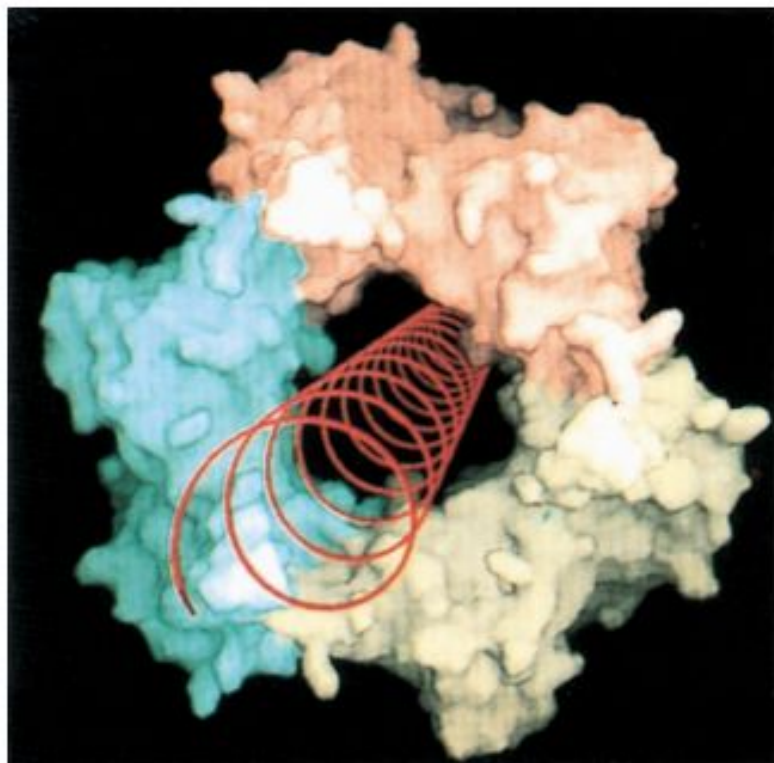


**Figure 21.12 Model of PCNA–DNA complex.** Each of the monomers of the PCNA trimer is represented by a different pastel color. The shape of the trimer is based on x-ray crystallography analysis. The red helix represents the probable location of the sugar–phosphate backbone of a DNA associated with the PCNA trimer. (Source: Krishna, T.S.R., X.-P. Kong, S. Gary, P.M. Burgers, and J. Kuriyan, Crystal structure of the eukaryotic DNA polymerase processivity factor PCNA. *Cell* 79 (30 Dec 1994) t. 3b, p. 1236. Reprinted by permission of Elsevier Science.)

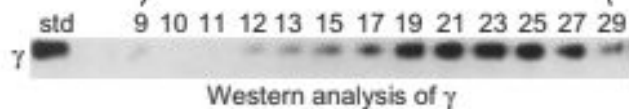
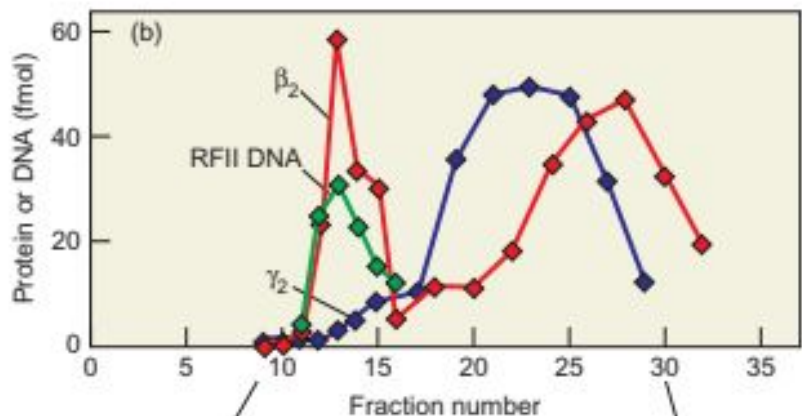
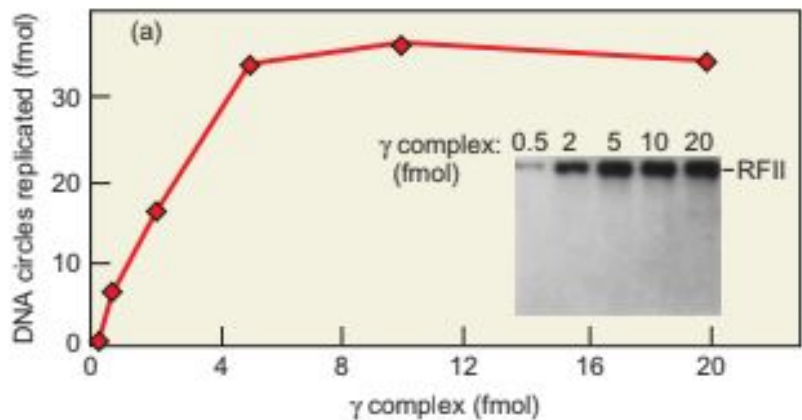


**Figure 21.13 Involvement of  $\beta$  and  $\gamma$  complex in processivity.**

**(a)** The  $\gamma$  complex acts catalytically in forming a processive polymerase. O'Donnell and coworkers added increasing amounts of  $\gamma$  complex (indicated on the x axis) to a primed M13 phage DNA template coated with SSB, along with  $\alpha\epsilon$  core, and the  $\beta$ -subunit of pol III holoenzyme. Then they allowed a 20-sec pulse of DNA synthesis in the presence of  $[\alpha\text{-}^{32}\text{P}]\text{ATP}$  to label the DNA product. They determined the radioactivity of part of each reaction and converted this to fmol of DNA circles replicated. To check for full circle replication, they subjected another part of each reaction to gel electrophoresis. The inset shows the result: The great majority of each product is full-circle size (RFII). **(b)** The  $\beta$ -subunit, but not the  $\gamma$  complex associates with DNA in the preinitiation complex. O'Donnell and colleagues added  $^3\text{H}$ -labeled  $\beta$ -subunit and unlabeled  $\gamma$  complex to primed DNA coated with SSB, along with ATP to form a preinitiation complex. Then they subjected the mixture to gel filtration to separate preinitiation complexes from free proteins. They detected the  $\beta$ -subunit in each fraction by radioactivity, and the  $\gamma$  complex by Western blotting, with an anti- $\gamma$  antibody as probe (bottom). The plot shows that the  $\beta$ -subunit (as dimers) bound to the DNA in the preinitiation complex, but the  $\gamma$  complex did not. (Source: Stukenberg, P.T., P.S. Studwell-Vaughn, and M. O'Donnell, Mechanism of the sliding  $[\beta]$ -clamp of DNA polymerase III holoenzyme. *Journal of Biological Chemistry* 266 (15 June 1991) f. 1a&c, p. 11329. American Society for Biochemistry and Molecular Biology.)

## The Clamp Loader

O'Donnell and his colleagues demonstrated the function of the clamp loader in an experiment presented in Figure 21.13. These scientists used the  $\alpha$ - and  $\epsilon$ -subunits instead of the whole core, because the  $\omega$ -subunit was not essential in their *in vitro* experiments. As template, they used a single-stranded M13 phage DNA annealed to a primer. They knew that highly processive holoenzyme could replicate this DNA in about 15 sec but that the  $\alpha\epsilon$  core could not give a detectable amount of replication in that time. Thus, they reasoned that a 20-sec pulse of replication would allow all processive polymerase molecules the chance to complete one cycle of replication, and therefore the number of DNA circles replicated would equal the number of processive polymerases. Figure 21.13a shows that each femtomole (fmol, or  $10^{-15}$  mol) of  $\gamma$  complex resulted in about 10 fmol of circles replicated in the presence of  $\alpha\epsilon$  core and  $\beta$ -subunit. Thus, the  $\gamma$  complex acts catalytically: One molecule of  $\gamma$  complex can sponsor the creation of many molecules of processive polymerase. The inset in this figure shows the results of gel electrophoresis of the replication products. As expected of processive replication, they are all full-length circles. This experiment suggested that the  $\gamma$  complex itself is not the agent that provides processivity. Instead, the  $\gamma$  complex could act catalytically to add something else to the core polymerase that makes it processive. Because  $\beta$  was the only other polymerase subunit in this experiment, it is the likely processivity-determining factor. To confirm this, O'Donnell and colleagues mixed the DNA template with 3H-labeled  $\beta$ -subunit and unlabeled  $\gamma$  complex to form preinitiation complexes, then subjected these complexes to gel filtration to separate the complexes from free proteins. They detected the preinitiation complexes by adding  $\alpha\epsilon$  to each fraction and assaying for labeled double-stranded circles formed (RFII, green). Figure 21.13b demonstrates that only a trace of  $\gamma$  complex (blue) remained associated with the DNA, but a significant fraction of the labeled  $\beta$ -subunit (red) remained with the DNA. (The unlabeled  $\gamma$  complex was detected with a Western blot using an anti- $\gamma$  antibody, as shown at the bottom of the figure.) It is important to note that, even though the  $\gamma$  complex does not remain bound to the DNA, it plays a vital role in processivity by loading the  $\beta$ -subunit onto the DNA.

This experiment also allowed O'Donnell and colleagues to estimate the stoichiometry of the b-subunit in the pre-initiation complex. They compared the fmol of b with the fmol of complex, as measured by the fmol of double-stranded circles produced. This analysis yielded a value of about 2.8 b-subunits/complex, which would be close to one b dimer/complex, in accord with other studies that suggested that b acts as a dimer.

Implicit in the discussion so far is the fact that ATP is required to load the b clamp onto the template. Peter Burgers and Kornberg demonstrated the necessity for ATP (or dATP) with an assay that did not require dATP for replication. The template in this case was poly(dA) primed with oligo(dT). The results showed that ATP or dATP is required for high-activity elongation of the oligo(dT) primer with dTMP.

How does the clamp loader pry apart the b dimer to allow it to clamp around DNA? O'Donnell, Kuriyan, and colleagues have determined the crystal structures of two complexes that give strong hints about how the clamp loader works. One of these was the structure of the active part of the clamp loader (a gdd9 complex). The other was the structure of a modified b–d complex composed of: a monomer of a mutant form of b (bmt) that is unable to dimerize; and a fragment of d that can interact with b.

The crystal structure of this modified b–d complex showed that the interaction between d and a b monomer would be expected to weaken the binding at one interface between the two b monomers in two ways. First, d acts as a molecular wrench by inducing a conformational change in the b dimer interface such that it no longer dimerizes as readily. Second, d changes the curvature of one b-subunit so that it no longer naturally forms a ring with the other subunit. Instead, it forms a structure that resembles a lock washer. Figure 21.14 illustrates these concepts. Notice that d binds to only one b monomer in the b clamp (there is only one d per b dimer in the pol III holoenzyme), so it weakens only one dimer interface, and therefore forces ring opening. If d bound to both b monomers, it would presumably cause the two monomers to dissociate entirely.



These structural studies and earlier biochemical studies, some of which we will discuss later in this chapter, showed that d on its own binds readily to a b monomer, but that d in the context of the clamp loader complex cannot bind to the b clamp unless ATP is present. So the role of ATP appears to be to change the shape of the clamp loader to expose the d-subunit so it can bind to one of the b-subunits and pry open the b clamp.

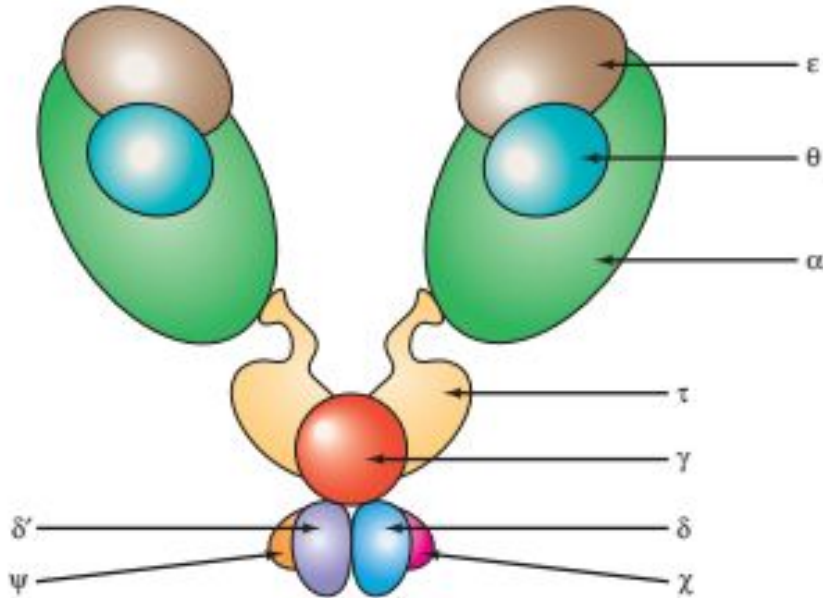
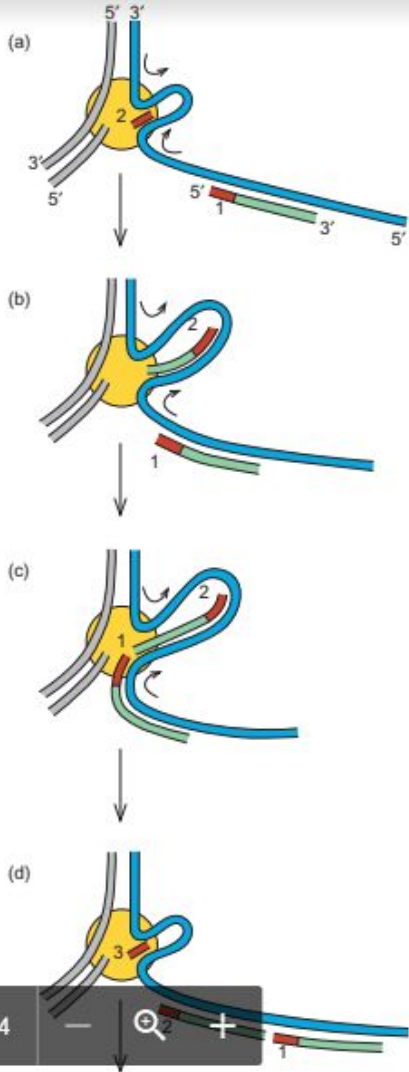


**Figure 21.15 Model of the Pol III\* subassembly.** Note that two cores and two  $\tau$ -subunits are present, but only one  $\gamma$ -complex ( $\gamma$ ,  $\delta$ ,  $\delta'$ ,  $\chi$ , and  $\psi$ ). The  $\tau$ -subunits are joined to the cores by their flexible C-terminal domains.

**Lagging Strand Synthesis** Structural studies on pol III\* (holoenzyme minus the b clamp) have shown that the enzyme consists of two core polymerases, linked through a dimer of the  $\tau$ -subunit to a clamp loader, as illustrated in Figure 21.15. The following reasoning suggests that the  $\tau$ -subunit serves as a dimerizing agent for the core enzyme: The  $\alpha$ -subunit is a monomer in its native state, but  $\tau$  is a dimer. Furthermore,  $\tau$  binds directly to  $\alpha$ , so  $\alpha$  is automatically dimerized by binding to the two  $\tau$ -subunits. In turn,  $\epsilon$  is dimerized by binding to the two  $\alpha$ -subunits, and  $\gamma$  is dimerized by binding to the two  $\epsilon$ -subunits. The two  $\tau$ -subunits are products of the same gene that produces the  $\gamma$ -subunit. However, the  $\gamma$ -subunit lacks a 24-kDa domain ( $\tau_c$ ) at the C-terminus of the  $\tau$ -subunits because of a programmed frameshift during translation. The two  $\tau_c$  domains provide flexible linkers between the core polymerases and the  $\gamma$  complex.



The fact that the holoenzyme contains two core polymerases fits very nicely with the fact that two DNA strands need to be replicated. This leads directly to the suggestion that each of the core polymerases replicates one of the strands as the holoenzyme follows the moving fork. This is straightforward for the core polymerase replicating the leading strand, as that replication moves in the same direction as the fork. But it is more complicated for the core polymerase replicating the lagging strand, because that replication occurs in the direction opposite to that of the moving fork. This means that the lagging strand must form a loop, as pictured in Figure 21.16. Because this loop extends as an Okazaki fragment grows and then retracts to begin synthesis of a new Okazaki fragment, the loop resembles the slide of a trombone, and this model is sometimes called the “trombone model.”

**Figure 21.16 A model for simultaneous synthesis of both DNA strands.** (a) The lagging template strand (blue) has formed a loop through the replisome (gold), and a new primer, labeled 2 (red), has been formed by the primase. A previously synthesized Okazaki fragment (green, with red primer labeled 1) is also visible. The leading strand template and its progeny strand are shown at left (gray), but the growth of the leading strand is not considered here. (b) The lagging strand template has formed a bigger loop by feeding through the replisome from the top and bottom, as shown by the arrows. The motion of the lower part of the loop (lower arrow) allows the second Okazaki fragment to be elongated. (c) Further elongation of the second Okazaki fragment brings its end to a position adjacent to the primer of the first Okazaki fragment. (d) The replisome releases the loop, which permits the primase to form a new primer (number 3). The process can now begin anew.

Because discontinuous synthesis of the lagging strand must involve repeated dissociation and reassociation of the core polymerase from the template, this model raises two important questions: First, how can discontinuous synthesis of the lagging strand possibly keep up with continuous (or perhaps discontinuous) synthesis of the leading strand? If the pol III core really dissociated completely from the template after making each Okazaki fragment of the lagging strand, it would take a long time to reassociate and would fall hopelessly behind the leading strand. This would be true even if the leading strand replicated discontinuously, because no dissociation and reassociation of the pol III core is necessary in synthesizing the leading strand. A second, related question is this: How is repeated dissociation and reassociation of the pol III core from the template compatible with the highly processive nature of DNA replication? After all, the  $\beta$  clamp is essential for processive replication, but once it clamps onto the DNA, how can the core polymerase dissociate every 1–2 kb as it finishes one Okazaki fragment and jumps forward to begin elongating the next?

The answer to the first question seems to be that the pol III core making the lagging strand does not really dissociate completely from the template. It remains tethered to it by its association with the core that is making the leading strand. Thus, it can release its grip on its template strand without straying far from the DNA. This enables it to find the next primer and reassociate with its template within a fraction of a second, instead of the many seconds that would be required if it completely left the DNA.

The second question requires us to look more carefully at the way the  $\beta$  clamp interacts with the clamp loader and with the core polymerase. We will see that these two proteins compete for the same binding site on the  $\beta$  clamp, and that the relative affinities of the clamp for one or the other of them shifts back and forth to allow dissociation and reassociation of the core from the DNA. We will also see that the clamp loader can act as a clamp unloader to facilitate this cycling process.

Theory predicts that the pol III\* synthesizing the lagging strand must dissociate from one b clamp as it finishes one Okazaki fragment and reassociate with another b clamp to begin making the next Okazaki fragment. But does dissociation of pol III\* from its b clamp actually occur? To find out, O'Donnell and his colleagues prepared a primed M13 phage template (M13mp18) and loaded a b clamp and pol III\* onto it. Then they added two more primed phage DNA templates, one (M13Gori) preloaded with a b clamp and the other (fX174) lacking a b clamp. Then they incubated the templates together under replication conditions long enough for the original template and secondary template to be replicated. They knew they would see replicated M13mp18 DNA, but the interesting question is this: Which secondary template will be replicated, the one with, or the one without, the b clamp? Figure 21.17 (lanes 1–4) demonstrates that replication occurred preferentially on the M13Gori template—the one with the b clamp. What if they put the b clamp on the other template instead? Lanes 5–8 show that in that case, the other template (fX174) was preferentially replicated. If the pol III\* kept its original b clamp, it could have begun replicating either secondary template, regardless of which was preloaded with a b clamp. Thus, the results of this experiment imply that dissociation of pol III\* from the template, and its b clamp, really does happen, and the enzyme can bind to another template (or another part of the same template), if another b clamp is present. To check this conclusion, these workers labeled the b clamp with  $^{32}\text{P}$  by phosphorylating it with  $[\text{g}^{32}\text{P}]\text{ATP}$ , then labeled pol III\* with  $^3\text{H}$  in either the  $\alpha$ - or  $\tau$ -subunits, or in the  $\gamma$  complex. Then they allowed these labeled complexes to either idle on a gapped template in the presence of only dGTP and dCTP or to fill in the whole gap with all four dNTPs and thus terminate. Finally, they subjected the reaction mixtures to gel filtration and determined whether the two labels had separated. When the polymerase merely idled, the labeled b clamp and pol III\* stayed together on the DNA template. By contrast, when termination occurred, the pol III\* separated from its b clamp, leaving it behind on the DNA. O'Donnell and coworkers observed the same behavior regardless of which subunit of pol III\* was labeled, so this whole entity, not just the core enzyme, must separate from the b clamp and DNA template upon termination of replication.

The *E. coli* genome is 4.6 Mb long, and its lagging strand, at least, is replicated in Okazaki fragments only 1–2 kb long. This means that over 2000 priming events are required on each template, so at least 2000  $\beta$  clamps are needed. Because an *E. coli* cell holds only about 300  $\beta$  dimers, the supply of  $\beta$  clamps would be rapidly exhausted if they could not recycle somehow. This would require that they dissociate from the DNA template. Does this happen? To find out, O'Donnell and colleagues assembled several  $\beta$  clamps onto a gapped template, then removed all other protein by gel filtration. Then they added pol III\* and reran the gel filtration step. Figure 21.18a shows that, sure enough, the  $\beta$  clamps dissociated in the presence of pol III\*, but not without the enzyme. Figure 21.18b demonstrates that these liberated  $\beta$  clamps were also competent to be loaded onto an acceptor template. It is clear from what we have learned so far that the  $\beta$  clamp can interact with both the core polymerase and the  $\gamma$  complex (the clamp loader). It must associate with the core during synthesis of DNA to keep the polymerase on the template. Then it must dissociate from the template so it can move to a new site on the DNA where it can interact with another core to make a new Okazaki fragment. This movement to a new DNA site, of course, requires the  $\beta$  clamp to interact with a clamp loader again. One crucial question remains: How does the cell orchestrate the shifting back and forth of the  $\beta$  clamp's association with core and with clamp loader? To begin to answer this question, it would help to show how and when the core and the clamp loader interact with the  $\beta$  clamp. O'Donnell and associates first answered the "how" question, demonstrating that the  $\alpha$ -subunit of the core contacts  $\beta$ , and the  $\delta$ -subunit of the clamp loader also contacts  $\beta$ . One assay these workers used to reveal these interactions was protein footprinting. This method works on the same principle as DNase footprinting, except the starting material is a labeled protein instead of a DNA, and protein-cleaving reagents are used instead of DNase. In this case, O'Donnell and colleagues introduced a six-amino acid protein kinase recognition sequence into the C-terminus of the  $\beta$ -subunit by manipulating its gene. They named the altered product  $\beta$ PK. Then they phosphorylated this protein in vitro using protein kinase and labeled ATP (an ATP derivative with an oxygen in the  $\gamma$ -phosphate replaced by  $^{35}\text{S}$ ); this procedure labeled the protein at its C-terminus.

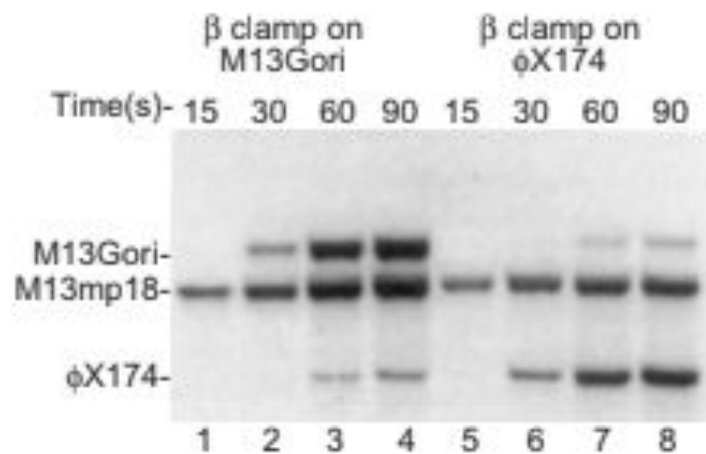
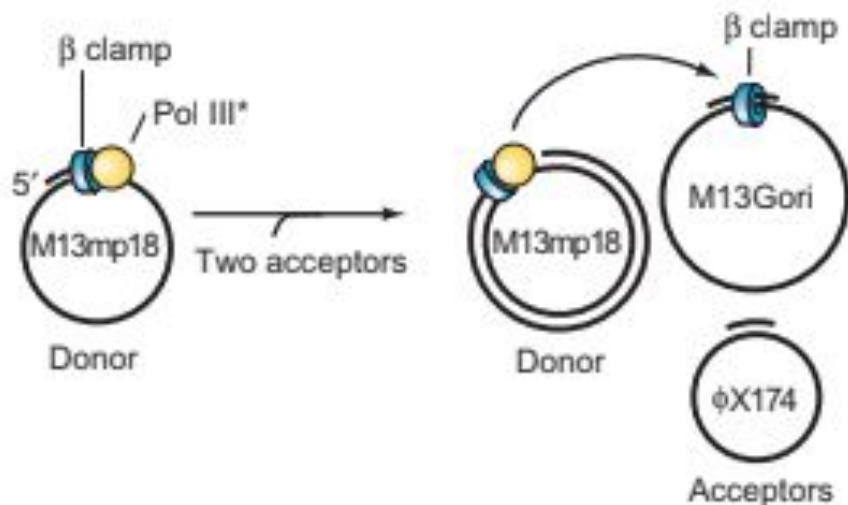


**Figure 21.17 Test of the cycling model.** If one assembles a pol III\* complex with a  $\beta$  clamp on one primed template (M13mp18, top left) and presents it with two acceptor primed templates, one with a  $\beta$  clamp (M13Gori) and one without ( $\phi$ X174), the pol III\* complex should choose the template with the clamp (M13Gori, in this case) to replicate when it has finished replicating the original template. O'Donnell and colleagues carried out this experiment, allowing enough time to replicate both the donor and acceptor templates. They also included labeled nucleotides so the replicated DNA would be labeled. Then they electrophoresed the DNAs and detected the labeled DNA products by gel electrophoresis. The electrophoresis of the replicated DNA products (bottom) show that the acceptor template with the  $\beta$  clamp was the one that was replicated. When the  $\beta$  clamp was on the M13Gori acceptor template, replication of this template predominated. On the other hand, when the  $\beta$  clamp was on the  $\phi$ X174 template, this was the one that was favored for replication. The positions of the replicated templates are indicated at left. (Source: Stukenberg, P.T., J. Turner, and M. O'Donnell. An explanation for leading strand replication. Polymerase

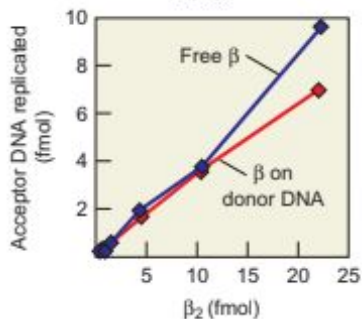
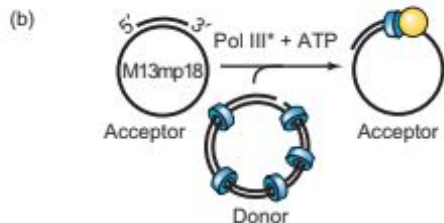
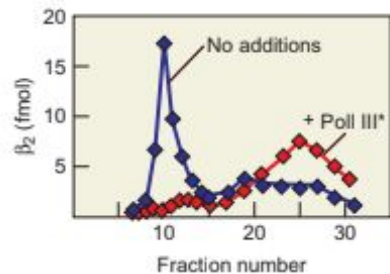
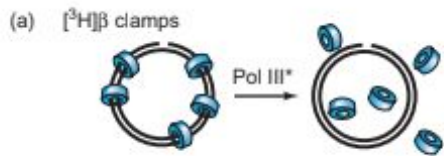


**Figure 21.18 Pol III\* has clamp unloading activity.** (a) Clamp unloading. O'Donnell and colleagues used the  $\gamma$  complex to load  $\beta$  clamps (blue, top) onto a gapped circular template, then removed the  $\gamma$  complex by gel filtration. Then they added pol III\* and performed gel filtration again. The graph of the results (bottom) shows  $\beta$  clamps that were treated with pol III\* (red) were released from the template, whereas those that were not treated with pol III\* (blue) remained associated with the template. (b) Recycling of  $\beta$  clamps. The  $\beta$  clamps from a donor  $\beta$  clamp–template complex treated with pol III\* (red) were just as good at rebinding to an acceptor template as were  $\beta$  clamps that were free in solution (blue). (Source: Adapted from Stukenberg, P.T., J. Turner, and M. O'Donnell, An explanation for lagging strand replication: Polymerase hopping among DNA sliding clamps. *Cell* 78:883, 1994.)

(Note that this is similar to labeling a DNA at one of its ends for DNase footprinting.) First they showed that the d-subunit of the clamp loader and the a-subunit of the core could each protect bPK from phosphorylation, suggesting that both of these proteins contact bPK.

Protein footprinting reinforced these conclusions. O'Donnell and colleagues mixed labeled bPK with various proteins, then cleaved the protein mixture with two proteolytic enzymes: pronase E and V8 protease. Figure 21.19 depicts the results. The first four lanes at the bottom of each panel are markers formed by cleaving the labeled b-subunit with four different reagents that cleave at known positions. Lane 5 in both panels shows the end-labeled peptides created by cleaving b in the absence of another protein. We observe a typical ladder of end-labeled products. Lane 6 in panel (a) shows what happens in the presence of d. We see the same ladder as in lane 5, with the exception of the smallest fragment (arrow), which is either missing or greatly reduced in abundance. This suggests that the d-subunit binds to b near its C-terminus and blocks a protease from cleaving there. If this d–b interaction is specific, one should be able to restore cleavage of the labeled bPK by adding an abundance of unlabeled b to bind to d and prevent its binding to the labeled bPK. Lane 7 shows that this is what happened. Lanes 8 and 9 in panel (a) are similar to 6 and 7, except that O'Donnell and coworkers used whole g complex instead of purified d. Again, the g complex protected a site near the C-terminus of bPK from cleavage, and unlabeled b prevented this protection.

Panel (b) of Figure 21.19 is just like panel (a), except that the investigators used the a-subunit and whole core instead of the d-subunit and whole g complex to footprint labeled bPK. They observed exactly the same results: a or whole core protected the same site from cleavage as did d or whole g complex. This suggests that the core and the clamp loader both contact b at the same site, and that the a- and d-subunits, respectively, mediate these contacts. In a further experiment, these workers used whole pol III\* to footprint bPK. Because pol III\* contains both the core and the clamp loader, one might have expected it to yield a larger footprint than either subassembly separately. But it did not. This is consistent with the hypothesis that pol III\* contacts b through either the core or the clamp loader, but not both at the same time.

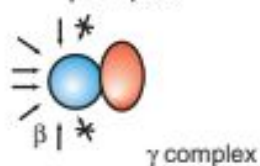


If the b clamp can bind to the core or the clamp loader, but not both simultaneously, which does it prefer? O'Donnell and colleagues used gel filtration to show that when the proteins are free in solution, b prefers to bind to the clamp loader, rather than the core polymerase. This is satisfying because free b needs to be loaded onto DNA by the g complex before it can interact with the core polymerase. However, that situation should change once the b clamp is loaded onto a primed DNA template; once that happens, b needs to associate with the core polymerase and begin making DNA. To test this prediction, O'Donnell and colleagues loaded 35S-labeled b clamps onto primed M13 phage DNA and then added either 3 H-labeled clamp loader (g complex) and unlabeled core, or 3 H-labeled core and unlabeled g complex. Then they subjected these mixtures to gel filtration to separate DNA–protein complexes from free proteins. Under these conditions, it was clear that the b clamp on the DNA preferred to associate with the core polymerase. Almost no g complex bound to the b clamp–DNA complex.

Once the holoenzyme has completed an Okazaki fragment, it must dissociate from the b clamp and move to a new one. Then the original b clamp must be removed from the template so it can participate in the synthesis of another Okazaki fragment. We have already seen that pol III\* has clamp-unloading activity, but we have not seen what part of pol III\* has this activity. O'Donnell and associates performed gel filtration assays that showed that the g complex has clamp-unloading activity. Figure 21.20 illustrates this experiment. The investigators loaded b clamps onto a nicked DNA template, then removed all other proteins. Then they incubated these DNA–protein complexes in the presence and absence of the g complex. We can see that the b clamps are unloaded from the nicked DNA much faster in the presence of the g complex and ATP than in their absence.

Thus the  $\gamma$  complex is both a clamp loader and a clamp unloader. But what determines when it will load clamps and when it will unload them? The state of the DNA seems to throw this switch, as illustrated in Figure 21.21. Thus, when  $\beta$  clamps are free in solution and there is a primed template available, the clamps associate preferentially with the  $\gamma$  complex, which serves as a clamp loader to bind the  $\beta$  clamp to the DNA. Once associated with the DNA, the clamp binds preferentially to the core polymerase and sponsors processive synthesis of an Okazaki fragment. When the fragment has been synthesized, and only a nick remains, the core loses its affinity for the  $\beta$  clamp. The clamp reassociates with the  $\gamma$  complex, which now acts as a clamp unloader, removing the clamp from the template so it can recycle to the next primer and begin the cycle anew.

(a)  $\beta + \delta$  or  $\gamma$  complex



(b)  $\beta + \alpha$  or core

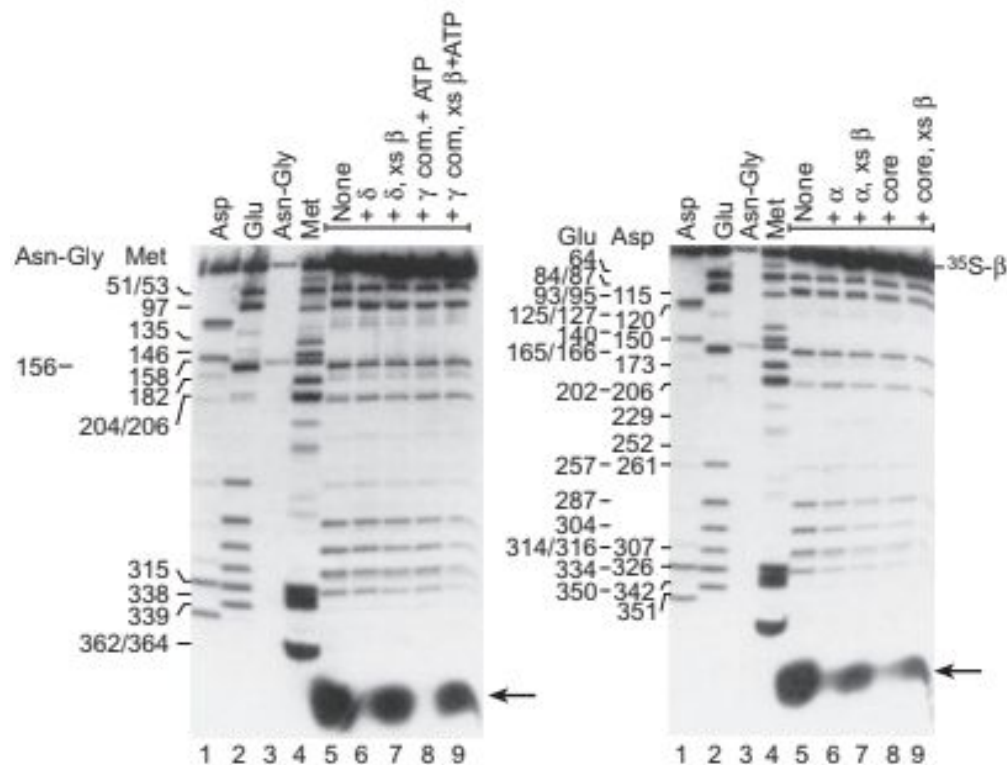
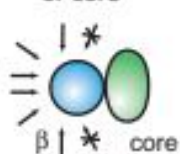


**Figure 21.19 Protein footprinting of  $\beta$  with the  $\gamma$  complex and core polymerase.** O'Donnell and colleagues labeled  $\beta^{\text{PK}}$  at its C-terminus by phosphorylation with protein kinase and [ $^{35}\text{S}$ ]ATP. Then they mixed this end-labeled  $\beta$  with either  $\delta$  or the whole  $\gamma$  complex (panel a) or with either  $\alpha$  or the whole core (panel b). Then they subjected the protein complexes to mild cleavage with a mixture of pronase E and V8 protease to generate a series of end-labeled digestion products. Finally, they electrophoresed these products and autoradiographed the gel to detect them. The first four lanes in each panel are digestion products that serve as markers. The amino acid specificity of each treatment is given at top. Thus, in lane 1, the protein was treated with a protease that cleaves after aspartate (Asp) residues. Lane 5 in both panels represents  $\beta^{\text{PK}}$  cleaved in the absence of other proteins. Lanes 6-9 in both panels represent  $\beta^{\text{PK}}$  cleaved in the presence of the proteins listed at the top of each lane. The  $\delta$ - and  $\alpha$ -subunits and the  $\gamma$  and core complexes all protect the same site from digestion. Thus, they reduce the yield of the fragment indicated by the arrow at the bottom of the gel. The drawings at top illustrate the binding between the  $\beta$  clamp and either the  $\gamma$  complex (a) or the core (b), emphasizing that both contact the  $\beta$  clamp at the same places near the C-terminus of each  $\beta$  monomer and prevent cleavage there (arrows with Xs). (Source: Naktilinis, V., J. Turner, and M. O'Donnell, A molecular switch in a replicating machine defined by an internal competition for protein rings. *Cell* 84 (12 June 1996) f. 3ab bottoms, p. 138. Reprinted by permission of Elsevier Science.)

## Termination in Eukaryotes

Eukaryotes face a difficulty at the end of DNA replication that prokaryotes do not: filling in the gaps left when RNA primers are removed. With circular DNAs, such as those in bacteria, there is no problem filling all the gaps because another DNA 3'-end is always upstream to serve as primer (Figure 21.23a). But consider the problem faced by eukaryotes, with their linear chromosomes. Once the first primer on each strand is removed (Figure 21.23b), there is no way to fill in the gaps because DNA cannot be extended in the 3'→5' direction, and no 3'-end is upstream, as there would be in a circle. If this were actually the situation, the DNA strands would get shorter every time they replicated. This is a termination problem in that it deals with the formation of the ends of the DNA strands, but how do cells solve this problem?

**Telomere Maintenance** Elizabeth Blackburn and her colleagues provided the answer, which is summarized in Figure 21.23c. The telomeres, or ends of eukaryotic chromosomes, are composed of repeats of short, GC-rich sequences. The G-rich strand of a telomere is added at the very 3'-ends of DNA strands, not by semiconservative replication, but by an enzyme called telomerase. The exact sequence of the repeat in a telomere is species-specific. In *Tetrahymena*, it is TTGGGG/AACCCC; in vertebrates, including humans, it is TTAGGG/AATCCC.

Blackburn showed that this specificity resides in the telomerase itself and is due to a small RNA in the enzyme that serves as the template for telomere synthesis. This solves the problem: The telomerase adds many repeated copies of its characteristic sequence to the 3'-ends of chromosomes. Priming can then occur within these telomeres to make the C-rich strand. There is no problem when terminal primers are removed and not replaced, because only telomere sequences are lost, and these can always be replaced by telomerase and another round of telomere synthesis.

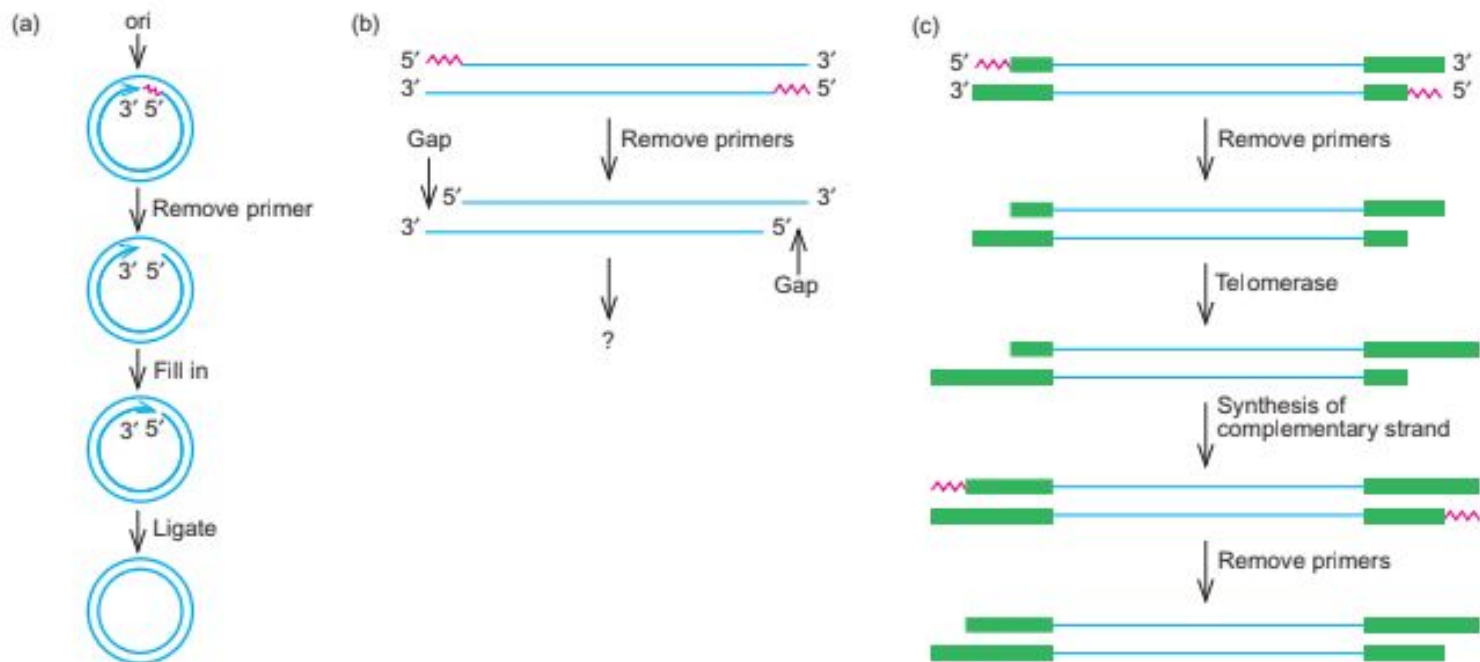


**Figure 21.23 Coping with the gaps left by primer removal.** (a) In bacteria, the 3'-end of a circular DNA strand can prime the synthesis of DNA to fill in the gap left by the first primer (pink). For simplicity, only one replicating strand is shown. (b) Hypothetical model to show what would happen if primers were simply removed from the 5'-end of linear DNA strands with no telomerase action. The gaps at the ends of chromosomes would grow longer each time the DNA replicated. (c) How telomerase can solve the problem. In the first step, the primers (pink) are removed from the 5'-ends of the daughter strands, leaving gaps. In the second step, telomerase adds extra telomeric

DNA (green boxes) to the 3'-ends of the other daughter strands. In the third step, DNA synthesis occurs, using the newly made telomeric DNA as a template. In the fourth step, the primers used in step three are removed. This leaves gaps, but the telomerase action has ensured that no net loss of DNA has occurred. The telomeres represented here are not drawn to scale with the primers. In reality, human telomeres are thousands of nucleotides long. (Source: (c) Adapted from Greider, C.W. and E.H. Blackburn, Identification of a specific telomere terminal transferase activity in tetramere extracts. *Cell* 43 (Dec Pt1 1985) f. 1A, p. 406.)

Blackburn made a clever choice of organism in which to search for telomerase activity: Tetrahymena, a ciliated protozoan. Tetrahymena has two kinds of nuclei: (1) micronuclei, which contain the whole genome in five pairs of chromosomes that serve to pass genes from one generation to the next; and (2) macronuclei, in which the five pairs of chromosomes are broken into more than 200 smaller fragments used for gene expression. Because each of these mini-chromosomes has telomeres at its ends, Tetrahymena cells have many more telomeres than human cells, for example, and they are loaded with telomerase, especially during the phase of life when macronuclei are developing and the new minichromosomes must be supplied with telomeres. This made isolation of the telomerase enzyme from Tetrahymena relatively easy.

In 1985, Carol Greider and Blackburn succeeded in identifying a telomerase activity in extracts from synchronized Tetrahymena cells that were undergoing macro-nuclear development. They assayed for telomerase activity in vitro using a synthetic primer with four repeats of the TTGGGG telomere sequence and included a radioactive nucleotide to label the extended telomere-like DNA. Figure 21.24 shows the results. Lanes 1–4 each contained a different labeled nucleotide (dATP, dCTP, dGTP, and dTTP, respectively), plus all three of the other, unlabeled nucleotides. Lane 1, with labeled dATP showed only a smear, and lanes 2 and 4 showed no extension of the synthetic telomere. But lane 3, with labeled dGTP, exhibited an obvious periodic extension of the telomere. Each of the clusters of bands represents an addition of one more TTGGGG sequence (with some variation in the degree of completion), which accounts for the fact that we see clusters of bands, rather than single bands. Of course, we should observe telomere extension with labeled dTTP, as well as with dGTP. Further investigation showed that the concentration of dTTP was too low in this experiment, and that dTTP could be incorporated into telomeres at higher concentration. Lanes 5–8 show the results of an experiment with one labeled, and only one unlabeled nucleotide. This experiment verified that dGTP could be incorporated into the telomere, but only if unlabeled dTTP was also present. This is what we expect because this strand of the telomere contains only G and T. Controls in lanes 9–12 showed that an ordinary DNA polymerase, Klenow fragment, cannot extend the telomere. Further controls in lanes 13–16 demonstrated that telomerase activity depends on the telomere-like primer.

[TTGGGG] <sub>n</sub> :	+	+	-
	Extract	Klenow	Extract
cold-dNT Ps:	all 3	ATTA	all 3
<sup>32</sup> P-dNT Ps:	ACGT	CGCG	ACGT

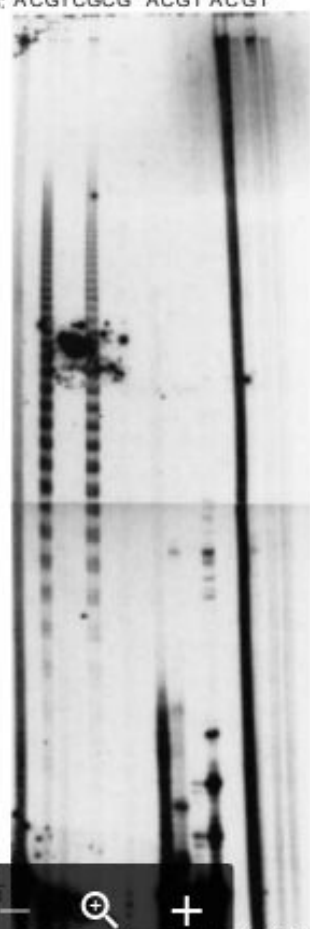


**Figure 21.24 Identification of telomerase activity.** Greider and Blackburn synchronized mating of *Tetrahymena* cells and let the offspring develop to the macronucleus development stage. They prepared cell-free extracts and incubated them for 90 min with a synthetic oligomer having four repeats of the TTGGGG telomere repeat sequence, plus the labeled and unlabeled nucleotides indicated at top. After incubation, they electrophoresed the products and detected them by autoradiography. Lanes 9–12 contained the Klenow fragment of *E. coli* DNA polymerase I instead of *Tetrahymena* extract. Lanes 13–16 contained extract, but no primer. Telomerase activity is apparent only when both dGTP and dTTP are present. (Source: Greider, C.W., and E.H. Blackburn, Identification of a specific telomere terminal transferase activity in tetramere extracts. *Cell* 43 (Dec Pt1 1985) f. 1A, p. 406. Reprinted by permission of Elsevier Science.)

Input  
(TTGGGG)<sub>n</sub>

18 / 914

1 2 3 4 5 6 7 8 9 10 11 12 13 14 15 16

How does telomerase add the correct sequence of bases to the ends of telomeres without a complementary DNA strand to read? It uses its own RNA constituent as a template. (Note that this is a template, not a primer.) Greider and Blackburn demonstrated in 1987 that telomerase is a ribonucleoprotein with essential RNA and protein subunits. Then in 1989 they cloned and sequenced the gene that encodes the 159-nt RNA subunit of the *Tetrahymena* telomerase and found that it contains the sequence CAACCCCAA. In principle, this sequence can serve as template for repeated additions of TTGGGG sequences to the ends of *Tetrahymena* telomeres as illustrated in Figure 21.25.

Blackburn and her colleagues used a genetic approach to prove that the telomerase RNA really does serve as the template for telomere synthesis. They showed that mutant telomerase RNAs gave rise to telomeres with corresponding alterations in their sequence. In particular, they changed the sequence 59-CAACCCCAA-39 of a cloned gene encoding the *Tetrahymena* telomerase RNA as follows:

wt: 59-CAACCCCAA-39

1: 59-CAACCCCCCAA-39

2: 59-CAACCTCAA-39

3: 59-CGACCCCAA-39

The underlined bases in each of the three mutants (1, 2, and 3) denote the base changed (or added, in 1). They introduced the wild-type or mutated gene into *Tetrahymena* cells in a plasmid that ensured the gene would be overexpressed. Even though the endogenous wild-type gene remained in each case, the overexpression of the transplanted gene swamped out the effect of the endogenous gene. Southern blotting of telomeric DNA from cells transformed with each construct showed that a probe for the telomere sequence expected to result from mutants 1 (TTGGGGG) and 3 (GGGGTC) actually did hybridize to telomeric DNA from cells transformed with these mutant genes. On the other hand, this did not work for mutant 2; no telomeric DNA that hybridized to a probe for GAGGTT was observed.



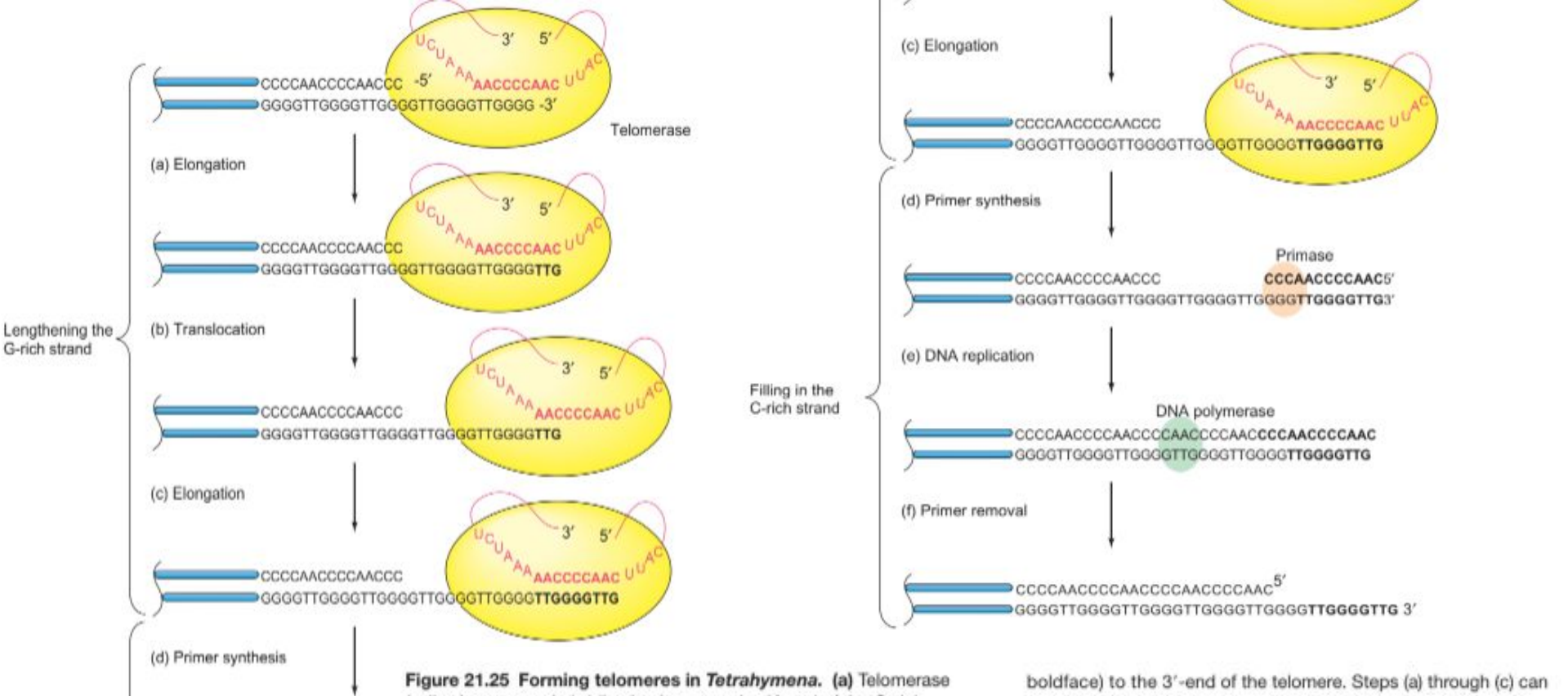


**Figure 21.25 Forming telomeres in *Tetrahymena*.** (a) Telomerase (yellow) promotes hybridization between the 3'-end of the G-rich telomere strand and the template RNA (red) of the telomerase. The telomerase uses three bases (AAC) of its RNA as a template for the addition of three bases (TTG, boldface) to the 3'-end of the telomere. (b) The telomerase translocates to the new 3'-end of the telomere, pairing the left-hand AAC sequence of its template RNA with the newly incorporated TTG in the telomere. (c) The telomerase uses the template RNA to add six more nucleotides (GGGTTG,

boldface) to the 3'-end of the telomere. Steps (a) through (c) can repeat indefinitely to lengthen the G-rich strand of the telomere. (d) When the G-rich strand is sufficiently long (probably longer than shown here), primase (orange) can make an RNA primer (boldface), complementary to the 3'-end of the telomere's G-rich strand. (e) DNA polymerase (green) uses the newly made primer to prime synthesis of DNA to fill in the remaining gap on the C-rich telomere strand and DNA ligase seals the nick. (f) The primer is removed, leaving a 12–16-nt overhang on the G-rich strand.

These results suggested that mutant telomerase RNAs 1 and 3, but not 2, served as templates for telomere elongation. To confirm this suggestion, Blackburn and colleagues sequenced a telomere fragment from cells transformed with mutant telomerase RNA 3. They found the following sequence:

59-CTTTTACTCAATGTCAAAGAAATTATTAATT(GGGGTT)30  
(GGGGTC)2GGGGT(GGGGTC)8GGGGTGGGGTC(GGGGTT)N-39

where the underlined bases must have been encoded by the mutant telomerase RNA. This nonuniform sequence differs strikingly from the normal, very uniform telomeric sequence in this species. The first 30 repeats appear to have been encoded by the wild-type telomerase RNA before transformation. These are followed by 11 mutant repeats interspersed with 2 wild-type repeats, then by all wild-type repeats. The terminal wild-type sequences may have resulted from recombination with a wild-type telomere, or from telomere synthesis after loss of the mutant telomerase RNA gene from the cell. Nevertheless, the fact remains that a significant number of repeats have exactly the sequence we would expect if they were encoded by the mutant telomerase RNA. Thus, we can conclude that the telomerase RNA does serve as the template for telomere synthesis, as Figure 21.25 suggests. The fact that telomerase uses an RNA template to make a DNA strand implies that telomerase acts as a reverse transcriptase. Thus, Blackburn and others set about to purify the enzyme to prove that this is indeed how it works. Although the enzyme eluded purification for 10 years, Joachim Lingner and Thomas Cech finally succeeded in 1996 in purifying it from another ciliated protozoan, *Euplotes*. This telomerase contains two proteins, p43 and p123, in addition to the RNA subunit that serves as the template for extending telomeres. The p123 protein has the signature sequence of a reverse transcriptase, indicating that it provides the catalytic activity of the enzyme. We therefore call it TERT, for telomerase reverse transcriptase. Because this enzyme was discovered when the Human Genome Project was well along, it did not take long to find a complementary sequence in the human genome and use it to clone the human TERT gene, hTERT, in 1997.

Structural analysis has shown that the C-terminal part of the TERT protein contains the reverse transcriptase activity, and the N-terminal part binds to the RNA. In fact, the RNA appears to be tethered to the protein so as to give the RNA, which is hundreds of nucleotides long, considerable flexibility. This allows the RNA to fulfill its template role by moving with respect to the active site of the enzyme as each nucleotide is added to the growing telomere. Until 2003, it appeared that the somatic cells of higher eukaryotes, including humans, lack telomerase activity, whereas germ cells retain this activity. Then, William Hahn and colleagues showed that cultured normal human cells do express telomerase at a low level, but only transiently, during S phase, when DNA is replicated. On the other hand, cancer cells have much higher telomerase activity, which is expressed constitutively—all the time. These findings have profound implications for the characteristics of cancer cells, and perhaps even for their control (see Box 21.1).

**Telomere Structure** Besides protecting the ends of chromosomes from degradation, telomeres play another critical role: They prevent the DNA repair machinery from recognizing the ends of chromosomes as chromosome breaks and sticking chromosomes together. This inappropriate joining of chromosomes would be potentially lethal to the cell.

Furthermore, cells have a DNA damage checkpoint that detects damage and stops cell division until the damage can be repaired. Because chromosome ends without telomeres look like broken chromosomes, they invoke the checkpoint, so cells stop dividing and eventually die. If telomeres really looked the way they are pictured in Figures 21.23 and 21.25, little would distinguish them from real chromosome breaks. In fact, the critical telomere length in humans is 12.8 repeats of the core 6-bp sequence. Below that threshold, human chromosomes began to fuse. How do telomeres allow the cell to recognize the difference between a real chromosome end and a broken chromosome?

For years, molecular biologists pondered this question and, as telomere-binding proteins were discovered, they theorized that these proteins bind to the ends of chromosomes and in that way identify the ends. Indeed, eukaryotes from yeasts to mammals have a suite of telomere-binding proteins that protect the telomeres from degradation, and also hide the telomere ends from the DNA damage factors that would otherwise recognize them as chromosome breaks. We will discuss the telomere-binding proteins from three groups of eukaryotes and see how they solve the telomere protection problem.

**The Mammalian Telomere-Binding Proteins: Shelterin** In mammals, the group of telomere-binding proteins is appropriately known as shelterin, because it “shelters” the telomere. There are six known mammalian shelterin proteins: TRF1, TRF2, TIN2, POT1, TPP1, and RAP1. TRF1 was the first of these proteins to be discovered. Because it bound to double-stranded telomere DNA, which includes repeats of the sequence TTAGGG, it was named TTAGGG repeat-binding factor-1 (TRF1). TRF2 is a product of a paralog of the TRF1 gene (paralogs are homologous genes in the same organism), and it also binds to the double-stranded parts of telomeres. POT1 (protection of telomeres -1) binds to the single-stranded 3'-tails of telomeres, beginning at a position just 2 nt away from the 5'-end of the other strand. In this way it is positioned to protect the single-stranded telomeric DNA from endonucleases, and the 5'-end of the other strand within the double-stranded telomeric DNA from 5'-exonucleases. TPP1 is a POT1-binding protein. Indeed, it appears to be a partner of POT1 in a heterodimer. TIN2 (TRF1-interacting factor-2) plays an organizing role in shelterin. It connects TRF1 and TRF2 together, and connects the dimer TPP1/POT1 to TRF1 and TRF2. Finally, RAP1, with the uninformative name “repressor activator protein-1,” binds to the telomere by interacting with TRF2. Other proteins besides shelterin bind to telomeres, but shelterin proteins can be distinguished from the others in three ways: They are found only at telomeres; they associate with telomeres throughout the cell cycle; and they are known to function nowhere else in the cell. Other proteins may fulfill one of these criteria, but not two or all three.

Shelterin can affect the structure of telomeres in three ways. First, it can remodel the telomere into a loop called a t-loop (for “telomere-loop”). In 1999, Jack Griffith and Titia de Lange and their colleagues discovered that mammalian telomeres are not linear, as had been assumed, but form a DNA loop they called a t-loop. These loops are unique in the chromosome and therefore quite readily set the ends of chromosomes apart from breaks that occur in the middle and would yield linear ends to the chromosome fragments. What is the evidence for t-loops? Griffith, de Lange and colleagues started by making a model mammalian telomeric DNA with about 2 kb of repeating TTAGGG sequences, and a 150–200-nt single-stranded 39-overhang at the end. They added one of the telomere-binding proteins, TRF2, then subjected the complex to electron microscopy. Figure 21.26a shows that a loop really did form, with a ball of TRF2 protein right at the loop–tail junction. Such structures appeared about 20% of the time. By contrast, when these workers cut off the single-stranded 39-overhang, or left out TRF2, they found a drastic reduction in loop formation.

One way for a telomere to form such a loop would be for the single-stranded 39-overhang to invade the double-stranded telomeric DNA upstream, as depicted in Figure 21.27. If this hypothesis is correct, one should be able to stabilize the loop with psoralen and UV radiation, which cross-link thymines on opposite strands of a double-stranded DNA. Because the invading strand base-pairs with one of the strands in the invaded DNA, this creates double-stranded DNA that is subject to cross-linking and therefore stabilization. Figure 21.26b shows the results of an experiment in which Griffith, de Lange, and coworkers cross-linked the model DNA with psoralen and UV, then deproteinized the complex, then subjected it to electron microscopy. The loop is still clearly visible, even in the absence of TRF2, showing that the DNA itself has been cross-linked, stabilizing the t-loop. Next, these workers purified natural telomeres from several human cell lines and from mouse cells and subjected them to psoralen–UV treatment and electron microscopy. They obtained the same result as in Figure 21.26b, showing that t-loops appear to form *in vivo*. Furthermore, the sizes of these putative t-loops correlated well with the known lengths of the telomeres in the human or mouse cells, reinforcing the hypothesis that these loops really do represent telomeres.

To test further the notion that the loops they observed contain telomeric DNA, Griffith, de Lange and colleagues added TRF1, which is known to bind very specifically to double-stranded telomeric DNA, to their looped DNA. They observed loops coated with TRF1, as shown in Figure 21.28a. If the strand invasion hypothesis in Figure 21.27 is valid, the single-stranded DNA displaced by the invading DNA (the displacement loop, or D-loop) should be able to bind *E. coli* single-strand-binding protein (SSB) if the displaced DNA is long enough. Figure 21.28b demonstrates that SSB is indeed visible, right at the tail-loop junction. That is just where the hypothesis predicts we should find the displaced DNA. Shelterin is essential for t-loop formation. In particular, TRF2 can form t-loops in a model DNA substrate. However, this remodeling reaction is weak in the absence of the other shelterin subunits. TRF1, the other telomere repeat-binding protein, is especially helpful, as it can bend, loop, and pair telomeric repeats. It is striking that this remodeling reaction can occur *in vitro* even in the absence of ATP. Based on all we know about shelterin proteins, de Lange proposed the model for t-loop formation depicted in Figure 21.29. Figure 21.29a shows the members of the shelterin complex bound to an unlooped telomere. Figure 21.29b is a model for the interaction of shelterin with a t-loop.

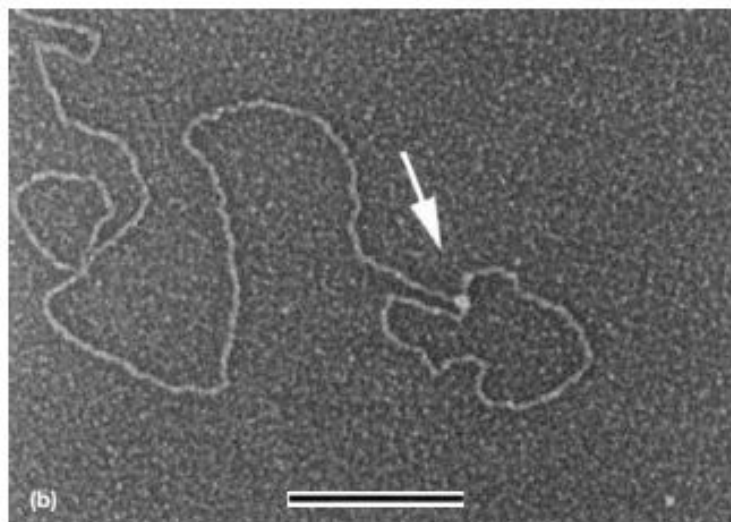


**Figure 21.28 Binding of TRF1 and SSB to t-loops. (a) TRF1.**

Griffith, de Lange, and colleagues purified natural HeLa cell t-loops, cross-linked them with psoralen and UV radiation, and added TRF1, which binds specifically to double-stranded telomeric DNA. Then they shadowed the loop with platinum and palladium and performed electron microscopy. The t-loop, but not the tail, is coated uniformly with TRF1. **(b) SSB.** These workers followed the same procedure as in panel (a), but substituted *E. coli* SSB for TRF1. SSB should bind to single-stranded DNA, and it was observed at the loop-tail junction (arrow), where the single-stranded displacement loop was predicted to be. The bar represents 1 kb. (Source: Griffith, J.D., L. Comeau, S. Rosenfield, R.M. Stansel, A. Bianchi, H. Moss, and T. de Lange, Mammalian telomeres end in a large duplex loop. *Cell* 97 (14 May 1999) f. 5, p. 510. Reprinted by permission of Elsevier Science.)

Figure 21.29b also hints at an explanation for the paradox that POT1 is a single-stranded telomere-binding protein and yet the single-stranded telomeric DNA is hidden in the t-loop. But the figure shows that formation of the t-loop also creates a D-loop, and the displaced single-stranded region is a potential binding site for POT1. There is also the possibility that not all mammalian telomeres form t-loops. Any telomeres that remain linear would provide obvious binding sites for POT1.

The second way shelterin affects the structure of telomeres is by determining the structure of the end of the telomere. It does this in two ways: by promoting 3'-end elongation, and protecting both the 5'- and 3'-ends from degradation. Finally, the third effect of shelterin on the structure of telomeres is to maintain telomere length within close tolerances. When the telomere gets too long, shelterin inhibits further telomerase action, limiting the growth of the telomere. POT1 plays a critical role in this process: When POT1 activity is eliminated, mammalian telomeres grow to abnormal lengths.

### **Telomere Structure and Telomere-Binding Proteins in Lower Eukaryotes**

Yeasts also have telomere-binding proteins, but they appear not to form t-loops. Thus, the proteins themselves must protect the telomere ends, without the benefit of hiding the single-stranded end within a D-loop. The fission yeast, *Schizosaccharomyces pombe*, has a group of telomere-binding proteins that resemble mammalian shelterin proteins. A protein called Taz1 plays the double-stranded telomere-binding role of mammalian TRF in fission yeast, and binds through Rap1 and Poz1 to a dimer of Tpz1 and Pot1. That resembles the TPP1-POT1 dimer in mammals, not only in structure, but in ability to bind to single-stranded telomeric DNA. These proteins can bind to a linear telomere, and they may also bend the telomere by 180 degrees by protein-protein interactions between proteins bound to the double-stranded telomere, and those bound to its single-stranded tail.



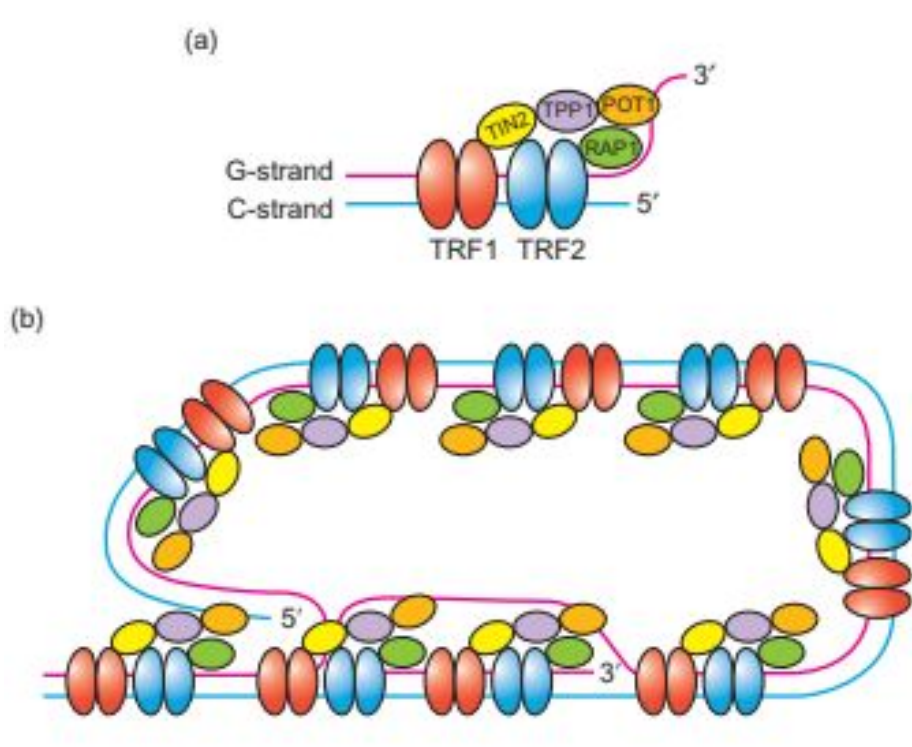


**Figure 21.29 The shelterin-telomere complex.** (a) Interaction with shelterin proteins and a linear telomere. TRF1 and TRF2 are shown interacting as dimers with the double-stranded part of the telomere, as POT1 interacts with the single-stranded part. The known interactions among shelterin proteins are also shown. (b) Model for the interaction of shelterin complexes with a t-loop. Colors are as in panel (a). Note the binding of POT1 (orange) to the single-stranded telomeric DNA in the D-loop, and the binding of TRF1 and TRF2 to the double-stranded telomeric DNA elsewhere in the t-loop.

This bending does not seem to form t-loops, however. The budding yeast *Saccharomyces cerevisiae* also has telomere-binding proteins, but their evolutionary relationship to mammalian shelterin proteins is limited to one protein: Rap1. However, unlike mammalian RAP1, yeast Rap1 binds directly to double-stranded DNA, as the mammalian TRF proteins do. RAP1 has two partners, Rif1 and Rif2. In addition, a second protein complex, composed of Cdc13, Stn1, and Ten1, binds to the single-stranded telomeric tail. Telomere-binding proteins were first discovered in the ciliated protozoan *Oxytricha*. This organism makes do with just two such proteins, TEBPa and TEBPb, which are evolutionarily related to POT1 and TPP1 in mammals. These proteins bind to the single-stranded 39-end of the organism's telomeres and protect them from degradation. By covering the ends of the telomeres, these proteins also prevent the telomeres from appearing like the ends of broken chromosomes—and all the negative consequences that would have.

## **The Role of Pot1 in Protecting Telomeres In *S. pombe*,**

Pot1, instead of limiting the growth of telomeres, as mammalian POT1 does, plays a critical role in maintaining their integrity. Indeed loss of Pot1 can cause the loss of telomeres from this organism. In 2001, Peter Baumann and Thomas Cech reported that they had found a protein in *S. pombe* that binds the single-stranded tails of telomeres. They named the *S. pombe* gene *pot1*, for protection of telomeres, and its product is now known as Pot1. To test their hypothesis that *pot1* encodes a protein that protects telomeres, Baumann and Cech generated a *pot11/pot12* diploid strain and germinated the spores from this strain. The *pot12* spores gave rise to very small colonies compared with the colonies from *pot11* spores. And the *pot12* cells tended to be elongated, to show defects in chromosome segregation, and to stop dividing. All of these effects are consistent with loss of telomere function.

To test directly the effect of *pot1* on telomeres, Baumann and Cech looked for the presence of telomeres in *pot12* strains by Southern blotting DNA from these strains and probing with a telomere-specific probe. Figure 21.30 shows the results. DNA from the *pot11* strains, and from the diploid strains containing at least one *pot11* allele, reacted strongly with the telomere probe, indicating the presence of telomeres. But DNA from the *pot12* strains did not react with the probe, indicating that their telomeres had disappeared. Thus, the *pot1* gene product, Pot1p (or Pot1), really does seem to protect telomeres. If Pot1 really protects telomeres, we would expect it to bind to telomeres. To check this prediction, Baumann and Cech cloned the *pot1* gene into an *E. coli* vector so it could be expressed as a fusion protein with a tag of six histidines

They purified this fusion protein and used a gel mobility shift assay (Chapter 5) to detect its binding to either the C-rich or G-rich strand of the telomere, or a double-stranded telomeric DNA. Figure 21.31a shows that Pot1 bound to the G-rich strand, but not to the C-rich or duplex DNA. Furthermore, an N-terminal fragment of Pot1 was even more effective in binding to the G-rich strand of the telomere (Figure 21.31b). It is interesting that the phenotype of the *pot12* strains, though it was originally quite aberrant, returned to normal after about 75 generations.

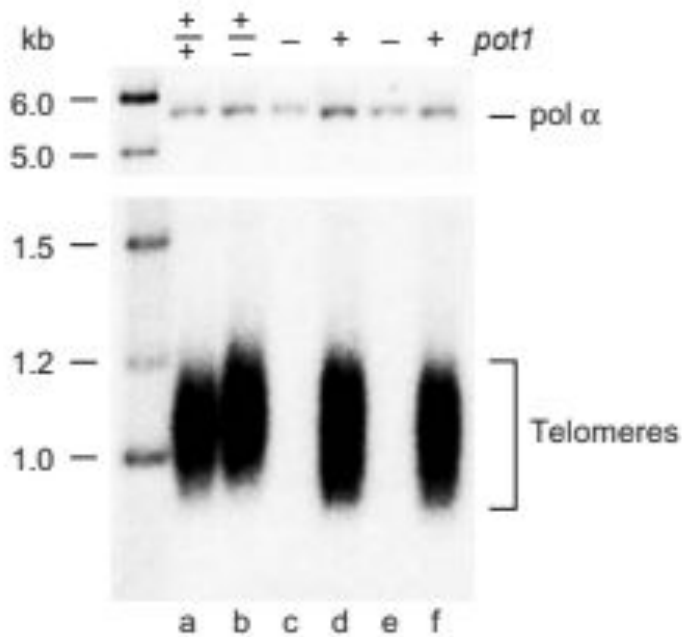


**Figure 21.30 Fission yeast strains defective in *pot1* lose their telomeres.** Baumann and Cech generated homozygous and heterozygous diploid, and *pot1*<sup>-</sup> and *pot1*<sup>+</sup> haploid strains of *S. pombe*, as indicated at top, then isolated DNA from these strains, digested the DNA with *Eco*RI, electrophoresed and Southern blotted the fragments, then probed the blot with a telomere-specific probe. As a control for uniform loading of the blot, the blot was also probed for DNA polymerase α, as indicated at top right. (Source: From Baumann and Cech, *Science* 292: p. 1172. © 2001 by the AAAS.)

The same effect had previously been observed in strains lacking telomerase. This behavior can be explained if yeast chromosomes lacking telomeres can protect their ends by circularizing. To test this hypothesis, Baumann and Cech cleaved DNA from surviving *pot12* strains with the rare cutter *Not*I (Chapter 4) and subjected the resulting DNA fragments to pulsed-field gel electrophoresis. If the chromosomes really had circularized, the *Not*I fragments at the ends of chromosomes should be missing and new fragments composed of the fused terminal fragments should appear. Figure 21.32 shows that this is exactly what happened for the two chromosomes tested, chromosomes I and II. The two fragments (I and L) normally at the ends of chromosome I were missing, and a new band (I1L), not present in *pot11* strains, appeared. Similarly, the two fragments (C and M) normally at the ends of chromosome II were missing, and a new band (C1M) appeared. Thus, the chromosomes in *pot12* strains really do circularize in response to loss of their telomeres.

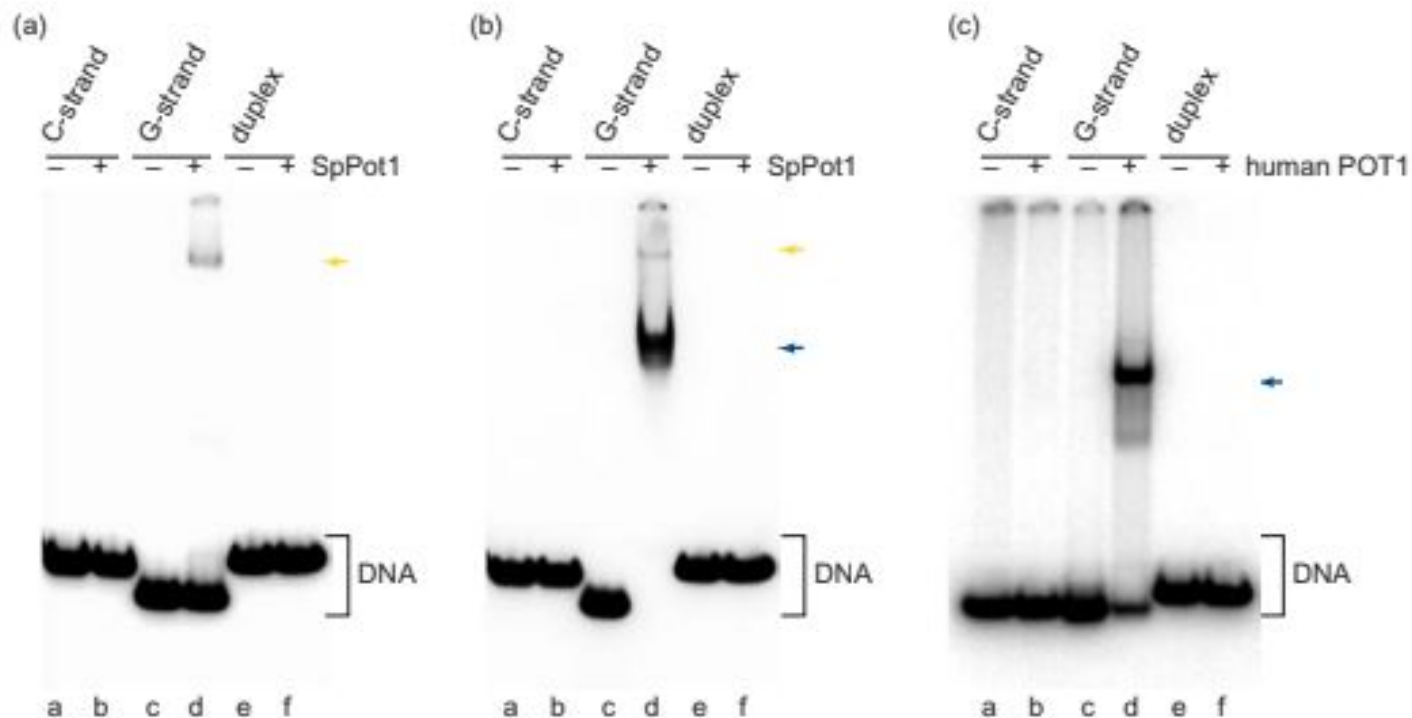


**Figure 21.31 Pot1 binding to telomeric DNA.** Baumann and Cech performed gel mobility shift experiments with *S. pombe* Pot1 and labeled *S. pombe* telomeric DNA (**a** and **b**) and human hPot1 and labeled human telomeric DNA (**c**). The telomeric DNA was either from the C-rich strand, the G-rich strand, or duplex DNA, as indicated at top. Panel (**a**) contained full-length Pot1. Panel (**b**) contained mostly

an N-terminal fragment of Pot1, with slight contamination from full-length Pot1. Panel (**c**) contained an N-terminal fragment of human POT1. Arrows indicate the positions of shifted bands containing full-length Pot1 (yellow arrows) or N-terminal fragments of Pot1 or human POT1 (blue arrows). (Source: From Baumann and Cech, *Science* 292: p. 1172. © 2001 by the AAAS.)

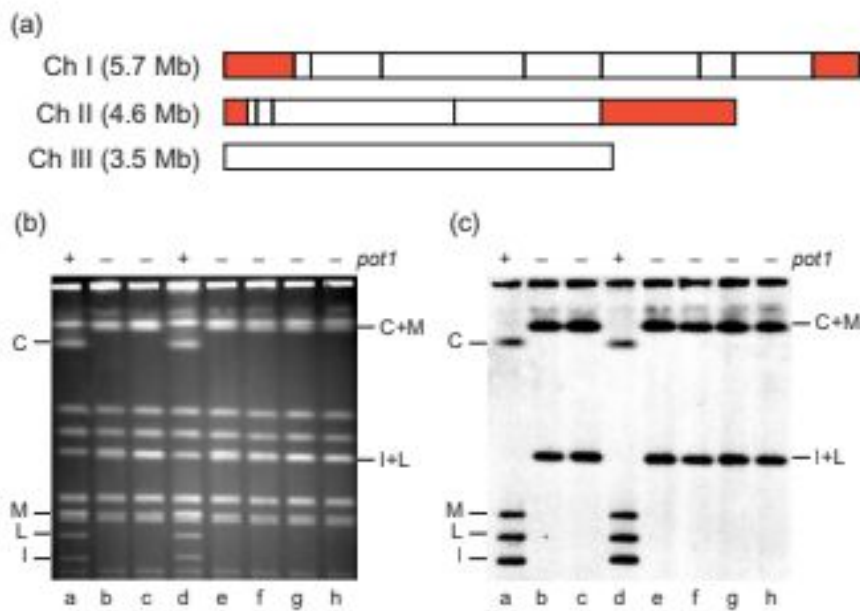


**Figure 21.32 Surviving *Pot1*<sup>-</sup> stains have circularized chromosomes.** (a) Maps of the three chromosomes of *S. pombe* showing the restriction sites for *NotI* as vertical lines. The terminal *NotI* fragments in chromosomes I and II are in red. Chromosome III is not cut by *NotI*. (b) Stained gel after pulsed-field gel electrophoresis of *NotI* DNA fragments from *pot1*<sup>+</sup> and *pot1*<sup>-</sup> cells, as indicated at top. The positions of terminal fragments (C, M, L, and I) of chromosomes I and II are indicated at left, and the positions of fused C+M and I+L fragments are indicated at right. (c) Baumann and Cech Southern blotted the gel from panel (b) and probed it with labeled DNA fragments C, M, L and I, representing the ends of chromosomes I and II. (Source: From Baumann and Cech. *Science* 292: p. 1172. © 2001 by the AAAS.)

The Role of Shelterin in Suppressing Inappropriate Repair and Cell Cycle Arrest in Mammals We have seen that telomeres prevent the cell from recognizing chromosome ends as chromosome breaks and invoking two processes that would threaten the life of the cell and even the organism. These processes are homology-directed repair (HDR) and nonhomologous end-joining (NHEJ). HDR would promote homologous recombination between telomeres on separate chromosomes, or between telomeres and other chromosomal regions, resulting in potentially drastic shortening or lengthening of telomeres. The shortening would be especially dangerous because it could lead to loss of the whole telomere. NHEJ would lead to chromosome fusion, which is often lethal to the cell because the chromosomes do not separate properly during mitosis. If the cell doesn't die, the results could be even worse for the organism because they can lead to cancer.

D-loop part of a t-loop. Presumably, POT1 blocks binding of RPA to this single-stranded DNA simply by out-competing it for those binding sites. POT1 has an advantage over RPA in that it is automatically concentrated at telomeres by being part of the shelterin complex.

Shelterin also blocks the two DNA repair pathways that threaten telomeres: NHEJ and HDR. TRF2 represses NHEJ at telomeres during the G1 phase of the cell cycle, before DNA replication, while POT1 and TRF2 team up to repress NHEJ at telomeres in the G2 phase, after DNA replication. POT1 and TRF2 also collaborate to block HDR at telomeres. Ku (Chapter 20) can also block HDR at telomeres. This is interesting, because Ku's other role is to promote NHEJ when chromosomes are broken. Thus, telomeres must take advantage of Ku's ability to suppress HDR, while keeping in check its ability to promote NHEJ.

In addition to HR and NHEJ, broken chromosomes also activate a checkpoint whereby the cell cycle can be arrested until the damage is repaired. If it is not repaired, the cells irreversibly enter a senescence phase and ultimately die, or they undergo a process called apoptosis, or programmed cell death, that results in rapid, controlled death of the cell. If normal chromosome ends invoked such a checkpoint, cells could not grow and life would cease. This is another reason that telomeres must prevent the cell from recognizing the normal ends of chromosomes as breaks. Chromosome breaks do not by themselves activate cell cycle arrest. Instead, they are recognized by two protein kinases that autophosphorylate (phosphorylate themselves) and thereby initiate signal transduction pathways that lead to cell cycle arrest. One of these kinases is the ataxia telangiectasia mutated kinase (ATM kinase), which responds directly to unprotected DNA ends. Ataxia telangiectasia is an inherited disease caused by mutations in the ATM kinase gene. It is characterized by poor coordination (ataxia), prominent blood vessels in the whites of the eyes (telangiectasias), and susceptibility to cancer, among other symptoms. The second kinase that senses chromosome breaks is the ataxia telangiectasia and Rad3 related kinase (ATR kinase), which responds to the single-stranded DNA end that appears when one DNA strand at a chromosome break is nibbled back by nucleases. As we have seen, mammalian telomeres have DNA ends that could activate the ATM kinase, and single-stranded DNA ends that could activate the ATR kinase, so both of these kinases need to be held in check at telomeres. How is this accomplished? It is shelterin's job to repress both the ATM and ATR kinase at normal chromosome ends. One of shelterin's components, TRF2, represses the ATM kinase pathway. In fact, loss of TRF2 activity leads to the inappropriate activation of the ATM kinase at mammalian telomeres, which leads to cell cycle arrest. Another shelterin subunit, POT1, represses the ATR kinase pathway. When POT1 is inactivated, the ATM pathway remains repressed, but the ATR pathway is activated. The simple formation of t-loops may explain the repression of the ATM pathway because the t-loops hide the DNA ends. However, t-loops cannot explain the repression of the ATR pathway, which is actually initiated by replication protein A (RPA), which binds directly to single-stranded DNA—and single-stranded DNA persists in the